12-2016

Direct Attachment of 4-Hydroxybenzoic Acid Polymers and Capture Agents to Flat Sheet and Microdialysis Membranes for Improved Mass Transport

Sarah Jane Phillips
University of Arkansas, Fayetteville

Citation

Direct Attachment of 4-Hydroxybenzoic Acid Polymers and Capture Agents to Flat Sheet and Microdialysis Membranes for Improved Mass Transport

A dissertation submitted in partial fulfillment
of the requirements for the degree of
Doctor of Philosophy in Chemistry

by

Sarah Phillips
Missouri State University
Bachelor of Science in Chemistry, 2009
Missouri State University
Master of Science in Chemistry, 2011

December 2016
University of Arkansas

This dissertation is approved for recommendation to the Graduate Council.

_____
Dr. Julie A. Stenken
Dissertation Director

_____   _____
Dr. David Paul   Dr. Shannon Servoss
Committee Member   Committee Member

_____   _____
Dr. Wesley Stites   Dr. Suresh Thallapuranam
Committee Member   Committee Member

ABSTRACT

Microdialysis (MD) sampling is a diffusion-based separation method which has the ability to sample any analyte that can diffuse across the semi-permeable membrane. However one challenge for MD is that for soluble proteins greater than 10 kDa, the relative recovery (RR) using a 100 kDa MD probe is between 1-5%.[1] There are two major barriers that lead to these low recovery values - nonspecific adsorption (NSA) and poor solute mass transport. To overcome these two barriers, the modification of PES-based MD membranes has been initiated by laccase. Previous researchers have used laccase to modify PES flat sheet and hollow fiber membranes using 4HBA to create a hydrophilic polymer chain network.[2] Furthermore by functionalizing the MD membranes with carboxylic acid functional groups from 4HBA, one can easily modify the surface.[3] This study focuses on characterization of the PES membrane surface before and after attachment of 4HBA polymers and heparin. First the attachment of 4HBA and heparin has been confirmed using XPS and ATR-FTIR. Next protein adsorption measurements were performed for 4HBA modified flat sheets which showed an initial increase in BSA adsorption followed by a decrease in BSA adsorption after 24 hours of modification. However, for positively charged lysozyme the protein adsorption increased upon modification. RR experiments were performed using FITC-labeled dextrans, lysozyme, CCL2, VEGF, TNF-α, KC/GRO and aFGF. After modification with 4HBA for 2 hours, RR of CCL2, KC/GRO, and VEGF increased 2 to 3 times compared to the control relative recovery however, this increase in RR was not observed for aFGF and TNF-α. This difference could be due to the isoelectric points (pI) of these proteins indicating an electrostatic interaction between the surface and the protein. For 24 hour 4HBA-heparin modified membranes CCL2 RR increased twofold for hours 3 and 4 and for 2 hour 4HBA-heparin modified membranes aFGF RR increase threefold.

ACKNOWLEDGEMENTS

First and foremost, I have to thank God for allowing me the opportunity to complete this degree and for providing me comfort and encouragement. Next, I would like to give thanks to my parents, Brenda and Dennis Phillips, for instilling a desire in me to learn and never give up. I next would like to thank my research advisor, Dr. Julie Stenken, without whom I would not be able to complete this research project. She has helped me grow immensely as a scientist and provided me many opportunities to learn many different techniques.

I am thankful for my dissertation committee members, Dr. David Paul, Dr. Shannon Servoss, Dr. Wesley Stites, and Dr. Suresh Thallapuranam, for their many suggestions that they have given me throughout this process. I would also like to thank all of the professors in the Missouri State University and University of Arkansas chemistry and chemical engineering departments for helping me learn more about chemistry, your willingness to discuss my project with me and allowing me to use instruments and equipment in your research labs. I would also like to thank Dr. Chris Mazzanti for giving me the opportunity to learn many different instruments in the teaching labs.

I would especially like to thank the lab members in the Stenken lab for being a willing audience to listen to all my ideas, providing good suggestions, and your ability to make this a fun place to work. Also thank you to all of the friends I have made in the chemistry department, I have enjoyed eating lunch together and the conversations that have occurred in passing. I would also like to thank the brothers in Alpha Chi Sigma for all of your help in support in networking and for providing a fun environment with other scientists.

DEDICATION

       This dissertation is dedicated to my grandfathers, Ed Harris, and Wade Phillips II. They were always so proud of me in terms of my education and I wish they could be here to see me complete this degree.

TABLE OF CONTENTS

LIST OF FIGURES

LIST OF TABLES

GLOSSARY

MIP-1	Macrophage inflammatory protein 1
MS	Mass spectrometry
NHS	N-hydroxysuccinimide
NMR	Nuclear magnetic resonance
OEG	Oligoethylene glycol
PBS	Phosphate buffered saline
PEG	Polyethylene glycol
PES	Polyethersulfone
PET	Polyethylene Terephthalate
pI	Isoelectric point
RANTES	Regulated and normal T cell expressed and secreted
RR	Relative recovery
SAMs	Self-assembled monolayers
SDS	Sodium dodecyl sulfate
SEC	Size exclusion chromatography
TGF-β	Transforming growth factor
TNF-α	Tumor necrosis factor-α
TOF	Time of flight
UV	Ultraviolet
VEGF	Vascular endothelial growth factor
XPS	X-ray photoelectron spectroscopy

Symbols

$[A]_{bound}$	Analyte concentration bound due to affinity interaction
$[A]_{external}$	Analyte concentration external to the probe
$[A]_{free}$	Free analyte concentration
$[AB]$	Concentration of analyte bound to affinity agent
$[B]_{free}$	Free affinity agent concentration
C_{10}	Concentration of species 1 at distance 0
C_{1l}	Concentration of species 1 at distance l
C_{inlet}	Concentration of analyte added in the perfusion fluid
C_{outlet}	Concentration of analyte in the dialysate
C_{sample}	Concentration of the analyte in the sample
D_{eff}	Effective diffusion coefficient
H	Partition coefficient
J	Flux
K_D	Equilibrium dissociation constant
k_{off}	Off-rate constant
k_{on}	On-rate constant
l	Length
M_x	Molecular weight
N_x	Number of molecules of M_x size

CHAPTER 1. INTRODUCTION

Significance

The work in this dissertation is focused on developing membranes to improve mass transport through covalent addition of 4-hydroxybenzoic acid (4HBA) polymers, and heparin to the microdialysis membrane surface. One significant challenge to microdialysis is that mass transport is low for large soluble signaling proteins (>10 kDa). These signaling molecules help cells, perceive and respond to their microenvironment and are found to be involved in processes such as inflammation, and immunity.[4] Another challenge for microdialysis is the nonspecific adsorption of protein molecules to the dialysis membrane and tubing, this decreases the effective pore size of the membrane and causes loss of analytes, leading to a decrease in recovery.[5] By attaching hydrophilic phenolic compounds (4-hydroxybenzoic acid polymers) onto the membrane surface, relative recovery of CCL2, KC/GRO, and VEGF, after 2 hours of modification increase two to three times and relative recovery of aFGF increased at hour 4. RR of TNF-α did not increase for the 2 hour 4HBA modification. The difference between these two groups of proteins is their isoelectric point's which can indicate an interaction between the charged surface and the overall charge of the protein. By covalent attachment of heparin to the membrane, relative recovery of CCL2 increased two times after hour 2 and VEGF increased for the 24 hour 4HBA modified MD probes and aFGF relative recovery, after a 2 hour 4HBA modification time, increased starting at hour 3.

Microdialysis Sampling

Microdialysis sampling is a diffusion-based separation method that allows analytes to freely diffuse across a semi-permeable dialysis membrane (Figure 1).[3]
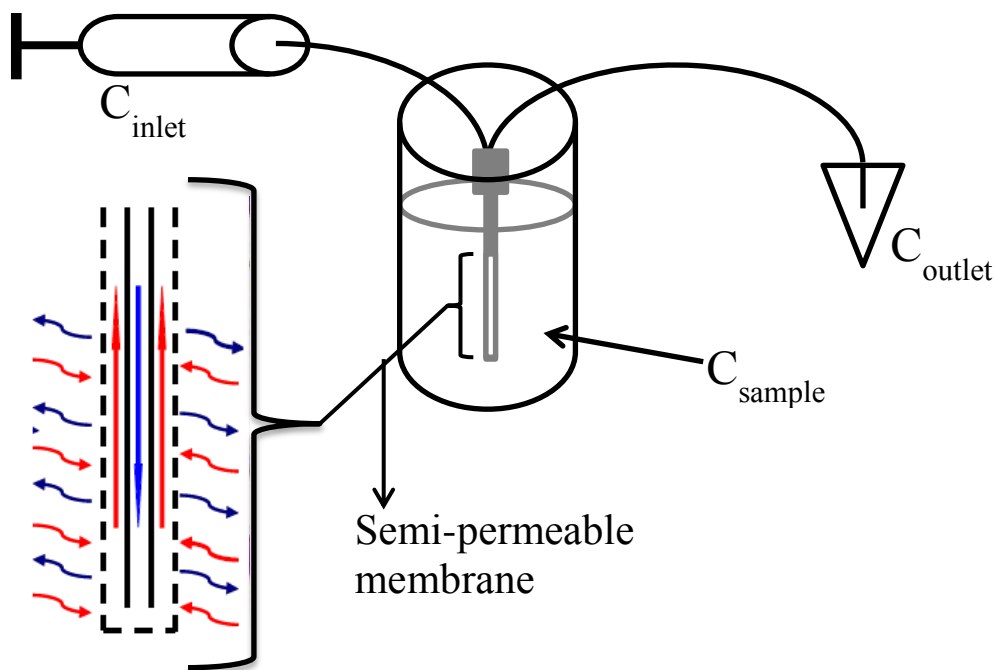
Figure 1. Microdialysis probe and relative recovery experimental design.

Commercially available membranes range in molecular weight cut-off (MWCO) from 6 to 1,000

kDa and are made up of a variety of membrane materials such as polyethersulfone,

polycarbonate, and polyarylethersulphone. Microdialysis sampling of a given analyte is

governed by the mass transport of the molecule from an external medium, through the

membrane, and into the perfusing fluid.[6] Factors such as membrane physical dimensions, device

accessible volume, perfusate flow rate, and analyte diffusion coefficients strongly influence

relative recovery.[6] Microdialysis sampling is an ideal technique to achieve real time monitoring

at the site of probe implantation within living systems.[7] The application of microdialysis is

emerging as an approach for clinical in vivo studies in both healthy and diseased subjects to

recover targeted molecules.[8-11] Microdialysis probes are made with a variety of MWCO's and

membrane chemistry. MWCO is defined as the molecular weight at which 80% of the analyte is

prohibited from membrane diffusion.[12] However, MWCO is typically determined from

equilibrium mass transport, which is not an exact representation of the non-equilibrium setting of microdialysis.[6] One of the parameters commonly measured for microdialysis is relative recovery (RR). This is used to estimate the concentration external to the probe.

$$RR = \frac{C_{outlet} - C_{inlet}}{C_{sample} - C_{inlet}}$$ [1]

As shown in Equation 1, RR is defined by the difference between the concentration of analyte in the dialysate (C_{outlet}) and the concentration of analyte added in the perfusion fluid (C_{inlet}), which is typically zero, divided by the difference between the concentration of the analyte in the sample (C_{sample}), and C_{inlet} multiplied by 100. RR is dependent on many factors such as the perfusion flow rate, membrane surface area, MWCO, and temperature, analyte, and matrix properties of the external media.[10, 13-15] As the flow rate decreases the concentration of analyte in the dialysate increases leading to an increase in relative recovery. Also as the surface area of the membrane increases, relative recovery increases due to the increase of contact between the solution and the membrane surface. An increase in MWCO leads to increased relative recovery however with increasing the MWCO, ultrafiltration leading to fluid loss in the dialysate becomes an issue. There are several techniques used to determine RR for in vivo studies, in vitro microdialysis, no-net flux, ultra-slow or zero flow rate method, internal standard, endogenous reference and retrodialysis.[16] The most commonly used technique is an in vitro recovery experiment, where the probe is placed in a solution containing a known amount of the analyte. The perfusion fluid is perfused through the probe and collected for quantification of the analyte. RR can then be calculated using Equation 1, knowing the external concentration in which the probe is placed and the amount collected in the perfusion fluid.

Challenges to Microdialysis Sampling

Microdialysis is a diffusion-based technique, so RR is highly dependent upon analyte diffusion properties.[7] Since microdialysis is not an equilibrium process due to the continuous flow of the perfusion fluid, RR is generally less than 100%.[7] One of the challenges for microdialysis sampling is that for soluble proteins greater than 10 kDa the RR using 100 kDa MWCO PES membranes ranges between 1 and 5% at flow rates of 0.5 and 1.0 µL/min.[1] Considering that proteins and peptides are large in size, their aqueous diffusion coefficients are small, thus causing mass transport through the probe to be limited resulting in lower recovery.[7, 17] Another challenge for membrane science is the nonspecific adsorption of protein molecules to the membrane surface and tubing; this decreases the effective pore size of the membrane and thus recovery. Due to the low concentration of certain proteins in vivo, low recovery introduces an issue of detection and quantification of these molecules.[7]

Use of Capture Agents in Microdialysis

Capture agents have been covalently attached to membranes previously to reduce nonspecific adsorption, improve biocompatibility, and for removal of specific molecules.[18, 19] The ideal capture agent should have both high binding capacity and a reasonably high permeability.[20] For example, quaternary amine ligands have been used for the removal of mammalian viruses, endotoxins, and DNA for biotechnology manufacturing.[21, 22] Acrylic acid polymer brushes have also been used as a cation-exchange ligand.[23] Also heparin and sulfonated polymers imitating heparin (sulfonated poly(styrene)-*b*-poly(methyl methacrylate)-*b*-poly(styrene) and poly(vinyl pyrrolidone)-*b*-poly(methyl methacrylate)-*b*-poly-(vinyl pyrrolidone), poly (acrylonitrile-co-acrylic acid-co-vinyl pyrrolidone)) have been used to reduce

nonspecific adsorption, improve hemocompatibility, and promote binding of heparin binding proteins.[24-26]

Theory

It has been previously shown that by adding capture agents to the perfusion fluid the diffusive mass transport driving force across the membrane is increased. This has been shown by including antibodies, heparin, and cyclodextrins in the perfusion fluid.[1-4] These molecules increase the diffusive mass transport driving force through the membrane due to the interaction between the analyte and the capture agent in the fluid perfused inside the membrane, as well as prevent nonspecific adsorption to the membrane surface.[4]

To understand the factors that alter a capture agent's ability to improve relative recovery enhancement, a hypothetical protein and affinity agent has been used of which the K_D, k_{on}, and k_{off} can be altered without altering the chemical structure of the protein and the affinity agent. This allows the study of how these parameters alter the binding interaction on the interior of the membrane surface and how these parameters alter relative recovery. It has been reported that the enhancement in relative recovery (RR) when the affinity agent is added in the perfusion fluid is due to the additive effect of the concentration of analyte (A) bound as shown in equation 2.[5]

$$RR = \frac{[A]_{bound} + [A]_{free}}{[A]_{external}} * 100 \qquad [2]$$

This is due to the analyte affinity agent complex being collected in the perfusion fluid and also the decrease in the concentration gradient which increases the analytes flux across the membrane.

The amount of A_{bound} in Equation 2 is a function of K_D at equilibrium. As the K_D value decreases the amount of analyte needed to saturate the total number of binding sites decreases as

well. This can be seen by the following chemical reaction, where the binding constant is defined

by Equation 3.

$A + B \leftrightarrows AB$
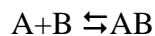
$$K_D = \frac{[A]_{free}[B]_{free}}{[AB]}$$ [3]

As the K_D value decreases the ratio between the concentrations of analyte free in solution

compared to the analyte bound ([AB]) decreases. At a set concentration of B the binding sites

become saturated at a lower concentration at a lower K_D value.

Although microdialysis is a non-equilibrium process due to the continuous flow of the

perfusion fluid, to achieve maximal relative recovery enhancement under typical low

concentration and low flux conditions for a protein the desired affinity agent should have a high

binding affinity and have a low K_D value. One of the challenges with looking only at K_D values

is that these values give no information about the rate at which equilibrium is reached. This

information is given by the k_{on} and k_{off} values. These values can be changed in such a way that

does not alter the K_D values as shown in Table 1, since the K_D value is equal to the k_{off}/k_{on}.

Table 1. On and Off Rates at a Constant K_D Value.

Condition	A	B	C	D
k_{on} (M^{-1}s^{-1})	1×10^6	1×10^5	1×10^4	1×10^3
k_{off} (s^{-1})	1×10^{-2}	1×10^{-3}	1×10^{-4}	1×10^{-5}
K_D (M)	1×10^{-9}	1×10^{-9}	1×10^{-9}	1×10^{-9}

Under condition A the k_{on} and k_{off} are larger than at condition D, but with looking at only

the K_D values these two conditions would appear identical. By looking at these conditions as a

function of time, the point at which equilibrium is reached is different. This can be shown using

Equation 4 and Equation 5 for association and dissociation rate.[6] When the analyte that is

binding is continually added, the association rate dominates the net rate in Equation 6, which are

the conditions that are occurring when performing microdialysis sampling in vitro.[6-8]

Association: $\frac{d[AB]}{dt} = k_{on}[A]_{free}[B]_{free}$ [4]

Dissociation: $\frac{-d[AB]}{dt} = k_D[AB]$ [5]

Net Rate $= \frac{d[AB]}{dt} = k_{on}[A]_{free}[B]_{free} - k_{off}[AB]$ [6]

When combining the kinetic information with the continual flux of analyte occurring

across the microdialysis probe equation 7 is formed.[7] This relates the change in concentration of

the analyte free in solution as a function of time at a set area of the microdialysis probe, where *J*

is equal to the flux (M/s), $[A]_o$ and $[B]_o$ are the concentration of A and B free in solution, and

[AB] is the concentration of analyte bound to the affinity agent. Although Equation 4 and 5 are

in relation to the change in concentration of analyte bound these can be used to form Equation 7

because the total amount of analyte A in solution is equal to the amount of analyte A transported

across the membrane surface minus the amount bound due to the affinity interaction plus the

amount released due to the dissociation of the analyte-affinity agent complex. This equation

shows how the concentration gradient is altered by the addition of an affinity interaction on the

membrane surface.

$\frac{d[A]_o}{dt} = J - k_{on}[A]_o[B]_o + k_{off}[AB]$ [7]

As can be seen in Equation 7 the affinity interaction in relation to k_{on} is subtracted from the flux

term when looking at the free concentration of analyte, A, as a function of time. As the affinity

interaction becomes a more dominant term due to a high k_{on} value the amount of free analyte in

solution approaches zero steepening the concentration gradient across the membrane surface

which leads to an increase in mass transport across the membrane. The release of the bound

protein in terms of k_{off} is added because the dissociation of the analyte-affinity interaction leads

to an increase in the concentration of the analyte in solution. This increase in concentration does

not affect the concentration gradient because it is carried away convectively due to the flow of

the perfusion fluid. From this equation the optimal kinetic parameters can be estimated to

determine at which k_{on} and k_{off} values the decrease in concentration of free analyte in solution is

maximized. This leads to an increase in the concentration gradient which alters the flux as

shown by Fick's second law (Equation 8), where J is the flux, D_{eff} is the effective diffusion

coefficient, l is the length, H is the partition coefficient and c is the concentration.[7]

$$J = \left[\frac{D_{eff}H}{l}\right](C_{10} - C_{1l}) \tag{8}$$

By changing the concentration gradient (C_{10}-C_{1l}) by lower the concentration of C_{1l} due to

addition of a capture agent the flux across the membrane is increased due to the binding of the

analyte dominating the rate equation, shown in Equation 7.[6, 9]

     For VEGF with a molecular weight of 15.5 kDa, a 2.5% relative recovery (from page

137), and a starting concentration outside the probe of 3,366 pg/mL the calculated flux (J) is

1.51×10^{-15} M/s. Assuming a total concentration of heparin 0.1 μM used in heparin affinity

microdiaysis[10], the change in concentration as a function of time can be determined. Based on

the slope of that line at a set K_D value of 100 nM and varying the k_{on} and k_{off} rates the change in

free analyte (A) over time can be plotted as shown in Figure 2.
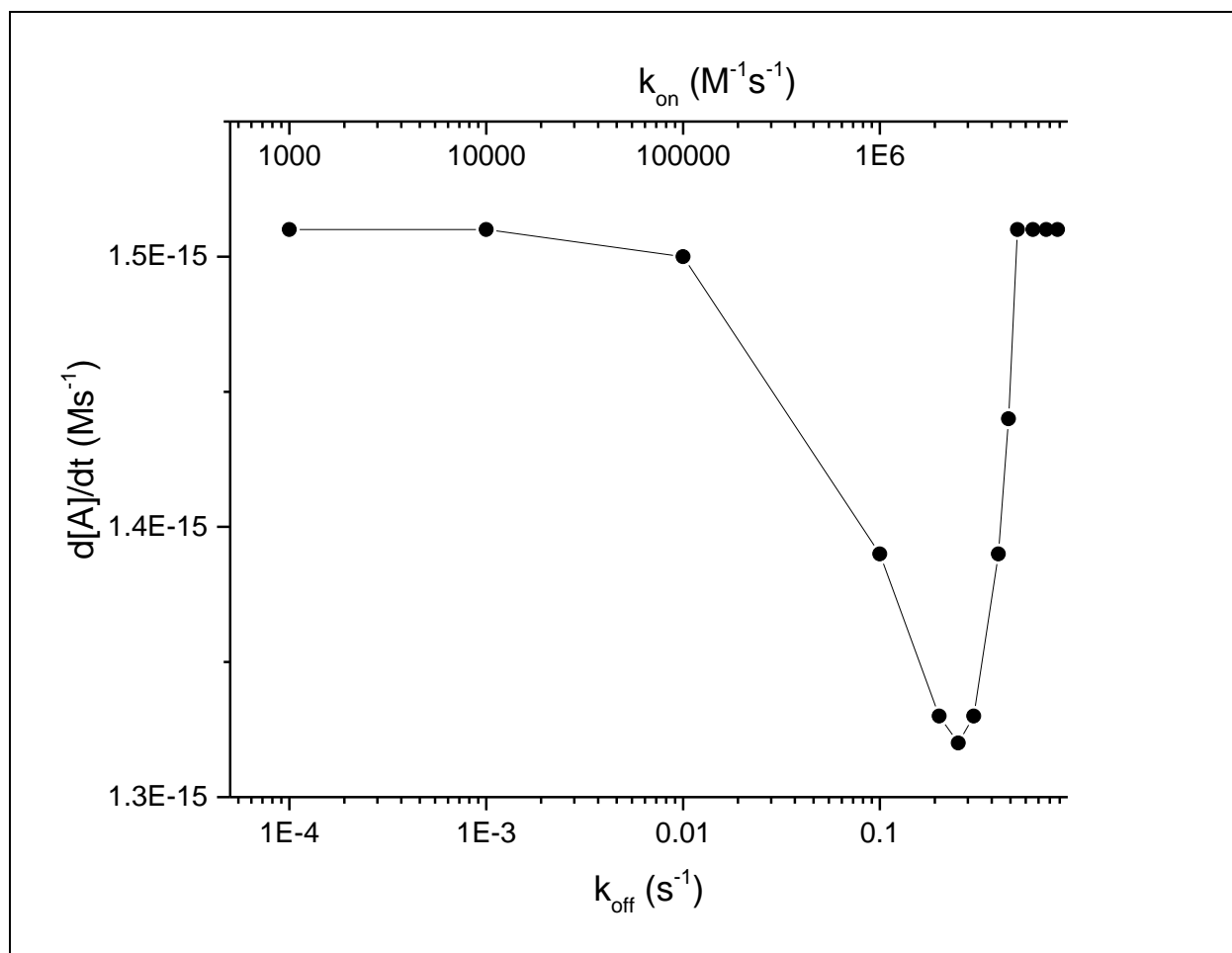
Figure 2. Change in concentration of A as a function of time related to the k_{off} (s^{-1}) and k_{on} ($M^{-1}s^{-1}$) at a set K_D value of 100 nM.

As can be observed from Figure 2 the approximate maximal drop in the free analyte concentration occurs approximately at a k_{on} of 2.5 $x10^6$ $M^{-1}s^{-1}$ and k_{off} of 0.25 s^{-1} with a K_D of 100 nM. This leads to maximal [AB] formation which is desired because this leads to the steepening in the concentration gradient which increases flux across the membrane At low k_{off} values the amount of analyte free in solution is greater due to correspondingly lower k_{on} value and at the higher koff values and correspondingly higher k_{on} values the amount of analyte free in solution calculated exceeds the amount of analyte transported across the membrane so the concentration is equal to the flux of analyte across the membrane. Although these are the

9

predicted ideal conditions, typically an affinity interaction has either a fast k_{on} ($\geq 1 \times 10^6$ $M^{-1}s^{-1}$) and a slow k_{off} ($\geq 1 \times 10^{-3}$ s^{-1}) and a high K_D (nM) value or a slow k_{on} ($\leq 1 \times 10^6$ $M^{-1}s^{-1}$) and a fast k_{off} ($\leq 1 \times 10^{-3}$ s^{-1}) and a lower K_D (μM) value. For example, CCL2 has a reported k_{on} of 9.97×10^3 $M^{-1}s^{-1}$ and a k_{off} of 1.39×10^{-2} s^{-1} and cam-related/down-regulated by oncogenes (Domain Fn2) (Drosophilia) has a reported k_{on} of 1.58×10^5 $M^{-1}s^{-1}$ and a k_{off} of 2.43×10^{-1} s^{-1}, which have reported fast k_{off} but slow k_{on} rates and μM K_D values.[11, 12] Also, hepatocyte growth factor has a reported k_{on} of 1.0×10^6 $M^{-1}s^{-1}$ and a k_{off} of 1.0×10^{-3} s^{-1} and kininogen-1 has a reported k_{on} of 1.27×10^6 $M^{-1}s^{-1}$ and a k_{off} of 4.03×10^{-4} s^{-1} which have reported fast k_{on} and slow k_{off} rates and nM K_D values.[13, 14] Two proteins which approach the ideal conditions calculated above are fibroblast growth factor 2 and stromal cell-derived factor 1 with k_{on} rates of 1.10×10^7 $M^{-1}s^{-1}$, and 2.16×10^6 $M^{-1}s^{-1}$ and k_{off} rates of 4.30×10^{-1} s^{-1} and 8.30×10^{-2} s^{-1} with K_D values of 3.90×10^{-8}, and 3.84×10^{-8}.[15, 16]

Antibodies

The use of antibodies as capture agents included in the perfusion fluid has been shown to increase recovery three to twenty times.[17] One of the downfalls to using antibodies is that they are specific to only one analyte. To resolve this issue, the use of antibody-immobilized microspheres used in flow cytometry applications were added to the perfusion fluid.[17] This allowed for multiple types of antibody-immobilized microspheres to be used, allowing for the quantification of multiple analytes and provided a platform for quantification of the analyte.[17] This method for enhanced recovery provided one disadvantage in the quantification step. If the analyte concentration was high the microspheres became saturated and thus outside of the calibration range of the assay meaning that the sample data was lost.[17]

<u>Heparin</u>

Another method used to capture multiple analytes is heparin. Heparin is part of a family of polysaccharides called glycosaminoglycans (GAG). GAG's are a component of the tissue extracellular matrix. In many cases, the binding of proteins to sulfated glycoconjugates, such as heparin, have ionic character and depend on the interaction of specific positively charged residues.[18] Yet when purifying a heparin sulfate(HS)-GAG-binding protein, the protein's interaction with a heparin-sepharose column is distinctly different from that of a cation exchange column of similar properties.[19] Heparin on average is comprised of approximately 25 disaccharide repeating units and has an average molecular weight of approximately 16 kDa.[20] Heparin contains $\alpha 1-4$ linked disaccharide repeat units consisting of sulfated uronic acid and glucosamine residues, resulting in a negatively charged polydisperse linear polysaccharide.[17] Its major repeating disaccharide unit is trisulfated iduronic acid and glucosamine, but also glucuronic acid, and N-acetyl glucosamine.[20] It is postulated that the conformational flexibility of the iduronate residue was central to the specific binding of HS-GAG oligosaccharides to a given protein.[19] Heparin is commonly used as an anticoagulant, and is typically isolated from mast cell or mucosa.[19] Heparin, has binding affinity to various growth factors such as acidic fibroblast growth factor (aFGF), vascular endothelial growth factor (VEGF), heparin-binding epidermal growth factor, and transforming growth factor-β (TGF-β).[21] Heparin is also known to bind to interleukin 8 (IL-8), chemokine ligand 2 (CCL2), macrophage inflammatory protein 1(MIP-1), regulated and normal T cell expressed and secreted (RANTES) and tumor necrosis factor α (TNF-α) with nM affinity.[22-25] Heparin is also known to bind thrombosponin at the Trp-Ser-Glu-Trp sequence present in the first type I repeat of thrombospondin. This sequence is widely distributed in the cytokine receptor superfamily (IL3, IL4, IL6, IL7).[18] Heparin-like

materials have been shown to exhibit good blood compatibility like heparin molecules by reducing clotting time and platelet adhesion.[26-30] Using heparin-immobilized microspheres as an additive in the perfusion fluid in microdialysis was shown to increase RR two to five fold for aFGF, VEGF, CCL2, and CCL5 (chemokine ligand 5).[31]

These methods allow for increased recovery for multiple analytes. Considering that cytokines are part of large signaling networks, the measurement of multiple cytokines rather than just one single cytokine can provide more relevant biomedical data.[17]

Covalent Attachment of Capture Agents to the Membrane Surface to Increase Transport

Considering that the use of capture agents in the perfusion fluid is shown to increase RR the question must be asked if RR could be increased by covalently attaching the capture agent to the inside of the membrane. By covalently attaching the capture agent to the membrane nonspecific adsorption can be reduced by adding a charged capture agent to the surface, as well as adding a reversible binding event to the membrane surface. With PES membrane surfaces proteins can irreversibly bind to the surface leading to membrane fouling.[32-34] By reducing irreversible binding of proteins to the surface this leads to an increase in collection of the analyte due to the reduction in fouling.[32-34] The difference between irreversible binding and reversible binding is that reversible binding can be easily removed as compared to irreversible binding.[32, 35] By adding the affinity agent to the surface this add reversible binding sites and also blocks binding sites that would lead to irreversible binding on the membrane surface. Initially what would be observed, if the fouling occurring on the membrane surface was the same with and without the modification, is a decrease in the concentration of the analyte due to the binding of the analyte dominating the rate equation shown in Equation 7 and Figure 2.[6, 9]

In Equation 7 for an immobilized affinity agent, J is equal to the flux (mol/cm^2 s), $[A]_o$ is the concentration of A free in solution (mol/cm^3), B_o is the moles of unbound affinity agent per cm^2, and AB is the moles of analyte bound to the affinity agent per cm^2. The k_{on} and k_{off} rates are in terms of (mol/cm^3)$^{-1}$s^{-1} and s^{-1} respectively.

For VEGF with a molecular weight of 15.5 kDa, a 2.5% relative recovery (from page 137), and a starting concentration outside the probe of 3,366 pg/mL the calculated flux (J) is 2.26×10^{-20} mol/cm^2 s. Assuming a total amount of heparin to be 20 nmol/cm^2, calculated from a reported value of 0.3 mg/cm^2 heparin bound to a polysulfone flat sheet[27], the change in amount of analyte A in moles as a function of time can be determined with various K_D, k_{on}, and k_{off} values as shown in Table 2, where J_o is the initial flux calculated above (2.26×10^{-20} mol/cm^2 s, and J_i is the flux calculated with addition of the affinity interaction.

Table 2. Change in analyte flux as a function of K_D, k_{on}, and k_{off} values.

K_D (mol/cm^3)	k_{on} (mol/cm^3)$^{-1}$s^{-1}	k_{off} (s^{-1})	Ji (mol cm^{-2}s^{-1})	J_0-J_i (mol cm^{-2}s^{-1})
1 mM	100	0.1	2.26×10^{-20}	0
100 μM	1,000	0.1	2.26×10^{-20}	0
10 μM	10,000	0.1	2.26×10^{-20}	0
1 μM	100,000	0.1	2.26×10^{-20}	0
100 nM	1,000,000	0.1	2.22×10^{-20}	4.0×10^{-22}
100 nM	100,000	0.01	2.25×10^{-20}	1.0×10^{-22}
10 nM	10,000,000	0.1	1.94×10^{-20}	3.2×10^{-22}
10 nM	1,000,000	0.01	2.22×10^{-20}	4.0×10^{-22}
10 nM	100,000	0.001	2.26×10^{-20}	0
10 nM	10,000	0.0001	2.26×10^{-20}	0

As shown in Table 2, with K_D values in the mM to µM range the flux of the analyte is not altered by the addition of the affinity interaction. Also with slower k_{off} values (≤ 0.001 s^{-1}) the flux of the analyte is not altered even with nM affinity. The decrease in flux of the analyte occurs for interactions with K_D values in the nM range with k_{off} rates of 0.01 to 0.1 s^{-1} and corresponding k_{on} rates of 1×10^7 to 1×10^5 (mol/cm^3)$^{-1}$s^{-1}. This phenomenon occurs before the saturation of the binding sites on the surface occurs. This leads to an increase in the concentration gradient which alters the flux as shown by Fick's second law shown in Equation 8. By changing the concentration gradient (C_{10}-C_{11}) by lower the concentration of C_{11} due to addition of a capture agent the flux across the membrane is increased due to the binding of the analyte dominating the rate equation shown in Equation 7.[6, 9] Using the concentration values calculated even at the maximum decrease concentration over time, the change in the flux would only be altered by 1.77%. This would not lead to a significant enhancement in the RR which explains why initially before the binding sites become saturated that the RR is not altered for heparin binding proteins (CCL2, aFGF, and VEGF).

Once the binding sites are saturated, the rate of binding and releasing of the analyte are equal so the net rate in Equation 6 is zero. When the net rate is zero, the relative recovery is not altered by the attachment of the affinity agent. What is interesting is that for analytes that have affinity for heparin (aFGF, and CCL2) the relative recovery increased at later collection times (hours 3, and 4) this could indicate that by adding reversible binding sites and the reduction in irreversible binding sites, that the reduction in irreversible binding sites initially offsets the loss due to binding at the surface at the earlier time points and is increasing the relative recovery at the later time points due to saturation of the heparin binding sites. This would also explain why the relative recovery of KC/GRO, an analyte that is not known to bind to heparin, increased for

all collections times because the initial phase described above where association is the dominate term in the rate equation, is not occurring.

Reducing Nonspecific Adsorption

Significance of the Nonspecific Adsorption Problem

Nonspecific adsorption is a combination of interactions that occur between two molecules, which are driven by electrostatic, Van der Waals and other forces; however, the main contributor to nonspecific adsorption is hydrophobic interactions.[61] Nonspecific adsorption in implantable devices used to measure the surrounding area can lead to reduced recovery, fouling of the device, and inaccurate measurements.[62-64] Membrane fouling is the term used to describe the undesirable deposition of retained particles, colloids, macromolecules, salt etc. at the membrane surface or inside the pores.[65] Fouling of membrane devices occurs through two mechanisms of action; the reduction of transmembrane pressure due to concentration polarization, and the buildup of material on the surface.[66] Concentration polarization leads to an accumulation of molecules in the mass transfer boundary layer adjacent to the membrane surface.[66] This accumulation of dissolved molecules on the surface can lead to reduced solvent activity and thus reduced solvent flow through the membrane.[66] In microdialysis experiments performed in vitro, the solution containing the analyte is typically stirred, which leads to a decrease in concentration polarization due to the increase in convection at the membrane surface.

Importance on Nonspecific Adsorption in Microdialysis

Another challenge for microdialysis is the nonspecific adsorption of protein molecules to the dialysis membrane and tubing, this decreases the effective pore size of the membrane and thus recovery.   PES, a commonly used as a membrane material in microdialysis is hydrophobic, which enhances interactions with many foulants.[67] PES membranes also have a high binding

affinity for proteins and microorganisms.[67] In kidney dialysis PES membranes can invoke severe

blood reactions due to adsorption and transformation of plasma proteins, activation of blood

cells, adherence of platelets and thrombosis which leads to an increased rate of mortality and

morbidity for hemodialysis patients.[68] BSA, fibrinogen and other major proteins are known to

adsorb onto implanted biomaterials including microdialysis probes.[69] Since calibration of the

microdialysis device is in terms of RR the recovery may be altered during or after protein

deposition, leading to an increase in the error in concentration determined based off of the RR.[69]

Theory of Nonspecific Adsorption

Fouling through the buildup of materials on the surface can occur through four modes of

action: adsorption, pore blockage, deposition, and gel formation.[66] Adsorption occurs when

specific interactions occur between the membrane and the solute that creates a monolayer on the

surface leading to additional hydraulic resistance.[66] If the degree of adsorption is concentration

dependent then the increase in concentration polarization will increase the adsorption.[66] Pore

blockage can also occur, leading to a reduction in the flux due to the blocked pore.[66] There are

four main mechanisms for pore blocking: complete pore blocking, internal pore blocking, partial

pore blocking, and cake filtration as shown in Figure 3.[66] Deposition or cake resistance occurs

when deposited particles on the surface can grow layer by layer leading to increased hydraulic

resistance.[66] Gel formation can also occur in the immediate vicinity of the membrane surface

depending on the level of concentration polarization.[66] Fouling of the membrane can lead to

reduction or even loss of recovery of desired analytes.
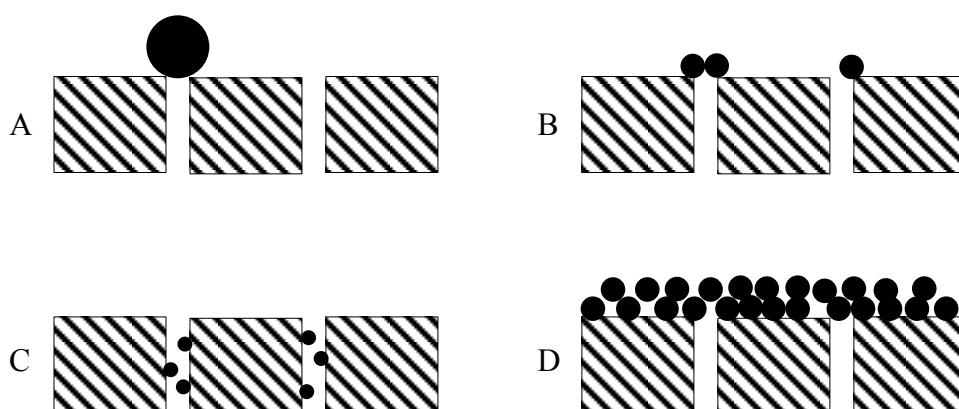
Figure 3. Mechanisms of fouling, (A) complete pore blockage, (B) partial pore blockage, (C) internal pore blockage, (D) cake filtration.

Design of Nonfouling Surfaces

Highly hydrated chemical groups with optimized physical properties of the surface are key to developing effective and stable nonfouling materials for long-term biomedical applications.[70] Polymers grafted to a hydrophobic surface can reduce protein adsorption simply because the polymer blocked protein adsorption sites.[70] Therefore, the blocking agents should have groups which are excellent in preventing nonspecific adsorption such as hydroxyl or poly(ethylene oxide) groups.[71] The adsorption and desorption of solutes on membranes will depend on many factors such as solution chemistry (pH, ionic strength), physiochemical properties, operating conditions, and solution additives.[71, 72] Specific surface functionalities and not the average degree of hydrophobicity or hydrophilicity determine adsorption behavior.[73] A general observation is that proteins adsorb weakly to neutral hydrophilic surfaces, are attracted or repelled by charged surfaces, and adsorb strongly to hydrophobic surfaces.[73] The adsorption process can be affected by the protein structure, protein stability, concentration, pH, and ionic strength.[74] The ionic strength of typical perfusion fluids used in microdialysis for Ringer's solution (154 mM NaCl, 5.4 mM KCl, 2.3 mM $CaCl_2$) is 158 mM and phosphate buffered saline (PBS) (137 mM NaCl, 10 mM Phosphate, 2.7 mM KCl) is 167.2 mM. These researchers were

17

able to observe lysozyme adsorption at ionic strengths up to 100 mM.[75] The adsorption of amino acids found in proteins is influenced considerably by moieties presented in the α-position in their structures. Hydrophilic moieties (carboxyl/amide) groups decrease amino acid adsorption on bare silica substrates, and hydrophobic phenyl moieties increase adsorption.[73]

It is hypothesized that the nonfouling ability of both polyhydrophilic and polyzwitterionic materials are tightly correlated with a hydration layer near the surface. A tightly bound water layer forms a physical and energetic barrier to prevent protein adsorption on the surface meaning that the energy required to displace the water is greater than the energy gained by the protein binding to the surface. Expulsion of water from the surface is the first step in order for protein adsorption to occur and if the surface is more hydrophilic then the water is held more tightly.[70] When a protein approaches the surface, the compression of the polymer chains causes steric repulsion to resist protein adsorption due to an unfavorable decrease in entropy.[70] Bulk water is structured because of hydrogen bonding between the water molecules.[65] For hydrophobic surfaces the orientation of water molecules in contact with a hydrophobic molecule is entropically unfavorable.[65] As a result the entropically unfavorable water molecules are expelled into the bulk and the total free energy of the system is reduced leading ultimately to protein adsorption.[65] These hydrophobic interactions can occur up to 80 nm away.[65]

Reduction in Nonspecific Adsorption in Microdialysis Sampling

In microdialysis sampling, perfusion fluid additives and modifications to the membrane have been made to reduce nonspecific adsorption. Many modifications to the perfusion fluid have been made to increase RR by reducing nonspecific adsorption. The addition of Poloxamer 407 is one method that has been used is to modify the membrane surface.[76] Poloxamer 407 is an nonionic surfactant with a structure containing hydrophilic polyethylene glycol (PEG) regions

and hydrophobic polypropylene glycol regions.[76] These hydrophobic regions adsorbed onto the surface exposing the hydrophilic PEG regions, reducing nonspecific adsorption by 33%.[76] Albumins have also been used as a perfusion fluid additive in order to coat the tubing and the membrane surface to reduce nonspecific adsorption leading to an increase in RR. Polysorbate 80 was also shown to reduce nonspecific adsorption of docetaxel to the polyurethane inlet tubing.[77] Other perfusion fluid additives include CHAPS, β-cyclodextrin, glucose, and dextran.[78]

Methods to Reduce Nonspecific Adsorption

Methods to reduce nonspecific adsorption focus on one of two approaches: creating a surface that repels protein adsorption or a chemical interaction that reduces nonspecific adsorption but for both strategies surface hydration is key to reducing nonspecific adsorption.[79] One common factor of non-fouling surfaces is their resistance to the release of bound water molecules from the surface. Water that is tightly bound to the polymer surface leads to a separation between the proteins in solution and the polymer.[79] One of the challenges with using hydrophilic polymers is their mechanical, thermal and chemical stability.[61] It has been shown that increasing the hydrophilicity of polymers significantly reduced protein adsorption and fouling as protein-polymer interactions are reduced.[61] Many methods have been used to repel protein adsorption by changing the properties of the surface. Some methods take the approach of increasing the hydration of the surface, these include: zwitterionic hydrogels, PEG and oligoethylene glycol (OEG). Other methods use blocking agents to block sites of nonspecific adsorption from analytes of interest. There are two main types of surface modifications: chemical and physical modifications.[61] Examples of physical modifications include exposure to flame, plasma radiation, and ion beams, and chemical modification include chemical reactions.[61]

Hydrophilic Polymers

Hydrophilic surface modifications to hydrophobic membranes can reduce the hydrophobic interaction between the protein and the polymeric membrane surface.[61] It has also been shown that polymers incorporating hydrophilic groups also showed good blood compatibility.[24] A nitrogen based plasma system has been used to modify PES membranes making the surface more hydrophilic leading to an increase in water flux and reduced protein fouling.[80] Many other types of materials have been used to increase the hydrophilicity of the surface by hydrogen bonding, including, tetraglyme[81], dextran[82], mannitol[83], polyamines functionalized with acetyl chloride[84], PEG-mimetic peptoids[85], and natural and synthetic peptides.[86, 87]

Other Covalent Modifications to Reduce Nonspecific Adsorption

Another approach is to use adsorbed protein films. These have been shown to be reasonable non-fouling surfaces for proteins in solution because proteins typically adsorb in monolayers. This is caused by the retention of hydration water by adsorbed protein molecules, preventing close interactions with the proteins in solution.[79]

Many different covalent modifications have been made to membranes in order to reduce nonspecific adsorption. Photo-induced graft polymerization has been used to covalently attach a phospholipid analog and was shown to reduce platelet adhesion to the membrane.[48] Photografting has also been used to attach acrylic acid which is negatively charged over a wide range of pH and was shown to reduce organic fouling and biofouling.[88]

Enzymatic Modification of Membrane Surfaces

Enzymes have also been used to facilitate the modification of membrane surfaces. The ideal enzyme to use for modification of membrane surfaces should have low cost of production,

inexpensive co-factors and substrates, be stable under reaction conditions, ability to exert its catalytic activity at high reaction rates under desired reaction conditions, and broad substrate specificity.[89] One of the enzymes used to modify membrane surfaces is laccase. Laccase is an enzyme that produces free radicals from phenolic acids using oxygen from air as an oxidant and producing water as the only by-product.[67] It is known to produce either a network or brush like structure depending on the substrate and reaction conditions used.[67]

Laccase

Laccases are copper containing polyphenol oxidases that oxidize polyphenols, methoxy-substituted phenols, and diamines, and using molecular oxygen as an electron acceptor.[90] Laccases induce the oxidation of C-O, C-C bonds, oxidative dimerization alicyclic esters, hydroxystilbenes, and the combination of oxidation followed by Diels-Alder reaction.[90] Laccases are more stable at or near neutral pH, and below room temperature but have a range of stability between pH 5-8 and up to 30°C.[89] Thermal inactivation is the main cause of denaturation, refolding can occur but is slow (3-12 hours) compared to 5-60 minutes for pH denaturation.[89] Laccase *Trametes versicolor* has the highest redox potential among laccases (785 mV vs standard hydrogen electrode) which is correlated with high activity.[89] Laccase is a monomer, organized in three sequentially arranged domains and has dimensions of about 65 x 55 x 45 $Å^3$.[91] Laccase in nature is involved in the wound response and the synthesis of lignin.[91]

Laccase contains a T1 (type-1) copper and a T2, T3 copper trinuclear cluster. The T1 copper is the primary oxidation site, and the T2/T3 copper cluster being the site at which the reduction of molecular oxygen takes place.[91] The enzyme catalyzes the one-electron oxidation of four reducing-substrate molecules followed by the four-electron reduction of molecular oxygen to water.[91] Then the reduction of molecular oxygen is accompanied by a one-electron

21

oxidation of reducing substrates.[91] This catalytic reaction starts with the abstraction of electrons from the substrate by the T1 copper and subsequent reduction of the T1 Cu^{2+} to T1 Cu^+, followed by the internal electron transfer from T1 to the T2/T3 copper cluster, and finally the binding and subsequent reduction of an oxygen molecule to divalent oxygen at the T2/T3 copper cluster.[89] The substrate binds in a small negatively charged cavity near the copper T1 site. The negative charges located at this site may have functional significance since they could stabilize the radical cation products that are formed during the catalytic cycle.[91] The oxygen-reducing site at the T2/T3 cluster has access to solvent through two channels, which lead to the T2 copper and T3 copper sites.[91] In between the two T3 coppers, there is an oxygen ligand, either a OH^- or O^{-2} molecule, that coordinates with the type-2 Cu and type-3 Cu.[91] The reoxidation of the coppers occurs at a rate of $5 \times 10^6 \, M^{-1} sec^{-1}$.[91] The overall outcome of the catalytic cycle is the reduction of one molecule of oxygen to two molecules of water and the concomitant oxidation of 4 substrate molecules to produce 4 radicals.[91]

The use of laccase to generate phenolic acid polymers and to attach phenolic compounds to the surface of PES has been shown to reduce nonspecific adsorption and as shown in this dissertation that it can be used to add functional groups onto the surface to covalently attach other molecules. This is due to two reaction types that occur, the grafting reaction of monomer onto the membrane surface and reaction of the monomers to form homopolymer in solution.[92] Laccase from *Trametes villosa* has also been reacted with 4-hydroxybenzoic acid (4HBA) to form a polymer with a number average molecular weight (M_n) of 8,500 Da for the 4 hour reaction and 8,400 Da for the 24 hour reaction with a polydispersity index (PDI) of 2.06 and 2.12 for the 4 and 24 hour reaction times respectively.[93] 4-hydroxybenzoic acid (4HBA) has been shown to be added to a PES surface using laccase *trametes versicolor* from with coverage in the

range of hundreds of mg/m^2 which is on average more than a monolayer.[94] This modification has also been shown to reduce BSA adsorption on PES flat sheet membranes and the average flux of the base membrane was never reduced more than 20% by the addition of the polymer.[92, 94] The reasons for these researchers choosing 4HBA is that it will add ionic and hydrogen bond-forming properties to the PES membranes as well as there is only one hydroxyl group which leads to growth of the chains mostly in one direction.[92] At pH 4 the grafting yield after 2 hour modification was 4 µg/cm^2, at pH 5 it is 11.7 µg/cm^2 and at pH 6 12.7 µg/cm^2.[92] This is attributed to the ionization of 4HBA at higher pH, which leads to a lower oxidation potential, and thus higher reaction rate and grafting yield.[92] The adsorbed amount of BSA decreases with increasing grafting yield and is close to 0 after 8 hours of modification at 28.8 mM 4HBA.[92] *Pycnoporus coccineus* and *Myceliophthore* laccases have also been used to graft 4HBA to poly(phenylene oxide)s.[95] To further study the laccase catalyzed reaction these researchers studied consumption of oxygen when laccase was in the presence of 1-naphthol using a Clark-type polarographic oxygen electrode and were able to determine K_M and V_{max} for the reaction.[96] These were determined based on the knowledge that the initial consumption rate of dissolved oxygen is equal to one-fourth the consumption rate of 1-naphthol due to the 1 to 4 stoichiometric ratio in the polymerization reaction.[96]

Characterization of Polymer Surfaces

Many techniques are used to characterize polymer surfaces. These include techniques to study how the physical properties of the surface are changed, how the surface is changed chemically, and how molecules interact with the surface. Commonly studied physical properties are hydrophobicity, thermal properties, and morphology. Techniques commonly used to study the chemical properties of a surface are attenuated total reflectance Fourier transform infrared

spectroscopy (ATR-FTIR), x-ray photoelectron spectroscopy (XPS), and matrix assisted laser desorption ionization spectroscopy (MALDI). Absorption of molecules onto the surface is also commonly measured using protein adsorption.

Techniques used to Study the Chemical Properties of a Polymer

ATR-FTIR

ATR-FTIR is a powerful technique that uses infrared spectroscopy to study the chemical functionalities at the surface. This technique allows for the investigation of solids and liquids without further sample preparation due to the phenomenon of total internal reflectance. This generates an evanescent wave due to the repeated reflection of the infrared radiation interacting on an optical crystal of high refractive index.[97] This technique has been used to identify functional groups present on surfaces, to confirm modifications made, and to study the buildup of foulants on a surface.[97] ATR-FTIR was used to confirm the synthesis of PES hollow fiber membranes.[98] Many researchers have also used ATR-FTIR to confirm a modification.[52, 73, 88, 90, 99-104] Some researchers have also used ATR-FTIR to study the buildup and removal of foulants on the surface.[87, 105]

XPS

XPS is an analytical technique used to characterize different chemical forms of elements within the top 10 nm of a surface.[106] Depth profiling can be performed using C_{60} or Ar as well as co-sputtering with both C_{60} and Ar.[107] Analysis of a sample is typically performed by first performing a survey scan which is a low resolution scan used to identify the elements present in the sample. After the survey scan, high resolution scans are performed for the specific elements present in the sample. From these high resolution scans the different functional groups can be seen as different peaks. Using peak fitting software, the area and intensity of these peaks can be

24

determined at specific binding energies. With this information and the known response factors

for each element, the different percentages of each functional group can be calculated. This

calculation is performed by taking the area multiplied by the response factor divided by the total

of the area time response factor for all peaks. This value is then multiplied by 100 to convert to a

percentage. These percentages can then be compared. XPS has been used to monitor the

addition of coupling agents needed to induce the bond formation between a fiber and a polymer

matrix.[108] XPS has been used to analyze modifications to membranes.[24, 61, 90, 109, 110] By using

XPS the characteristic types of atoms and bonds for the capture agent and 4HBA will be an

indication of successful coupling.

Analysis of Polymer Samples to Determine Molecular Weight Information

Polymers formed in a polymerization reaction are by nature complex due to the

distribution of molecular weights present. One way to characterize these distributions is to

calculate the number average molecular weight (9), and weight average molecular weight (10)

which then in turn can be used to calculate the polydispersity (11),

$$Number\ average\ molecular\ weight = \frac{\Sigma N_x M_x}{\Sigma N_x} \tag{9}$$

$$Weight\ average\ Molecular\ weight = \frac{\Sigma C_x M_x}{\Sigma C_x} \tag{10}$$

$$Polydispersity = \frac{Weight\ Average\ Molecular\ Weight}{Number\ Average\ Molecular\ Weight} \tag{11}$$

where N_x is the number of molecules of M_x size, M_x is molecular weight, and $C_x = N_x M_x$. To

calculate these values two techniques are typically used, mass spectrometry, and size exclusion

chromatography.

Size exclusion chromatography (SEC) is a technique that separates molecules based on

their size (hydrodynamic volume) at a set solvent strength and typically a pure solvent.[111] The

hydrodynamic volume depends on a variety of factors, including interactions between solvent

and polymer molecules, chain branching, restricted rotation caused by resonance, and conformational effects arising from the polarity, and steric bulkiness of the substituent groups.[112] Unless a molar mass sensitive detector is used SEC requires calibration using standards of known molar mass distribution. These standards are typically polyethylene, PEG or polystyrene. In order to perform this technique, the standards need to mimic the physiochemical properties of the sample. From these standards a calibration curve is formed from the relationship between the log of molecular weight at peak max and the retention time.[113] A commonly used detector for SEC is a light scattering detector which is widely used for obtaining weight average molecular weights between 10-10,000 kDa.[112] A challenge for SEC is that highly branched samples have abnormal SEC elution behavior this is due to large molecules spending too much time diffusing in and out of the column packing creating an Argentinean bolas effect (entanglement of a part of the macromolecule in the column packing) and sieving in the voids between packing spheres.[114] One way to help with this problem is to use multiple separations for branched polymers.[114] An example of using multiple separations is to perform SEC/MALDI where the sample is fractionated into individual fraction that have a polydispersity index (PDI) <1.07, and then analyzed using MALDI-TOF.[115] Also the information obtained from the MALDI-MS can be used to create a calibration curve for SEC making the calibration more accurate.[111] An added advantage to using this technique is that structural data about monomers, repeating units and end groups are also provided by SEC/MALDI.[115]

For polymers with molecular weights less than 50,000 Da, end group analysis, titration, elemental analysis, radioactive tagging, and spectroscopy (IR, NMR (nuclear magnetic resonance)), can be used to determine molecular weight information.[112] In order to use end group analysis for M_n the polymer cannot be branched.[112] It also must be noted that in a linear

polymer there are twice as many end groups as polymer molecules, and that if the polymer contains different groups at each end of the chain and only one characteristic end group is being measured, the number of this type is equal to the number of polymer molecules.[112]

When characterizing polymers using mass spectrometry, MALDI, or liquid chromatography electrospray ionization (LC-ESI-MS) are typically used. MALDI involves embedding the analyte in a matrix. The matrix being a compound that absorbs at the wavelength of the laser. This energy is then transferred from the matrix to the analyte leading to ionization of the analyte molecule as well as desorption of the matrix and the analyte. MALDI-TOF (time of flight) MS (mass spectrometry) has been shown to be able to detect synthetic polymers in excess of 1,000 kDa.[111] One of the strengths of using MALDI-MS is in the simplicity of the mass spectra which contains mostly singly-charged quasi-molecular ions and relatively high tolerance for contamination.[111] In order to use MALDI-MS to determine the number average molecular weight, weight average molecular weight, and the polydispersity, the ionization efficiency needs to be ideally the same for each molecular weight of the polymer in order for the intensity to be used. In order for these requirements to be fulfilled there needs to be a narrow-distribution of homo-polymers with a polydispersity of approximately 1.2 or less.[111] One way to overcome the issue of complex polymer systems with several mass distributions is to use a separation technique in conjunction with MALDI-MS.[111]

LC-ESI-MS can also be used to analyze polymers. ESI works by passing a liquid through an intense electric field that disperses the sample into a fine spray into a bath gas which evaporates the charged droplets producing gas-phase ions. These ions are then sent into the mass analyzer. Some of the issues with using ESI for polymers are the insolubility of polymers in ESI-compatible solvents, and their electroneutrality prohibits ion formation using the ESI

mechanism.[111] The ability of ESI to produce multiply-charged ions extends the mass range but this can lead to complexity in the mass spectra for even narrowly dispersed polymers. To reduce this complexity coupling the ESI to a separation technique can be done.

Techniques used to Study the Interaction between the Surface and the Environment

For surfaces that are placed in a biological sample a commonly measure parameter is protein adsorption. Commonly used proteins solutions are bovine serum albumin (BSA), lysozyme, and serum. Protein adsorption can be measured using a variety of methods such as surface plasmon resonance, quartz crystal microbalance and reflectometry but these techniques require specialized equipment. A commonly feasible method for most labs to measure protein adsorption onto a surface is by difference between a solution containing a known protein concentration and the surface, and a solution containing the same known concentration of protein. This change can be measured using absorbance value at 280 nm[61, 67, 92, 116-120], using the bicinchoninic assay (BCA)[121-126], or using fluorescently labeled proteins[99, 103, 127, 128]. Another method is to desorb the proteins bound to the surface using sodium dodecyl sulfate (SDS) and sodium hydroxide.[87]

The difference method using the absorbance at 280 nm uses the intrinsic absorbance from aromatic amino acids present in the protein, mostly tyrosine and tryptophan.[129] It is necessary to use standards of the protein you are interested in, in our case BSA and lysozyme, because the molar absorptivity of the each protein is different due to the different amount of aromatic amino acids as well as how exposed those amino acids are. One of the dawbacks to this method is that as the time of incubation of the surface with the protein solution increases, the protein denatures exposing more of the aromatic residues which thus leads to an increase in the absorbance value at 280 nm although the protein concentration has not changed. Another consideration that must

be made is that other compounds can also absorb light at 280 nm. In our case the PES itself in a solution of PBS at pH 7.4 absorbed at 280 nm. This was corrected for by performing a measurement of a solution containing only PBS and the PES membranes. The change in absorbance per unit area was then calculated from this information and subtracted from the change in absorbance per unit area from the membranes placed in the protein solution.

The difference method using the BCA assay is a colorimetric assay that uses the reduction of Cu^{2+} to Cu^+ by proteins in an alkaline medium with detection of the Cu^+ by bicinchoninic acid.[130] The first step involves the chelation of copper (Cu^{2+}) in an alkaline medium to form a blue complex in the presence of sodium potassium tartrate by the biuret reaction.[130] The next step involves bicinchoninic acid which reacts with the cuprous cations formed in step one generating a purple colored product from the chelation of two molecules of BCA with one cuprous ion.[130] The BCA/copper complex displays a strong linear absorbance at 562 nm with increasing protein concentration.[130] The BCA color formation is strongly influenced by cysteine, tyrosine and tryptophan but the universal peptide backbone also contributes to the color formation.[130] BCA is dependent on the amino acid composition of the protein therefore when using a BSA standard the concentrations are relative and not absolute.[130] Also as incubation time of the surface with the protein solution increases, the protein structure will change which can also affect the concentration calculated using the calibration curve.

Using a FITC-labeled protein to measure protein adsorption by difference, one must consider the effect the label will have on the protein structure. FITC-labeling occurs through the amine residues on the proteins by incubating the FITC and protein in a solution with a pH of 9.0 or greater, followed by separation of the free FITC from the FITC-labeled protein.[131] The

protein adsorption is then calculated based on the difference in fluorescence intensity from a solution containing the surface and the solution.

Another type of method to measure protein adsorption is a method that removes the adsorbed protein from the surface using SDS and NaOH. In this method the surface is placed in a solution containing the protein of interest for a set amount of time.[87] The surface is then removed and placed in a solution containing SDS and NaOH which desorbs the protein bound to the surface. Then the concentration of protein is measured in the SDS/NaOH solution.[87] One of the disadvantages to this method is that depending on the interactions between the surface and the protein the removal with SDS and NaOH may become more or less effective. This can become an issue when comparing a modified surface to an unmodified surface, especially if the modification is reducing nonspecific adsorption. This can falsely lead to an increase in protein adsorption when in fact the removal was more effective on one surface versus another.

Another factor in measuring protein adsorption is the amount of time that the surface is incubated in the protein solutions. Commonly used incubation times are 1 hour,[98, 132] 2 hours,[52, 99, 100] 3 hours,[122] and 24 hours[116, 119, 120, 133].

Objective

The work to be described in this dissertation has two main objectives. The first objective seeks to address the challenges with protein adsorption onto the dialysis membrane. This nonspecific adsorption onto the dialysis membrane can severely affect the capabilities to recover important signaling proteins of interest. This objective was met by covalently modifying the membrane by attaching phenolic compounds onto the membrane and testing the RR of five different cytokines and lysozyme. The second objective focuses on attaching an affinity agent, heparin, onto the membrane surface, increasing the mass transport across the membrane by

reducing irreversible adsorption. The analytes chosen are CCL2, aFGF, and VEGF. The reason

for choosing these analytes was to test if the off rates (k_{off}) would have an effect on the RR

enhancement. The k_{off} is defined as the rate of dissociation between two molecules with units of

s^{-1}. CCL2 has a reported slow k_{off} rate of $(1.64 \pm 0.66) \times 10^{-3}$ s^{-1}. [134] VEGF and aFGF have

reported fast k_{off} rates of 0.10 ± 0.03 s^{-1} and 0.10 ± 0.03 s^{-1}.[134] Also, aFGF, CCL2, and VEGF

have different isoelectric points (pI), of 5.7, 9.3 and 8.5, respectively. Because heparin is highly

sulfonated, it is highly negatively charged, which also may be a factor in RR enhancement due to

the charge-charge interactions between the protein and heparin. Covalently attaching heparin

onto the membrane surface and measuring the change in recovery of three heparin binding

proteins has met this objective.

CHAPTER 2. MODIFICATION OF PES FLAT SHEETS AND MICRODIALYSIS MEMBRANES WITH 4-HYDROXYBENZOIC ACID POLYMERS TO REDUCE NONSPECIFIC ADSORPTION AND IMPROVE RELATIVE RECOVERY

<u>Introduction</u>

Due to the chemical and physical stability of polyethersulfone (PES), PES is widely used in membrane science. One of the challenges with using PES is that it is hydrophobic in nature. For that reason, when PES is placed in a solution, it leads to an increase in nonspecific adsorption on the surface. Previous research has shown that polymers grafted to a hydrophobic surface can reduce protein adsorption simply by nonspecifically blocking protein adsorption sites.[70] Therefore, the polymer should have groups which prevent nonspecific adsorption, such as hydroxyl or poly(ethylene oxide) groups.[71] By modifying the surface with a hydrophilic polymer, 4HBA, the surface becomes more hydrophilic but the chemical and physical properties of PES are not changed. This chapter addresses a method of attaching 4HBA-initiated polymers onto the surface using the enzyme laccase, and the characterization of nonspecific adsorption and its effect on RR in microdialysis. Initially, experiments were performed on PES flat sheets to confirm the modification with 4HBA polymers using the enzyme laccase, and to analyze protein adsorption onto the surface. After characterizing this reaction onto flat sheets this method was then applied to hollow fiber microdialysis membranes.

<u>Materials and Methods</u>

Materials

Laccase form *Trametes versicolor*, sodium acetate, fluorescein isothiocyanate dextran 4,000, fluorescein isothiocyanate dextran 10,000, fluorescein isothiocyanate dextran 20,000 and

methyl orange were purchased from Sigma Aldrich (St. Louis, MO), 4-hydroxybenzoic acid was purchased from TCI (Portland, OR). 3-chloro-4-hydroxybenzoic acid, and 2-5-dihydroxybenzoic acid was purchased from Alfa Aesar (Haverhill, MA). HPLC grade methanol and water were purchased from Fisher Scientific (Waltham, MA). Glacial acetic acid was purchased from VWR international (Radnor, PA). NAP-25 Sephedex G-25 column were purchased from GE healthcare (Chicago, IL). Bovine Serum Albumin fraction V, was purchased from Rockland (Pottstown, PA) and was certified immunoglobulin and protease free. Lysozyme was purchased from MP biomedicals (Solon, OH). 100 kDa PES flat sheet membranes (UE50) were purchased from Sterlitech (Kent, WA). Fluorescein isothiocyanate isomer 1 was purchased from Alfa Aesar (Haverhill, MA). Dibasic sodium phosphate (ACS grade) was purchased from EMP (Howell, NJ). Sodium chloride bioXtra grade, potassium chloride (99.0%), and monobasic potassium phosphate (ACS grade) where purchased from Sigma Aldrich (St. Louis, MO). CMA 20 microdialysis probes were purchased from Harvard Apparatus (Holliston, MA). CCL2, and TNF-α optiEIA ELISA kit was purchased from BD bioscience (San Jose, CA) Recombinant rat KC/GRO, and mouse aFGF, and VEGF Duo set ELISA kits were purchased from R&D systems (Minneapolis, MN).Recombinant mouse FGF1 was purchased from Sino Biologicals (Beijing, China) and recombinant mouse VEGF was purchased from Life Technologies (Carlsbad, CA).

Addition of 4HBA onto PES Flat Sheets

Modification of 100 kDa polyethersulfone (PES) flat sheets were performed with a solution containing 28.8 mM 4HBA or 3Cl4HBA, and 0.5 U/mL of laccase from *Trametes versicolor* that were dissolved in 0.1 M sodium acetate buffer pH 5.0. The solution was filtered using a 0.2 μm PES filter and the membranes were placed in the solution for 24 hours on a plate shaker at room temperature. Following modification, the membranes were placed in a solution

of 0.1 M sodium acetate buffer pH 5.0 at room temperature overnight. The membranes were

then analyzed using XPS.

XPS Methods for PES Flat Sheets

Four different control solutions were used. The 4HBA control contained 28.8 mM

4HBA in 0.1 M sodium acetate at pH 5.0. Laccase control contained 0.5 U/mL laccase in 0.1 M

sodium acetate at pH 5.0. The 3Cl4HBA control contained 28.8 mM 3Cl4HBA in 0.1 M sodium

acetate at pH 5.0. Sodium acetate control contained only 0.1 M sodium acetate at pH 5.0. The

procedure for the controls was the same as the modified flat sheet membranes. Three 1 cm x 1

cm flat sheet 100 kDa PES membranes was placed in these solutions and each one was analyzed

individually. Then one from each group of flat sheet membranes was analyzed in three different

areas. XPS high resolution spectra for C1s, O1s, and Cl 2p, and survey scans were performed.

ATR-FTIR Method

A separate set of membranes where prepared as stated above but allowed to react in the

4HBA polymerization solution for 1, 2, 3, and 4 days. The membranes were then placed in a

desiccator overnight to dry the membrane before analysis with the ATR-FTIR.

Protein Adsorption Methods

FITC-labeling of both BSA and lysozyme was performed by placing 400 μg of FITC into

10 μL of DMSO, and dissolving 4 mg of BSA or lysozyme into 990 μL of 0.1 M phosphate at

pH 8.0. These two solutions were then combined and incubated at 37°C for 2 hours. Then, the

solution was filtered using a NAP-25, Sephedex G-25 size exclusion column to separate the

FITC-labeled protein from the free FITC. The concentration of FITC-labeled protein was

determined based on the absorbance at 280 nm. Later, the membranes were then placed in a

solution of FITC-BSA (74 μg/mL) or FITC-lysozyme (5.5 μg/mL) and a solution without

membranes (control solution) were incubated for 48 hours. Then, fluorescence measurements were made using an excitation wavelength of 485 nm, and the emission was measured from 500-650 nm. As a result, the emission maxima were between 517 nm and 520 nm for FITC-BSA and for FITC-lysozyme were between 515 nm and 517 nm. To determine the concentration, a calibration curve was made for both FITC-BSA and FITC-lysozyme using the stock solutions from above. After the concentration was determine, the difference between the concentration of the control solution and the solution containing the membranes was calculated. Then, the difference was used to determine the amount of protein adsorbed per unit of surface area using Equation 12.

$$Protein\ Adsorption\ (\mu g/cm^2) = \frac{Concentration\ (\mu g/mL)*volume\ (mL)}{Surface\ Area\ (cm^2)} \qquad [12]$$

Attachment of 4HBA onto Microdialysis Membranes

For the modification of the PES microdialysis membranes a solution containing 28.8 mM of 4HBA, and 0.5 U/mL of laccase from *Trametes versicolor* that was dissolved in 0.1 M sodium acetate buffer pH 5.0. Then, the solution was filtered using a 0.2 μm PES filter and perfused at a rate of 1 μL/min for either 2 hours or 24 hours. Following modification, the probe was flushed with 0.1 M sodium acetate buffer pH 5.0 overnight at a flow rate of 3 μL/min. Following modification, the microdialysis membranes were either used for a relative recovery experiment or cut longitudinally and the inside was analyzed for reaction with 4HBA using XPS. An initial survey scan was performed to determine the elements present in the sample. This was followed by high resolution scans of C1s, O1s and S2p to determine the binding energies present and the percentages of those binding energies.

Relative Recovery Determination

FITC-Dextrans

Initially an experiment was performed to determine if the presence of laccase alters the membrane in a way that changes the recovery of FITC-4 and FITC-10. The microdialysis probes were placed in a stirred solution containing 0.5 U/mL laccase in sodium acetate pH 5 for 2 hours, and perfused for 2 hours in laccase solution. Relative recovery of FITC-4 and FITC-10 was determined using a CMA 20 microdialysis probe at a flow rate of 1 μL/min with a perfusion fluid of 4% (w/v) Dextran 500 in Ringer's solution (154 mM NaCl, 5.4 mM KCl, and 2.3 mM CaCl$_2$) at pH 7.2-7.4. The probe was placed in a solution of either 500 μM FITC-4 or 200 μM FITC-10 in perfusion fluid and samples were collected every 20 minutes for a total of 60 minutes. Then, the absorbance values were measured in triplicate for each sample at 493 nm, and concentrations were determined based off a calibration curve measured that day.

To test the impact of the modification with 4HBA, FITC-4, FITC-10 and FITC-20 RR was determined. This experiment was performed using a CMA 20 microdialysis probe modified for 0, 2 and 24 hours with 4HBA at a flow rate of 1 μL/min using PBS at pH 7.4. The solution the probe was placed in contained 500 μM FITC-4, 200 μM FITC-10 or 100 μM FITC-20 in PBS pH 7.4, and samples were collected every 20 minutes for a total of 60 minutes. Absorbance values were measured in triplicate for each sample at 493 nm, and concentrations were determined based off a calibration curve measured the same day.

Proteins

After testing RR of FITC-4, FITC-10, and FITC-20, RR was analyzed for lysozyme using control, 2 hour and 24 hour 4HBA modified membranes using the same microdialysis probes as above. RR of lysozyme was performed using 500 μg/mL of lysozyme with a perfusion fluid of

PBS at pH 7.4 at a flow rate of 1 μL/min. Samples were collected every 30 minutes for a total of 2 hours and were analyzed using a standard BCA assay. Next RR of CCL2, VEGF, TNF-α, KC/GRO (keratinocyte chemoattractant/ growth regulated oncogene), and aFGF were performed. To test the RR of these analytes the probes were placed in a solution containing 6,000 pg/mL of CCL2, 800 ng/mL of aFGF, 4,000 pg/mL KC/GRO, 5,000 pg/mL TNF-α or 200 ng/ml of VEGF in PBS 0.1% BSA at pH 7.4. These concentrations were chosen in order to observe concentrations in the dialysate that are within the detection range for the corresponding ELISA. The perfusion fluid was prepared using PBS 0.1 % BSA at pH 7.4 and perfused at 1 μL/min, and the samples were collected every hour and analyzed using a standard CCL2, aFGF, KC/GRO, TNF-α or VEGF ELISA.

Results and Discussion

Addition of 4HBA Polymers onto PES Flat Sheets

After modification with 4HBA and laccase using the procedure described above, images of the membrane were taken. As shown in Figure 4, upon the addition of 4HBA polymer onto the PES flat sheets the membrane surface becomes browner in color which is due to the oxidation of the 4HBA polymer on the surface. The results from XPS analysis are shown in Figure 5 and Tables 3 and 4. In Figure 5(A), the high resolution scan of C1s shows the presence of 3 peaks for the 4 different controls (laccase control, 4HBA control, 3Cl4HBA control, and sodium acetate control); these are the C-C/C-H peak at 284.77 eV, the ether linkage (C-O-C) at 286.23 eV and the C-S peak at 288.81 eV. For the 4HBA modified and 3Cl4HBA modified, there is a peak present between C-O-C and C-S which corresponds to the carboxylic acid functional group at 287.85 eV. This indicates that the membrane is modified because the controls (4HBA control, laccase control, 3Cl4HBA control, and sodium acetate control) do not

37

contain carboxylic acid functional groups. In Figure 5(B), the Cl2p high resolution scan showed the presence of C-Cl peak at 200.32 eV and 201.92 eV which indicates the attachment of 3Cl4HBA. Also, the C-Cl peaks are not present in the 3Cl4HBA control indicating the 3Cl4HBA does not adsorb to the surface, but is covalently bound. In Figure 5(C), the O1s high resolution survey scan shows the presence of 2 peaks for the 4 controls; these are from the O-C (531.72 eV) and O-S (533.35eV) functional groups. In the 4HBA and 3Cl4HBA modified flat sheet membranes, there is a merging of these 2 peaks indicating the presents of a third functional group, possibly a carboxylic acid functional group. In Figure 5(D), the survey scan for the 4HBA modified, 3Cl4HBA modified and the sodium acetate control is shown. From the information obtained from the high resolution spectra, the percentages of each functional group was calculated and tabulated in Table 3 for one flat sheet analyzed in 3 different areas and in Table 4, for 3 different flat sheets.

    For the laccase control, the C-C, C-O-C, O-C and O-S percentages were significantly different than the other control membranes. This is most likely due to laccase being a protein, and proteins are known to adsorb onto PES surfaces. For the 4HBA modified membranes, due to the O-S bond only being present in PES, the O-S decreased. For 4HBA, the COOH functional group was also present which is the end group of the 4HBA polymer at a percentage of 8.62±0.74%. For 3Cl4HBA, the C-Cl doublet was present a percentage of 3.50±0.71% and 1.75±0.36%, the COOH functional group was present at 5.10±1.63% and the O-S decreased. Results in Table 4, for three different locations on one flat sheet show similar trends to the results in Table 3 indicating uniformity in the modification procedure. For the 4HBA modified flat sheets, the COOH functional group appeared at a percentage of 6.82±2.19% which was not present in any other control flat sheets. Also, the O-S and C-O-C functional group was

significantly less than the control membranes. For the 3Cl4HBA modified membranes, the

chlorine doublet for C-Cl was present at a percentage of $2.88\pm0.24\%$ and $1.44\pm0.12\%$, and the

COOH functional group at $5.10\pm1.82\%$. Also, the C-O-C percentage increased and the O-S

environments decreased compared with the control membranes.
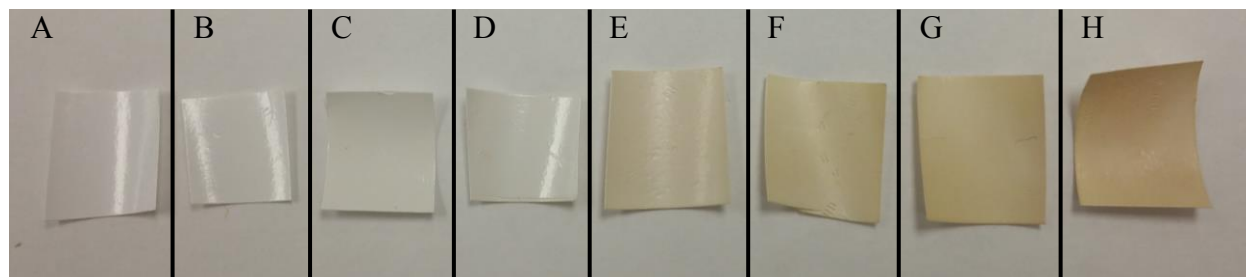
Figure 4. PES membranes before and after 4-hydroxybenzoic acid modification. (A) PES, (B) sodium acetate control, (C) laccase control, (D) 4HBA control, (E) 1 day 4HBA modification, (F) 2 day 4HBA modification (G) 3 day 4HBA modification, (H) 4 day 4HBA modification.
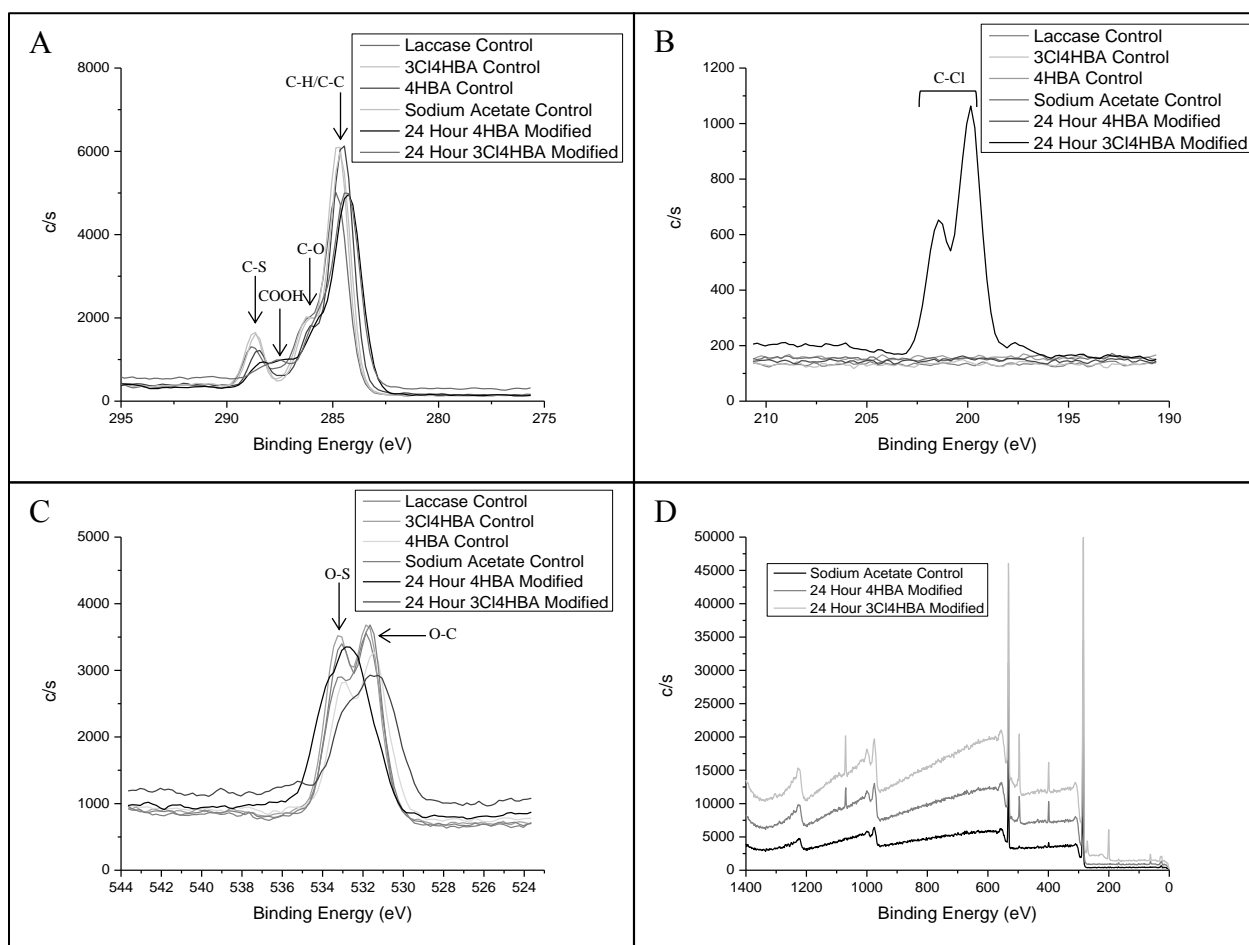
Figure 5. XPS spectra for PES flat sheets. XPS overlays for high resolution scans of C1s (A), Cl2p (B), and O1s (C), and XPS survey scan overlay (D) for PES flat sheets.

Table 3. **PES flat sheet membranes analyzed using XPS in three different areas on one flat sheet membrane. Percentages are determined from the peak areas of the C 1s, O 1s, and Cl 2p high resolution XPS spectra. The element listed first indicates the source of the photoelectron. * indicates a significant difference from the sodium acetate control, 4HBA control, and 3Cl4HBA control at the 95% confidence level using a single factor ANOVA with Bonferroni post hoc test. ND indicates not detected ($\leq$0.1).**

	C-C	C-O-C	C-S	COOH	O-C	O-S	Cl⁻	Cl⁻	C-Cl	C-Cl
Binding Energy (eV)	284.77±0 0.093	286.23 ±0.093	288.81 ±0.09	287.85 ±0.14	531.72 ±0.19	533.35 ±0.12	197.92 ±0.07	199.52 ±0.07	200.32 ±0.04	201.92 ±0.04
Sodium Acetate Control	55.32 ±3.33%	13.89 ±0.95%	7.79 ±0.95%	ND	12.54 ±0.96%	10.46 ±1.07%	ND	ND	ND	ND
4HBA Control	57.25 ±0.78%	11.00 ±4.26%	7.20 ±0.79%	ND	13.09 ±1.43%	9.41 ±1.40%	ND	ND	ND	ND
3Cl4HBA Control	51.28 ±3.86%	14.88 ±1.51%	9.00 ±0.60%	ND	13.77 ±1.47%	11.40 ±1.04%	ND	ND	ND	ND
Laccase Control	47.00 ±5.47%*	23.28 ±0.89%*	8.51 ±0.57%	ND	14.06 ±4.39%*	7.15 ±1.32%*	ND	ND	ND	ND
4HBA Modified	58.66 ±5.01%	11.77 ±1.55%	3.53 ±1.15%*	8.62± 0.74%*	14.44 ±6.89%	3.62 ±1.40%*	ND	ND	ND	ND
3Cl4HBA Modified	53.02 ±4.53%	17.69 ±2.51%*	1.12 ±0.02%*	5.10± 1.63%*	12.53 ±1.95%	6.24 ±1.45%*	0.14 ±0.012%*	0.077 ±0.005%*	3.50 ±0.71%*	1.75 ±0.36%*

Table 4. Three PES flat sheet membranes analyzed using XPS. Percentages are determined from the peak areas of the C 1s, O 1s, and Cl 2p high resolution XPS spectra. The element listed first indicates the source of the photoelectron. * indicates a significant difference from the sodium acetate control, 4HBA control, and 3Cl4HBA control at the 95% confidence level using a single factor ANOVA with Bonferroni post hoc test. ND indicates not detected (≤ 0.1).

	C-C	C-O-C	C-S	COOH	O-C	O-S	Cl⁻	Cl⁻	C-Cl	C-Cl
Binding Energy (eV)	284.77 ±0.02	286.24 ±0.07	288.83 ±0.10	287.95 ±0.12	531.69 ±0.24	533.31 ±0.31	197.86 ±0.01	199.46 ±0.07	200.35 ±0.04	201.95 ±0.03
Sodium Acetate Control	51.07 ±0.90%	15.58± 1.36%	8.35± 0.71%	ND	14.43 ±2.57%	10.56 ±2.38%	ND	ND	ND	ND
4HBA Control	51.00 ±4.86%	15.49 ±0.22%	7.99 ±1.48%	ND	14.65 ±0.97%	10.88 ±2.68%	ND	ND	ND	ND
3Cl4HBA Control	49.32 ±2.86%	16.17 ±1.31%	8.57 ±0.45%	ND	15.34 ±1.73%	10.60 ±0.45%	ND	ND	ND	ND
Laccase Control	46.62 ±3.76%	20.38 ±3.60%*	8.07± 0.47%	ND	17.08 ±0.43%	7.84 ±0.38% *	ND	ND	ND	ND
4HBA Modified	56.63 ±2.14%	12.06 ±2.24%*	3.64 ±1.21%*	6.82 ±2.19%*	12.67 ±1.90%	7.36 ±1.55% *	ND	ND	ND	ND
3Cl4HBA Modified	49.13 ±6.49%	19.62 ±2.94%*	0.81 ±0.45%*	5.10 ±1.82%*	14.68 ±4.86%	7.06 ±4.33% *	0.22 ±0.091%*	0.11 ±0.044%*	2.88 ±0.24%*	1.44 ±0.12%*
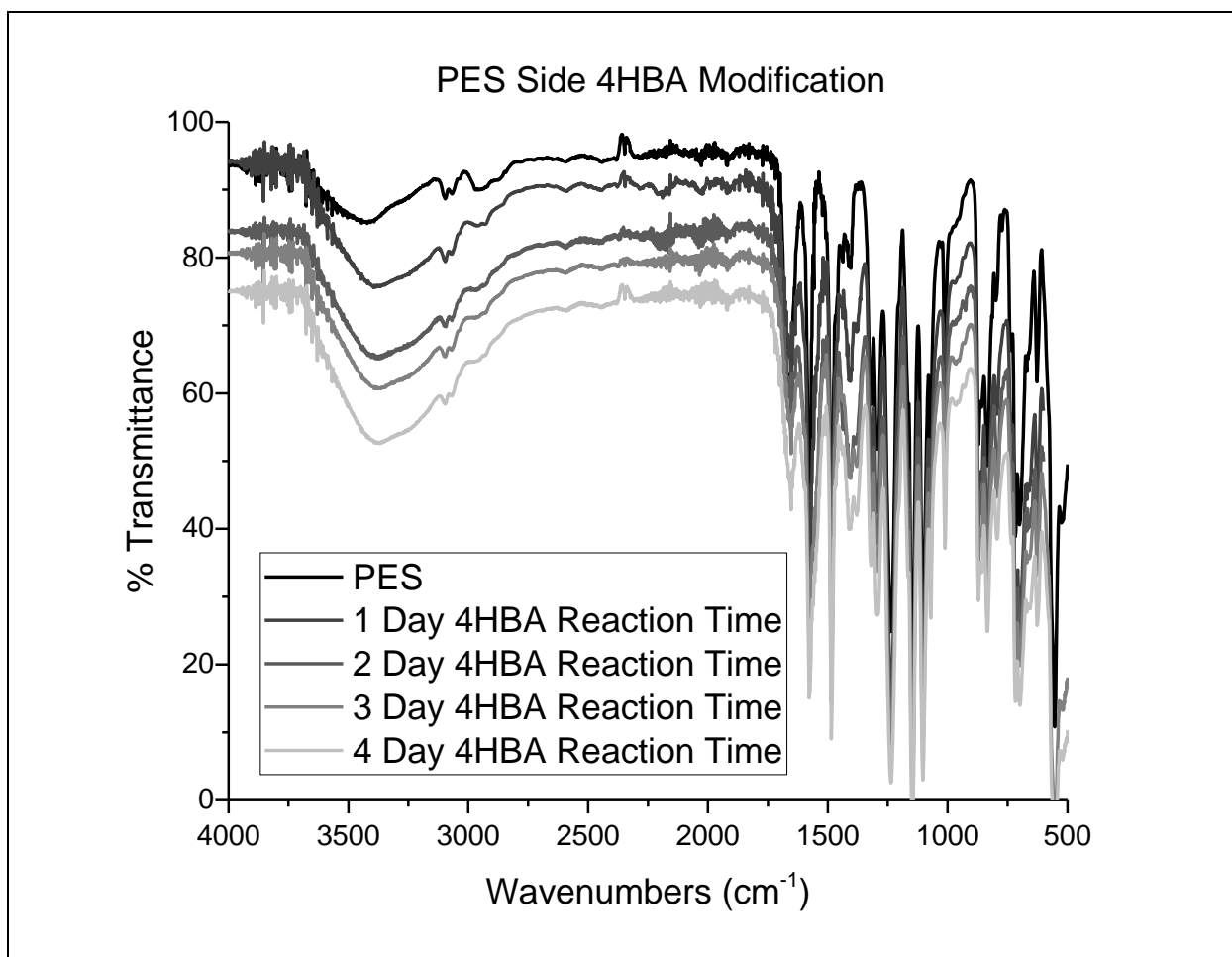
Figure 6. IR spectra of the PES side of the flat sheet membrane for PES, 1 day modification, 2 day modification, 3 day modification, 4 day modification after attachment of 4-hydroxybenzoic acid polymers.
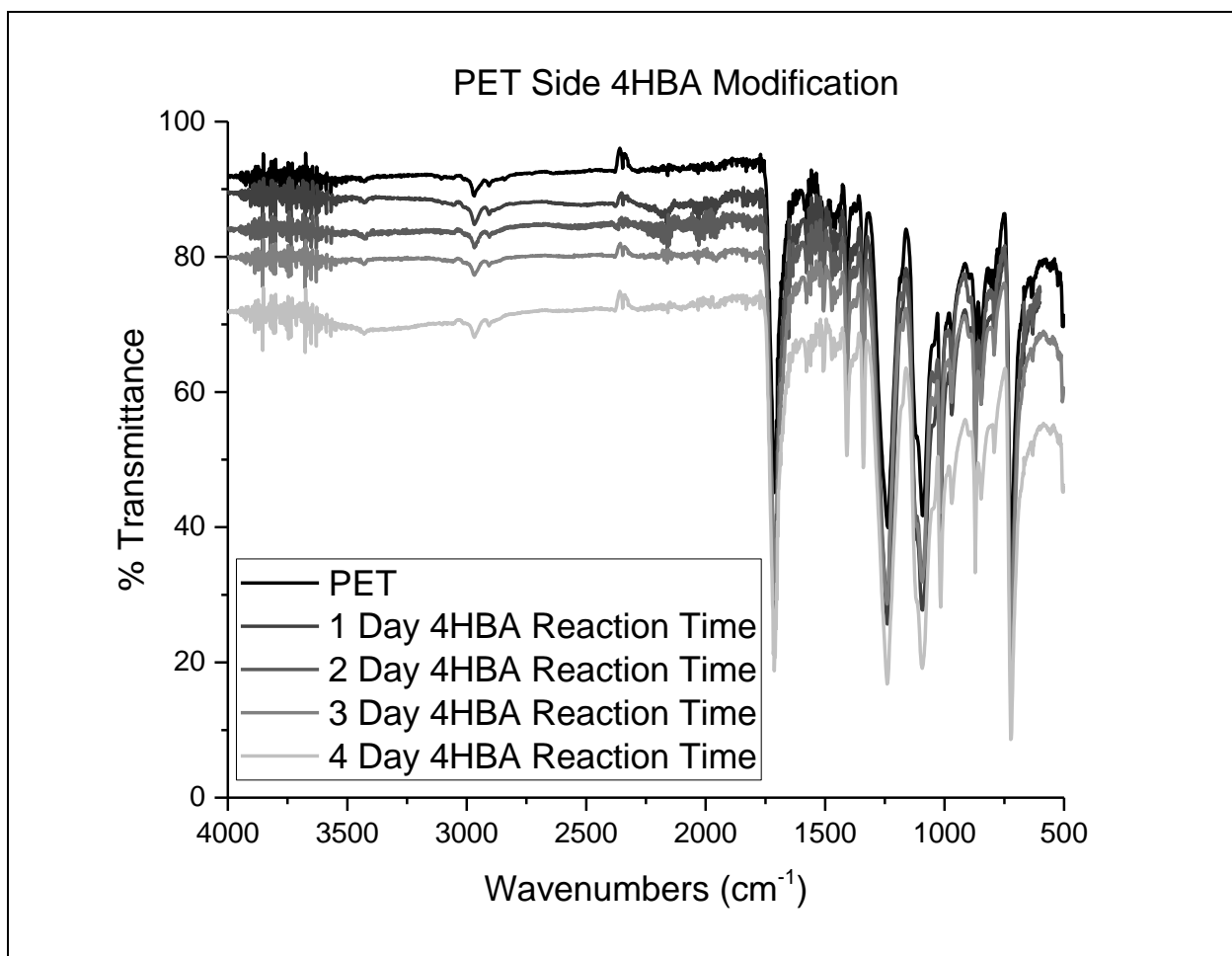
Figure 7. IR spectra of the PET side of flat sheet membrane for PES, 1 day modification, 2 day modification, 3 day modification, 4 day modification after attachment of 4-hydroxybenzoic acid polymers.

The ATR-FTIR spectra in Figure 6 show the presence of a hydroxyl peak from the conjugated carboxylic acid functional group at 3300 cm^{-1} for the PES side of the membrane. This peak increases in size as the modification time increase. The polyethylene terephthalate (PET) side of the membrane in Figure 7 shows that it is unaffected by the 4HBA modification. The presence of the carboxylic acid functional group is evidence of the attachment of 4HBA polymers on the PES surface. The combined results from XPS and IR confirm the attachment of 4HBA polymers on the surface of PES flat sheets.

Protein Adsorption Experiments

After confirming the attachment of 4HBA onto PES flat sheets, the amount of BSA and lysozyme adsorbed onto the surface was measured. This was done to investigate whether the modification would reduce nonspecific adsorption of BSA and lysozyme. Lysozyme was chosen because of its isoelectric point (pI) of 11, which makes the overall charge on the protein at pH 7.4 positive; BSA was chosen because its pI is 4.7, which makes the overall charge on the protein at pH 7.4 negative. Since the 4HBA polymer introduces a carboxylic acid functional group (pK$_a$=4.54) onto the surface which is deprotonated at pH 7.4, the comparison of the amount of BSA and lysozyme adsorbed onto the surface can give insight into the dominate mechanism of protein adsorption upon addition on the 4HBA polymer. Reduction in protein adsorption can occur through charge repulsion and by strengthening the water polymer interaction.[70] If BSA adsorption decreases and lysozyme increases, a charge-charge interaction dominates. This is due to the carboxylic acid being deprotonated at pH 7.4 so lysozyme would be attracted to the surface and BSA would be repelled. However, if BSA and lysozyme adsorption decrease then the water-polymer interaction dominates. This is due to water being

more tightly bound to the surface due to the interaction with the carboxylic acid functional group and the water must be displaced in order for proteins to adsorb to the surface.

Initially both BSA and lysozyme were fluorescein isothiocyanate (FITC) labeled. After FITC labeling BSA and lysozyme, the membranes were placed in a solution of FITC-BSA (74 µg/mL) or FITC-lysozyme (5.5 µg/mL). Then the difference between a solution without the membrane and with the membrane was used to determine the amount of protein adsorbed onto the surface. This was performed for the following reasons: 1) to determine if the modification with 4HBA altered the amount of protein adsorbing to the surface, and 2) investigate the dominate mechanism (charge attraction/repulsion, water polymer interaction) of protein adsorption.
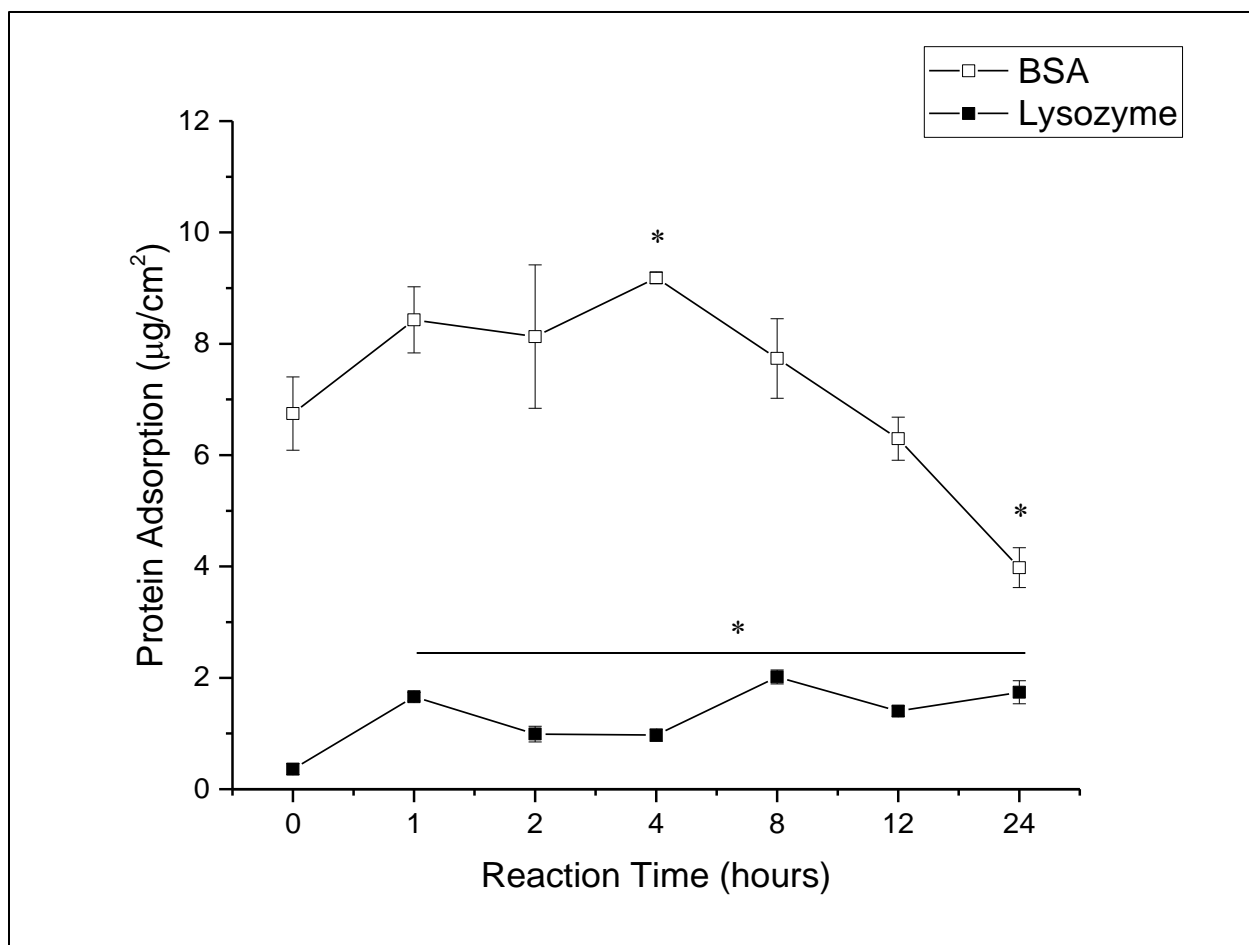
Figure 8. BSA (□) and lysozyme (■) adsorption onto PES membranes modified with 4-hydroxybenzoic acid (4HBA) polymers for between 1 and 24 hours compared to control membranes. * indicates significant difference at the 95% confidence level compared to the 0 hour reaction time using a single factor ANOVA with Bonferroni post hoc test. The error bars represent the standard deviation in protein adsorption calculated from 3 different solutions containing PES membranes modified with 4HBA for different reaction times.

The results for FITC-lysozyme adsorption, shown in Figure 8, show an increase in the adsorption of FITC-lysozyme after 4HBA modification. In addition, the results for the FITC-BSA experiment, shown in Figure 8, show an initial increase in BSA adsorption which becomes significant at the 4 hour of reaction time followed by a decrease in BSA adsorption after 8 hours of reaction time. At a 24 hour reaction time, FITC-BSA adsorption is significantly lower compared to the control. For BSA, the initial increase in protein adsorption could be due to the graft density of the polymer on the surface which is not sufficient enough to exclude BSA. This could be due to the BSA being able to go between the polymer chains, and BSA becoming trapped within the chains of the polymer which will lead to an increase in protein adsorption. Moreover, the decrease in protein adsorption observed at the 24 hour reaction time is due to the exclusion of BSA from becoming trapped within the polymer chains due to the increase in size and graft density with the longer reaction time. At increased graft density there are more carboxylic acid functional groups which could increase charge-charge repulsion, leading to a decrease in BSA adsorption. For lysozyme, the increase in protein adsorption is possibly caused by the 4HBA modification's ability to trap lysozyme because lysozyme is smaller at 14 kDa compared to BSA at 66.5 kDa.   Also, the increase in lysozyme adsorption could be due to the charge-charge interaction with the deprotonated carboxylic acid functional group.   Overall this experiment shows that for BSA, there is a decrease in protein adsorption with the 24 hour reaction time, but for lysozyme there is an overall increase in protein adsorption due to a combination of graft density and charge-charge interactions between the polymer and the protein.

Modification of Microdialysis Membranes with 4-Hydroxybenzoic Acid Polymers

Following the confirmation of the covalent attachment of 4HBA polymers onto PES flat

sheet, the reaction was applied to PES microdialysis membranes. The attachment of 4HBA

polymers onto the microdialysis membranes was confirmed using XPS. Then, RR values of

FITC-labeled dextrans of 4 kDa, and 10 kDa, were determined to analyzed the effect of the

reaction on transport as well as the effect of nonspecific adsorption of the reactants (4HBA and

laccase). Finally, RR of lysozyme, CCL2, VEGF, KC/GRO, TNF-α, and acidic fibroblast

growth factor (aFGF) was determined and compared to unmodified microdialysis probes.

XPS Characterization

The results from XPS analysis for both control and 24 hour 4HBA modified membranes

(Table 4) show the presence of the carboxylic acid functional group at 287.90 ± 0.17 eV with

$9.73 \pm 5.94\%$. There is also a decrease in the O-S functional group at 532.99 ± 0.88 eV from

$3.15 \pm 0.64\%$ to not detectable values. There is also a decrease in S2p which is only found in

PES from $3.12 \pm 1.14\%$ to $0.85 \pm 0.18\%$. This confirms the attachment of 4HBA polymer onto

to the microdialysis membrane because 4HBA is the only source of the carboxylic acid

functional group. Also, the decrease in O-S, and S2p, only found in PES, shows the addition of

polymer onto the surface is sufficient to not allow the photoelectrons from O-S to escape.

Table 5. XPS data from control and 24 hour 4HBA modified microdialysis membranes. Percentages are determined from the peak areas of the C1s, O1s, and S2p high resolution XPS spectra. N=3, * indicates a significant difference from the control at the 95% confidence level using a single factor ANOVA with Bonferroni post hoc test. ND indicates not detected (≤0.1%).

	C-C/C-H	C-O	COOH	S2p	O-C	O-S
eV	284.71 ± 0.11	285.98 ± 0.30	287.90 ± 0.17	168.09 ± 0.25	531.63 ± 0.57	532.99 ± 0.88
Control	54.65 ± 10.40%	22.54 ± 6.76%	ND	3.12 ± 1.14%	15.14 ± 5.07%	3.15 ± 0.64%*
4HBA Modified	49.83 ± 11.88%	17.68 ± 6.50%	9.73 ± 5.94%*	0.85 ± 0.18%*	14.81 ± 4.36%	ND

Effect of Laccase and 4-Hydroxybenzoic Acid on the Relative Recovery of FITC-4 and FITC-10

FITC-4 and FITC-10 RR of three different microdialysis probes were analyzed to determine if nonspecific adsorption of laccase onto the surface would alter the transport across the membrane. Results shown in Figure 9 and 10 show that FITC-4 and FITC-10, RR is not significantly different, indicating that laccase does not adsorb to the microdialysis membrane in a way that inhibits the RR of FITC-4 and FITC-10. This indicates that laccase is not adsorbing onto the surface to an extent that would inhibit the transport of FITC-4 and FITC-10.
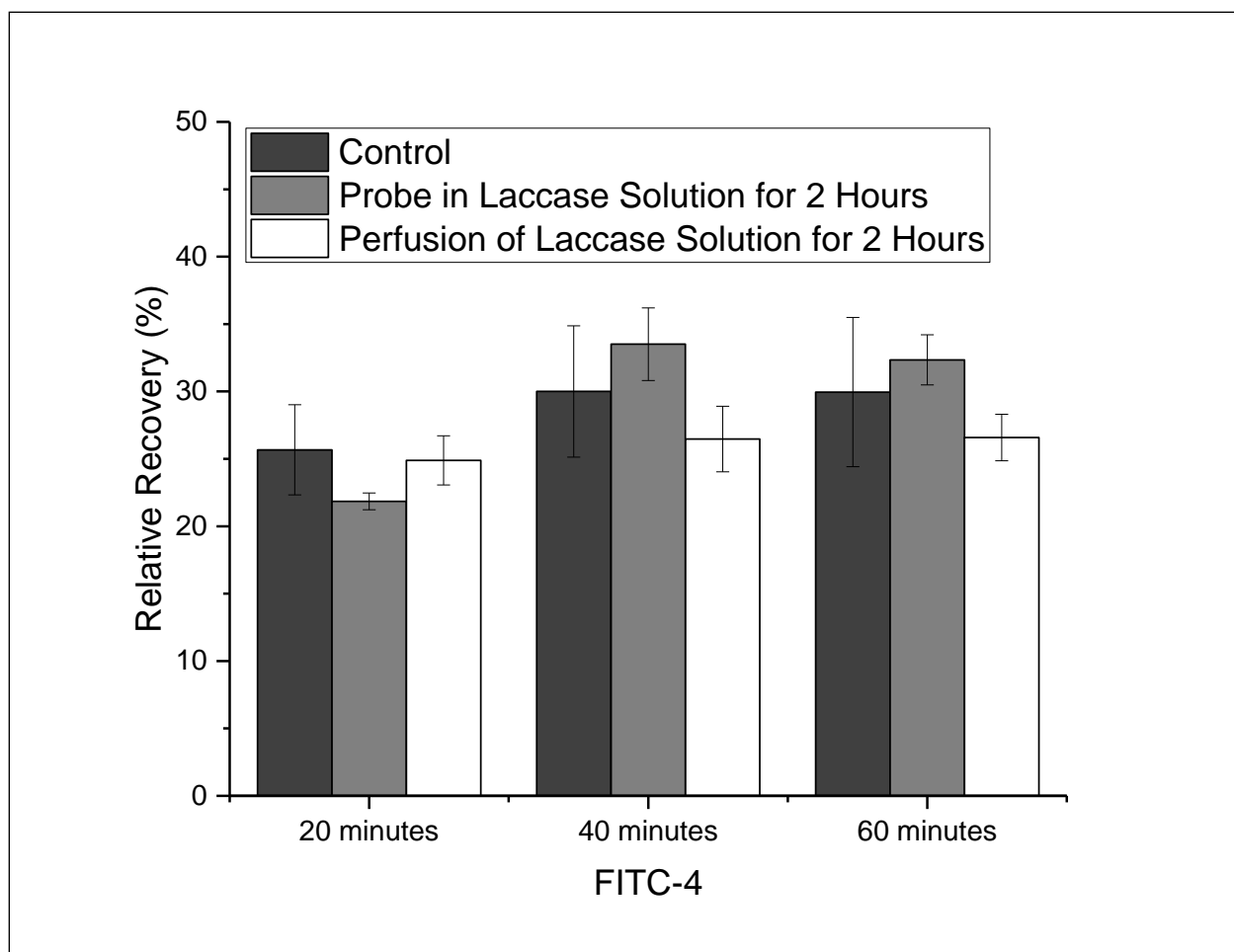
Figure 9. Analysis of the effect of nonspecific adsorption of laccase on FITC-4 relative recovery. Three different groups were analyzed, control probes perfused and placed in a solution that does not contain laccase, probes perfused with a 0.5 U/mL laccase solution, and probes placed in a solution containing 0.5 U/mL of laccase. These results correspond to 3 different probes tested for RR of FITC-4 at 3 different times, with each time point measured in triplicate. Error bars represent ± SD from mean.
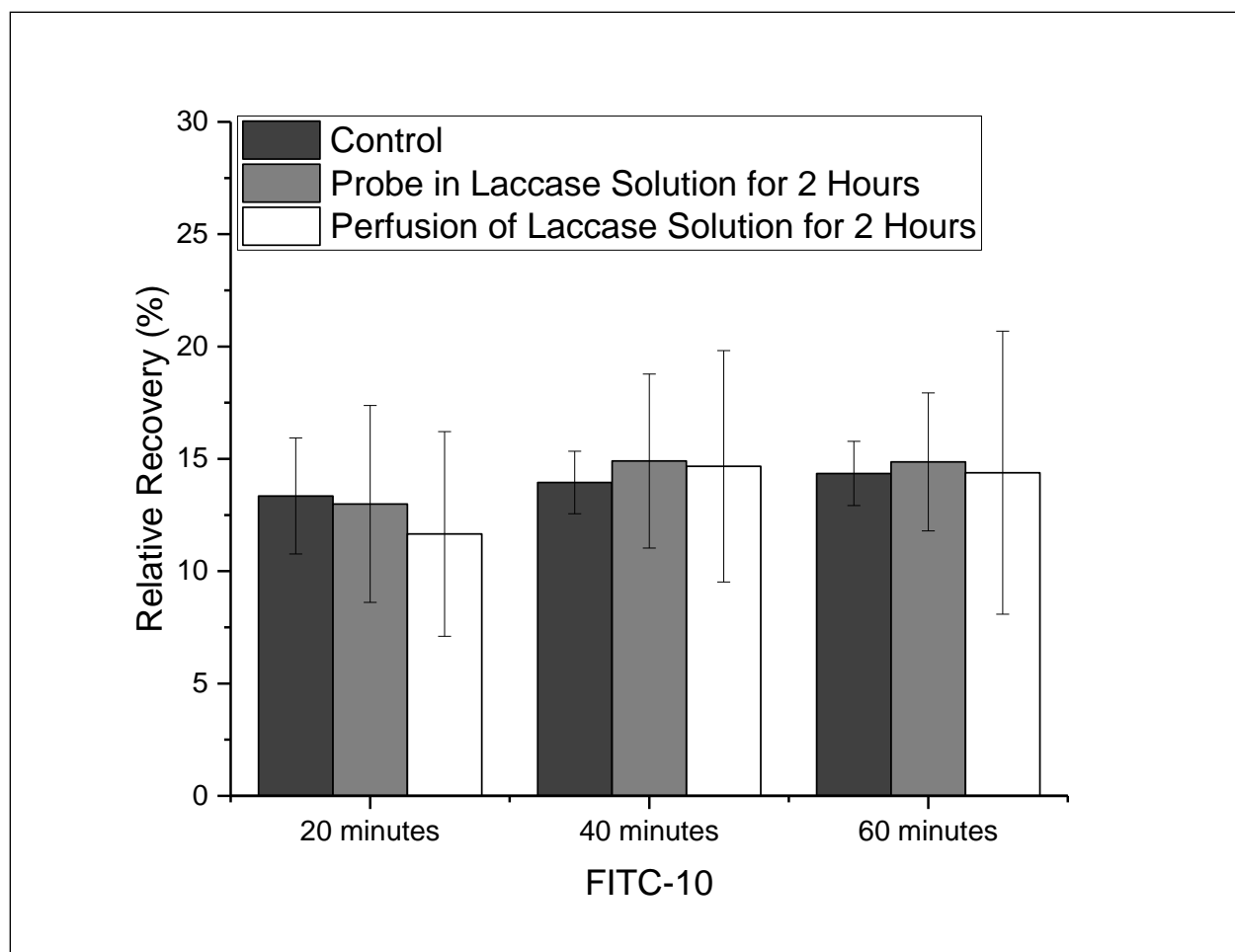
Figure 10. Analysis of the effect of nonspecific adsorption of laccase on FITC-10 relative recovery. Three different groups were analyzed, control probes perfused and placed in a solution that does not contain laccase, probes perfused with a 0.5 U/mL laccase solution, and probes placed in a solution containing 0.5 U/mL of laccase. These results correspond to 3 different probes tested for RR of FITC-10 at 3 different times, with each time point measured in triplicate. Error bars represent ±SD from mean.

FITC-4, FITC-10, FITC-20 Relative Recovery after 2 and 24 Hour Reaction Time

Next, FITC-4, FITC-10, and FITC-20 RR was tested after modification with 4HBA and laccase for 2 and 24 hours. This was performed to see if the modification would hinder the RR of these molecules. The results from this experiment are shown in Figures 11-13. For FITC-4 (Figure 11), there is a 20% decrease in RR after modification for 2 hours and a 61% decrease for the 24 hour modification time. For FITC-10 (Figure 12), the RR decreased by 40% for the 2 hour modification and 73% for the 24 hour modification. FITC-20 (Figure 13) showed a 40% decrease for the 2 hour modification time and a 76% decrease for the 24 hour modification. For the 2 hour modification time, there is only a slight decrease, of 20%, in RR of FITC-4 which then increases to 40% for FITC-10 and FITC-20. Moreover for the 24 hour modification, FITC-4, FITC-10 and FITC-20 RR decrease by approximately 70%. This could indicate that the longer modification time leads to denser polymer formation. This leads to an increase in pore blockage which decreases RR.
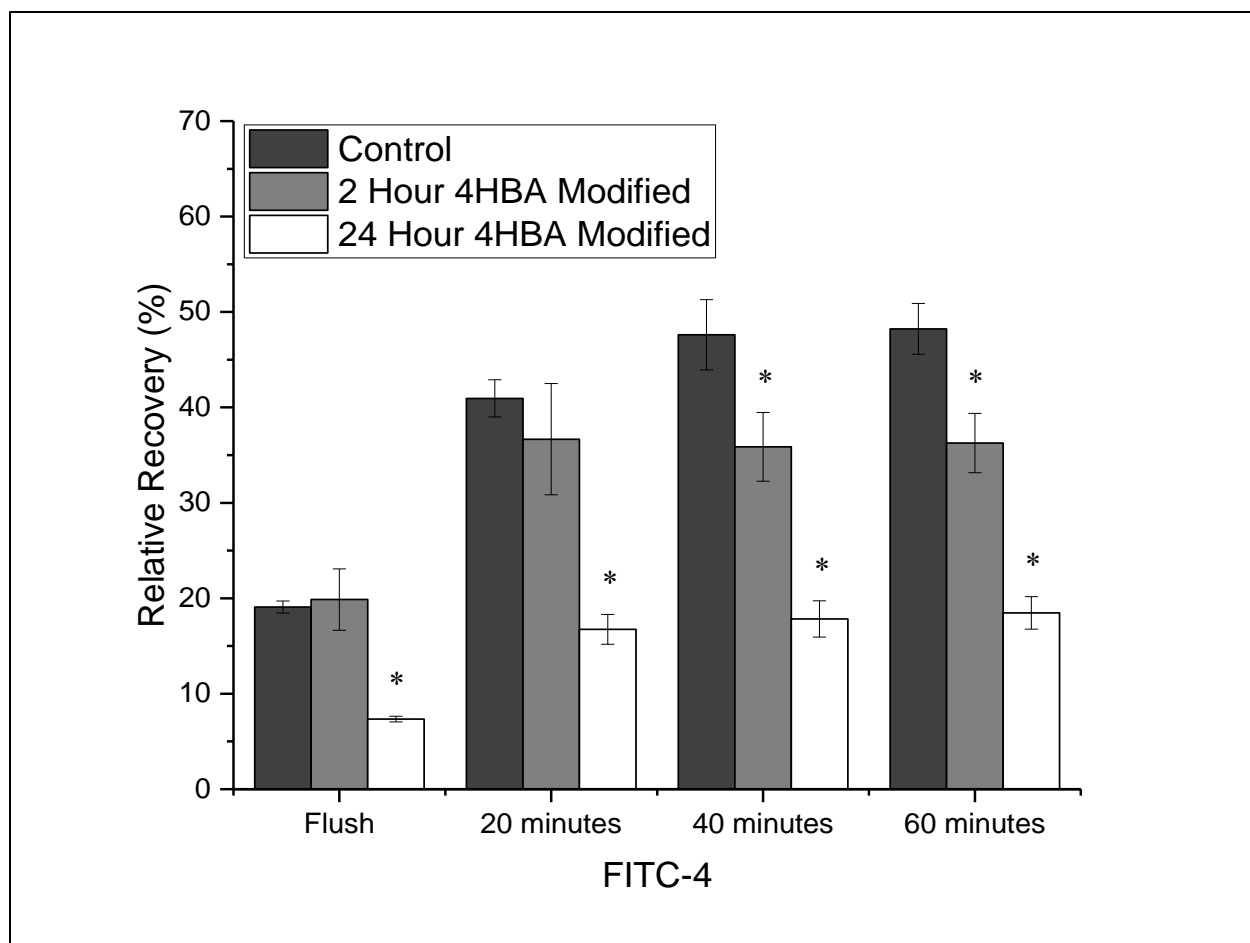
Figure 11. FITC-4 relative recovery for control, 2, and 24 hour 4HBA modified microdialysis probes. N=3, * indicate significant difference at the 95% confidence level using a two factor ANOVA with Bonferroni post hoc test.
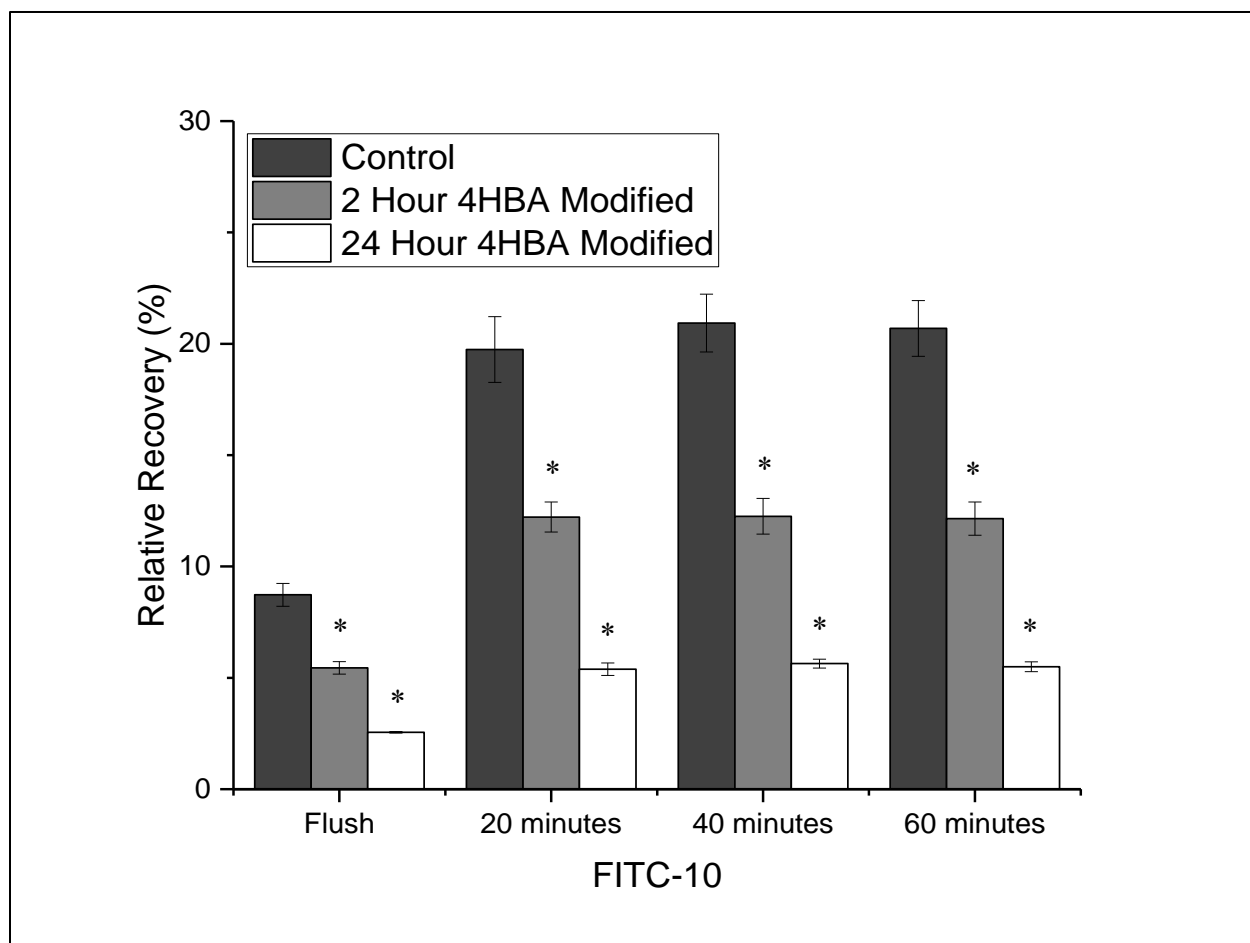
Figure 12. FITC-10 relative recovery for control, 2, and 24 hour 4HBA modified microdialysis probes. N=3, * indicate significant difference at the 95% confidence level using a two factor ANOVA with Bonferroni post hoc test.
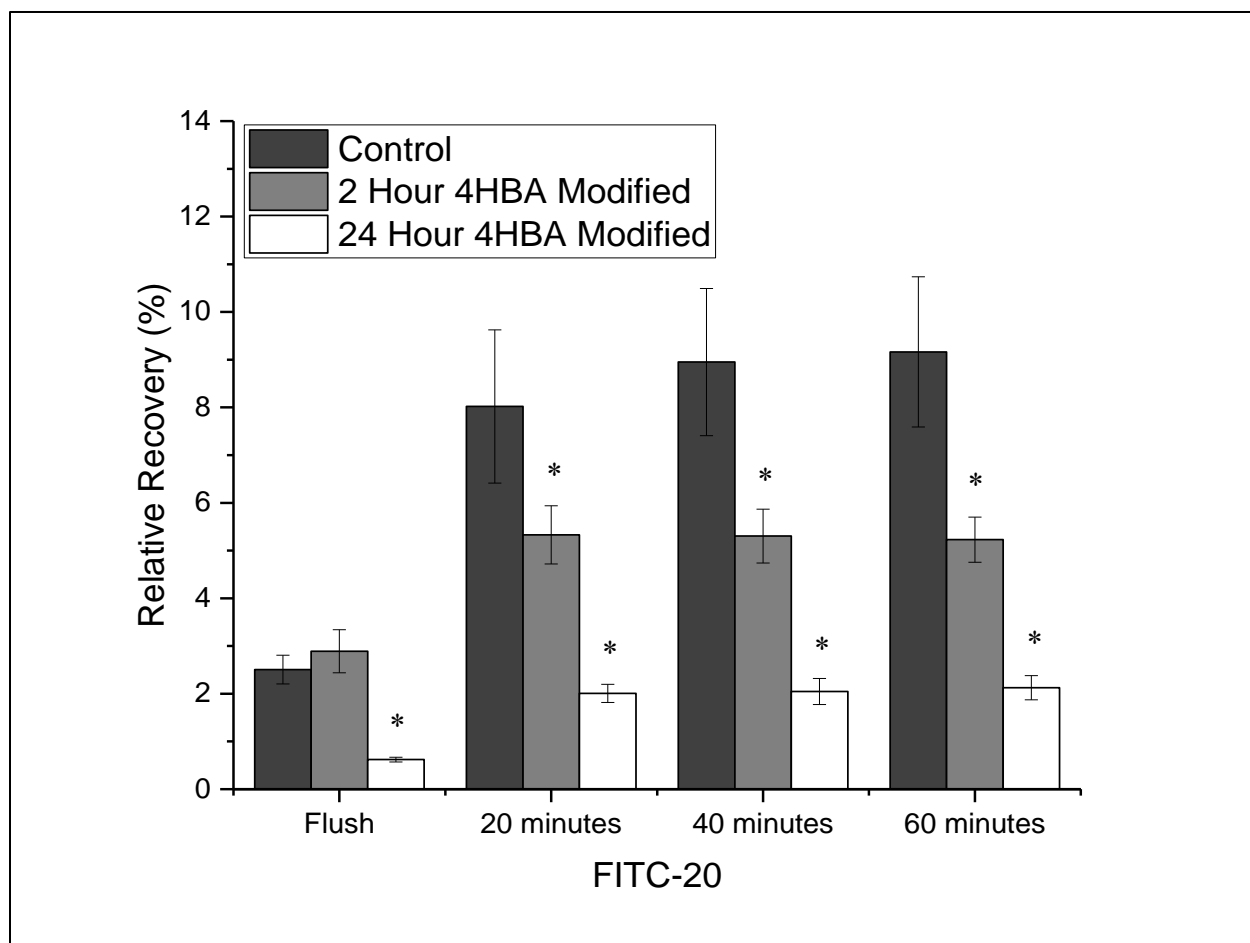
Figure 13. FITC-20 relative recovery for control, 2, and 24 hour 4HBA modified microdialysis probes. N=3, * indicate significant difference at the 95% confidence level using a two factor ANOVA with Bonferroni post hoc test.

Relative Recovery of Lysozyme

After observing the reduction in FITC-4, FITC-10 and FITC-20 RR by modification with 4HBA, lysozyme was tested to investigate if the reduction of the RR would occur by comparing protein and dextran RR. Lysozyme is a 14 kDa protein but is more globular in structure compared to dextran which is more linear.[135, 136] Figure 14 shows that there is no significant reduction in lysozyme RR for the 2 hour 4HBA modified microdialysis probes, but for the 24 hour 4HBA modified microdialysis probes the lysozyme concentration were below the detection limit of 25 μg/mL with a 500 μg/mL solution outside the probe. This suggests that pore blocking and/or charge-charge attraction is occurring after 24 hours of modification with 4HBA and laccase.
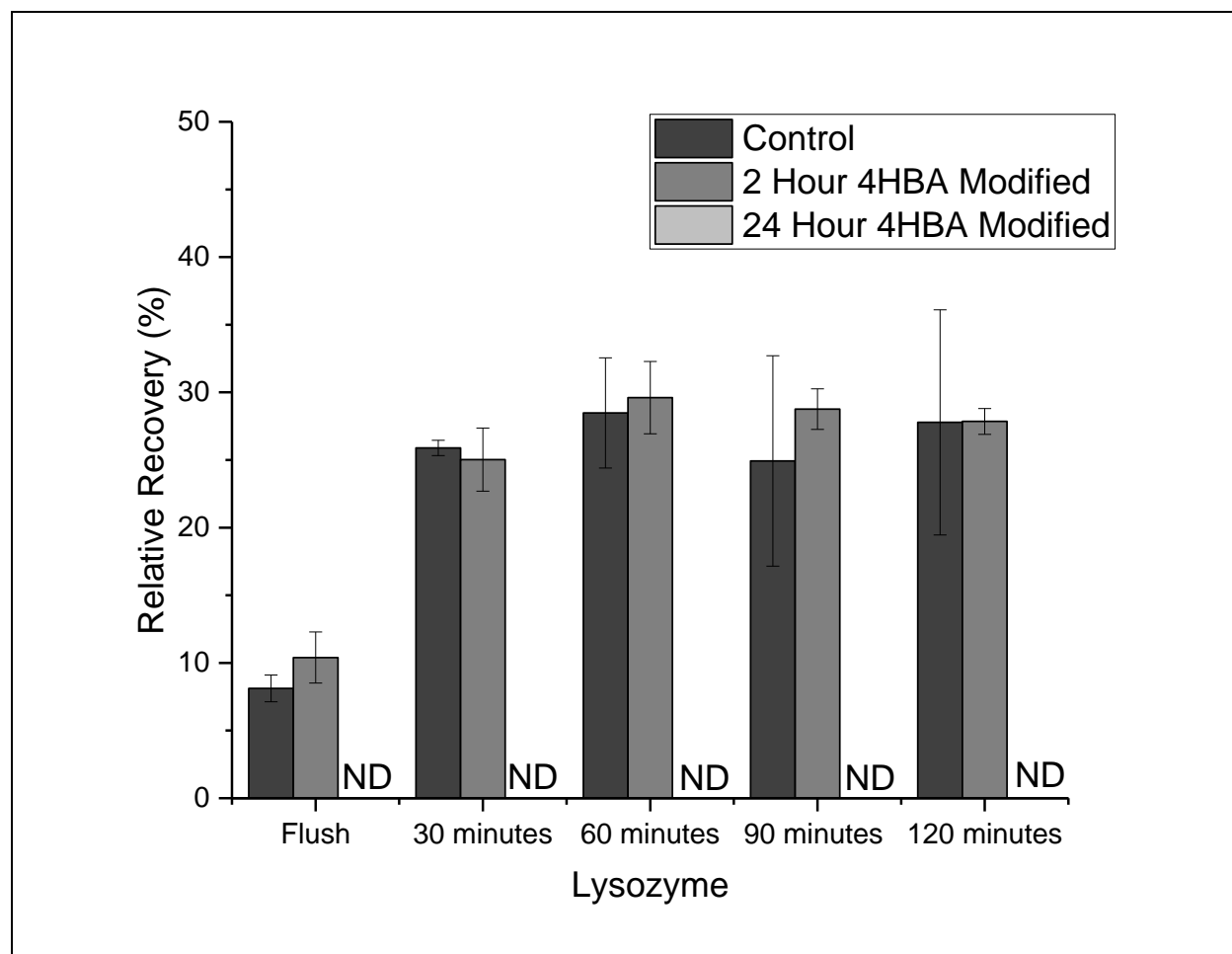
Figure 14. Lysozyme relative recovery for control, 2 hour, and 24 hour 4HBA modified microdialysis probes. Probes were placed in a solution containing 500 μg/mL of lysozyme. ND indicates not detected (detection limit of 25 μg/mL), N=3.

Relative Recovery of CCL2, VEGF, KC/GRO, aFGF, and TNF-α

        After measuring the RR of lysozyme, the RR of CCL2, aFGF, KC/GRO, TNF-α, and

VEGF were measured. The reason for choosing these analytes is due to their varying molecular

weights as well as isoelectric points shown in Table 6. The 4HBA modification introduces a

carboxylic acid functional group, which is deprotonated at pH 7.4, onto the membrane surface.

Different analytes may interact differently with the surface based on the charge-charge

interactions between the protein and the membrane surface. Also by varying molecular weight,

recovery enhancement may be altered due to the change in size of the pores based on the

modification time. For these experiments, 2 hour and 24 hour 4HBA modified membranes will

be compared with control microdialysis probes.

Table 6. Molecular weight and isoelectric point (pI) values for proteins whose relative recoveries were analyzed.

Protein	Molecular Weight (kDa)	pI
TNF-α	17.2	5.0
aFGF	15.5	5.7
VEGF	21	8.5
KC/GRO	7.8	9.1
CCL2	13.1	9.3
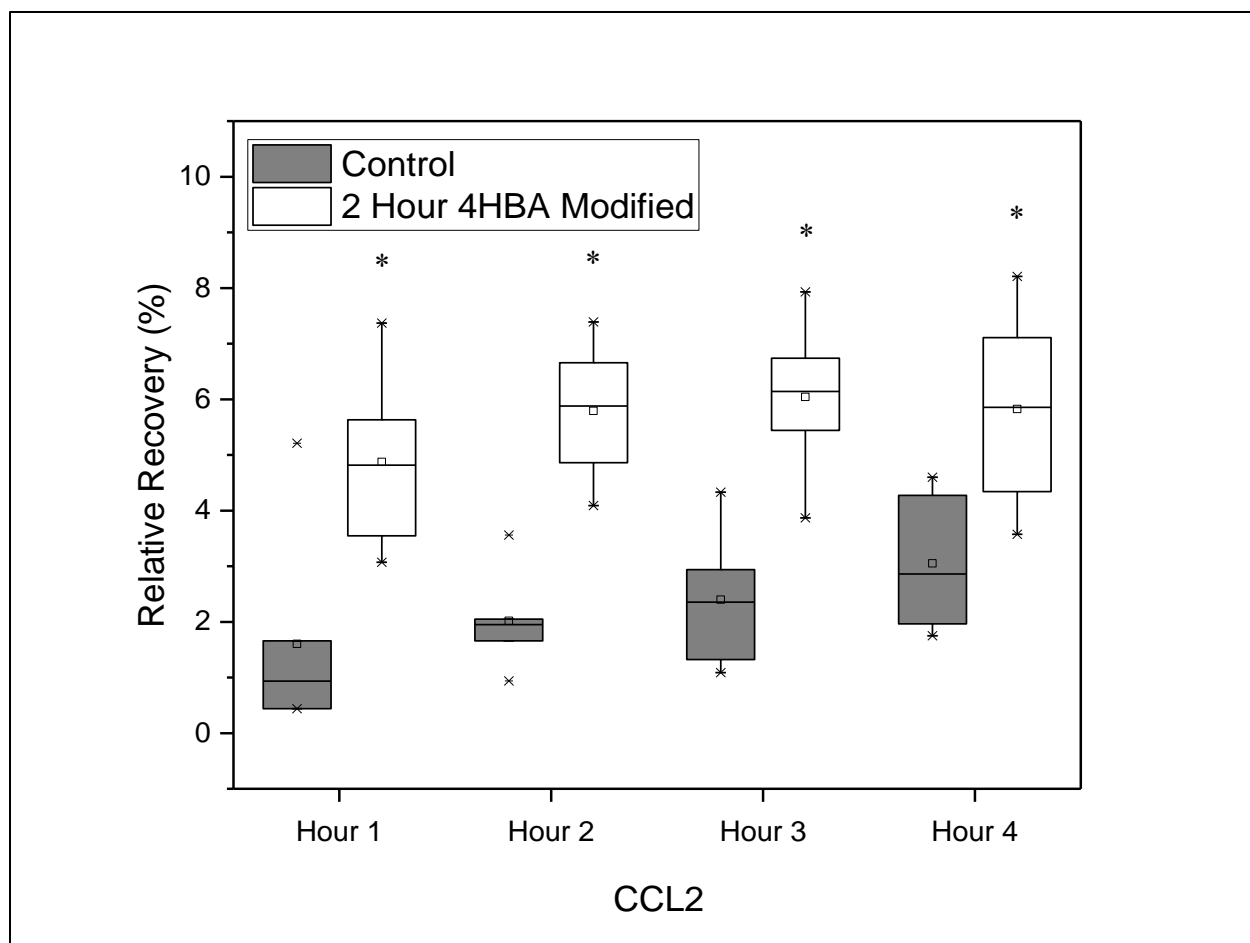
Figure 15. Box and whiskers plot of CCL2 relative recovery of control and 2 hour 4HBA modified microdialysis probes. N=6 The box represents the 25th-75th percentiles. The line through the box represent the median, whiskers represent the 5th and 95th percentile, and the □ represents the mean. * Indicates significantly different than the control at the 95% confidence level (p≤ 0.05) as determined by a 2 factor ANOVA with Bonferroni post hoc test.
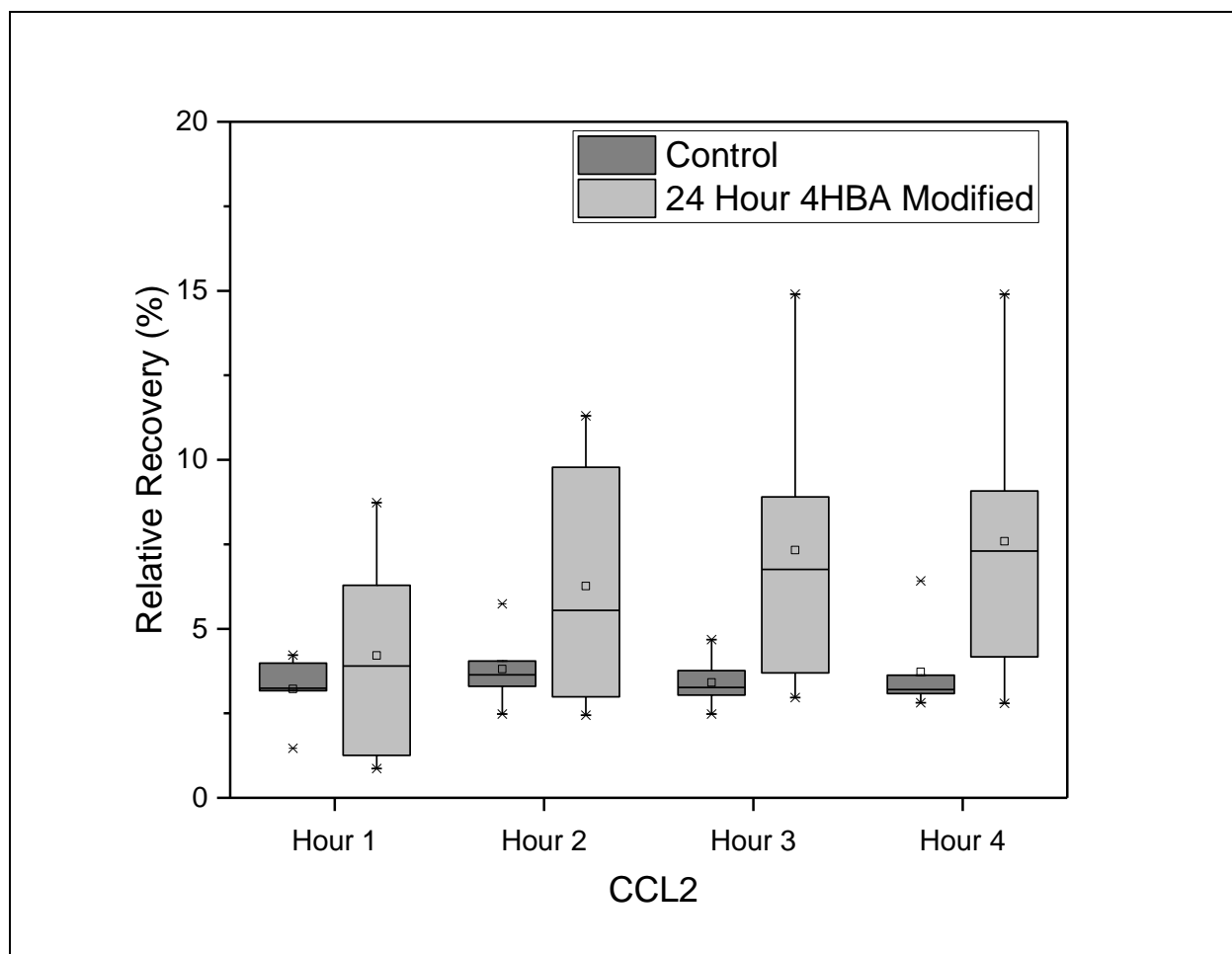
Figure 16. Box and whiskers plot of CCL2 relative recovery of control and 24 hour 4HBA modified microdialysis probes. N=6 Significance was compared between the control and 24 hour 4HBA modified microdialysis probes and the control at the 95% confidence level as determined by a 2 factor ANOVA with Bonferroni post hoc test.

For CCL2, the 2 hour modification showed a significant increase in RR between 90 and 190 % (Figure 15). For the 24 hour modification, CCL2 RR did not increase significantly overall (Figure 16). CCL2 is a 13.1 kDa protein so it is similar in molecular weight to lysozyme at 11 kDa. The lack of RR increase could be due to partial pore blockage which was observed with the FITC-labeled dextrans. Also, the isoelectric point of CCL2 is 9.25 which gives the protein an overall positive charge. This could explain the increase in RR for the 2 hour 4HBA modified membranes because CCL2 could bind to the surface due to the overall negative charge provided by the carboxylic acid functional group added by 4HBA. However, this was not observed in the 24 hour modified membranes due to the partial blockage of pores due to the increase in size and/or graft density with a longer modification time.
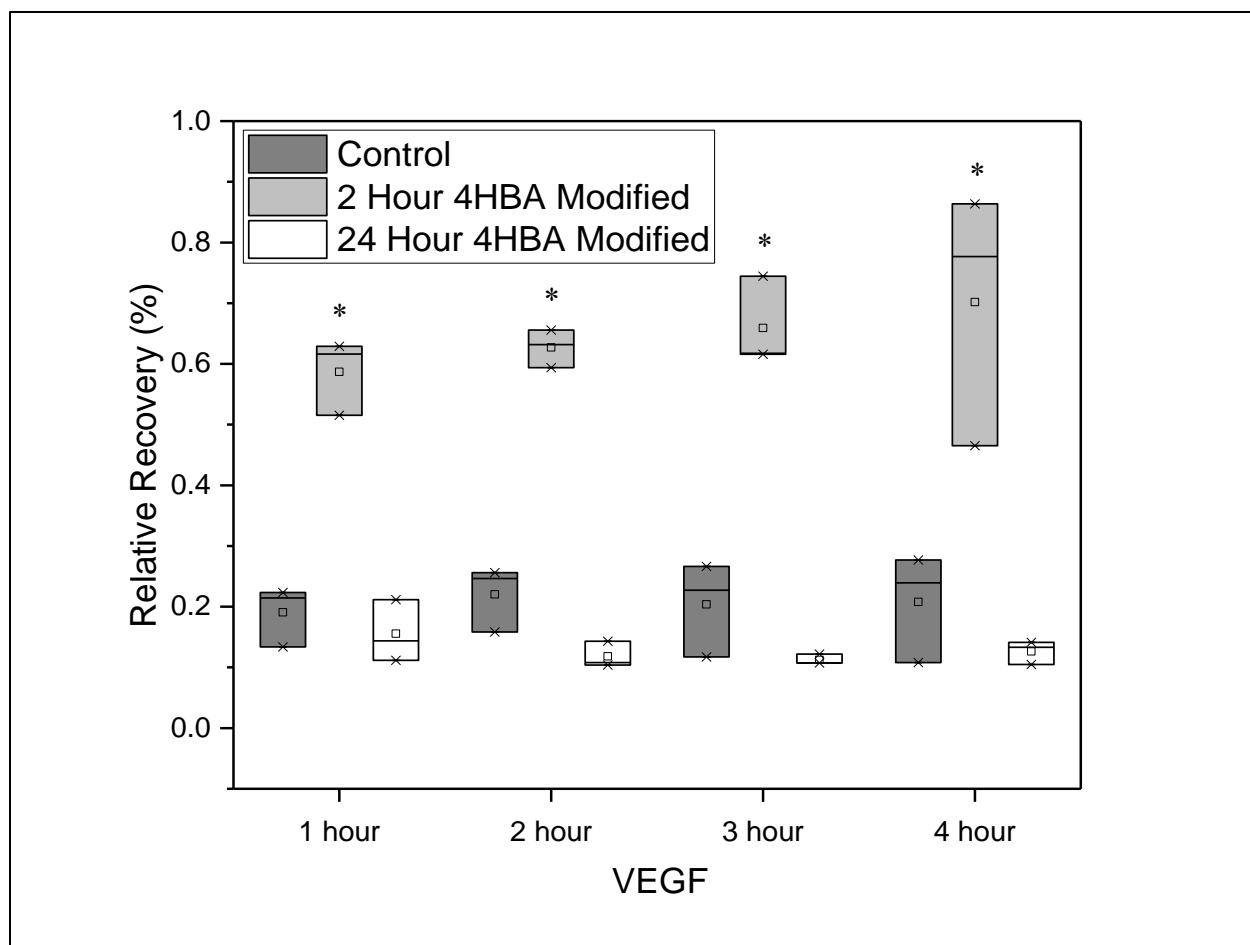
Figure 17. Box and whiskers plot of VEGF relative recovery of control, 2 and 24 hour 4HBA modified microdialysis probes. N=3 * Indicates significantly different than the control at the 95% confidence level as determined by a 2 factor ANOVA with Bonferroni post hoc test.

A comparison of RR for VEGF between control and 4HBA modified membranes is shown in Figure 17. This figure shows an increase in RR for the 2 hour 4HBA modification but not for the 24 hour modification. This absence of an increase in RR for the 24 hour 4HBA modification could be due to the pores size becoming reduced because of the longer modification time.
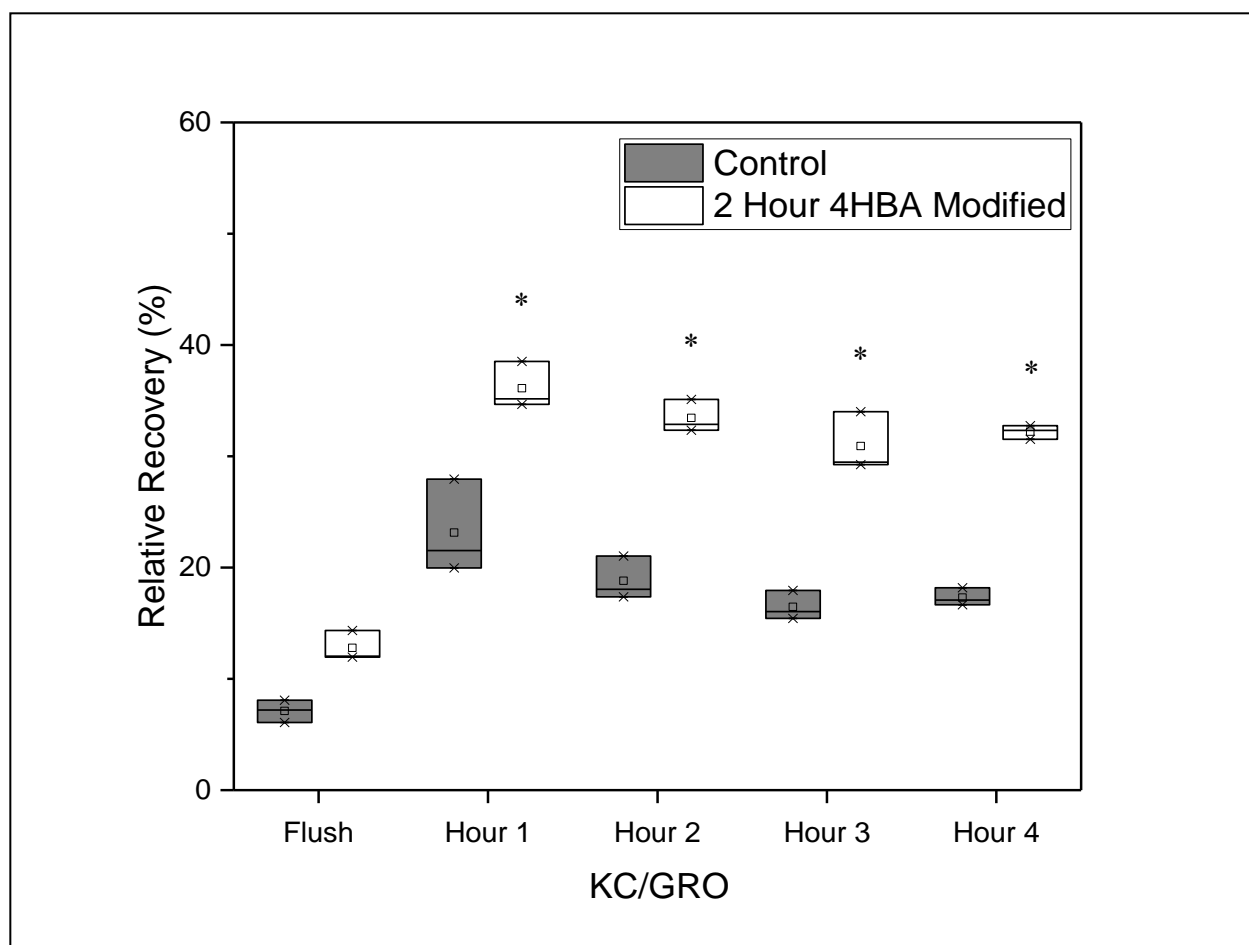
Figure 18. Box and whiskers plot of KC/GRO relative recovery of control, and 2 hour 4HBA modified microdialysis probes. N=3 * Indicates significantly different than the control at the 95% confidence level as determined by a 2 factor ANOVA with Bonferroni post hoc test.

KC/GRO is a 7.8 kDa protein with an isoelectric point of 9.1. KC/GRO relative recovery was analyzed because at pH 7.4 the protein has an overall positive charge. As seen with CCL2 and VEGF which also have isoelectric points above 7.4, the relative recovery increased upon modification with 4HBA for 2 hours. In Figure 18, the relative recovery of KC/GRO was shown to increase by the addition of the 4HBA polymer after modification for 2 hours. This is consistent with the increase in relative recovery after modification with 4HBA for 2 hours for proteins with isoelectric points above 7.4.
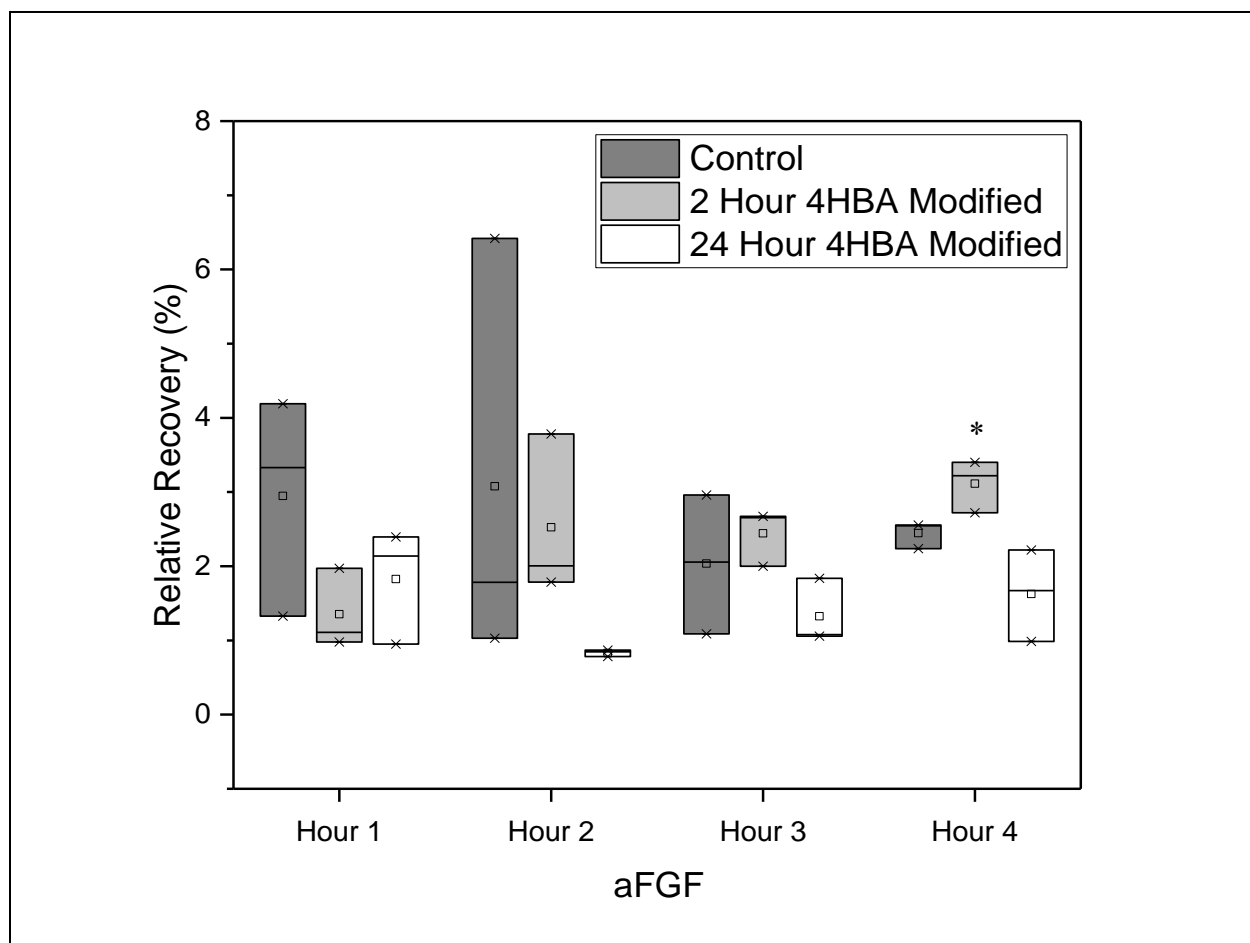
Figure 19. Box and whiskers plot of aFGF relative recovery of control, 2 and 24 hour 4HBA modified microdialysis probes. N=3 * Indicates significantly different than the control at the 95% confidence level as determined by a 2 factor ANOVA with Bonferroni post hoc test.
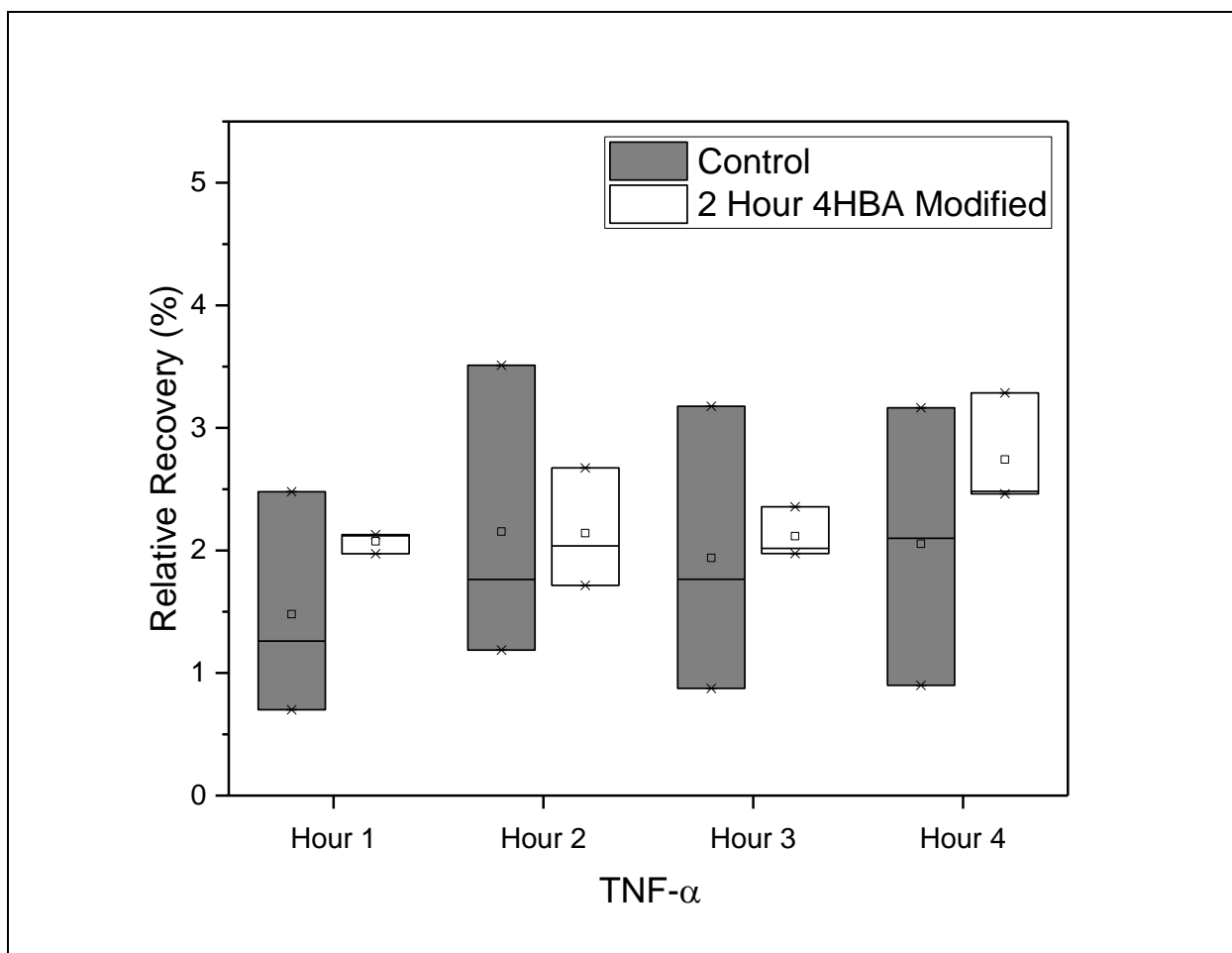
Figure 20. Box and whiskers plot of TNF-α relative recovery of control, 2 hour 4HBA modified microdialysis probes. N=3 * Indicates significantly different than the control at the 95% confidence level as determined by a 2 factor ANOVA with Bonferroni post hoc test.

For aFGF, there was a significant increase in RR at hour 4 between the control and 2 hour 4HBA modified membranes (Figure 19). CCL2 (13.1 kDa) is slightly smaller than aFGF (15.5 kDa), and also aFGF has an overall negative charge based on the isoelectric point (pI 5.6). The charge-charge repulsion between aFGF, and 4HBA could explain the lack of RR increase. RR of TNF-α a 17.2 kDa protein with an isoelectric point of 5.0 was analyzed for the 2 hour 4HBA modification. The RR for TNF-α after 2 hour 4HBA modification, as shown in Figure 20, was

not significantly different than the control RR this could be due to charge-charge repulsion between the negatively charged surface and TNF-α which has an overall negative charge.

For CCL2, VEGF, and KC/GRO the RR increased for the 2 hour modification. RR did not increase with the 2 hour 4HBA modification for aFGF and TNF-α. This RR increase was not observed for CCL2 and VEGF for the 24 hour modification time. For aFGF the increase in RR was only observed at hour 4 for the 2 hour modification time. TNF-α and aFGF have isoelectric points of 5.0, and 5.7 compared to CCL2, VEGF, and KC/GRO at 9.3, 8.5, and 9.1. The modification adds a negative charge onto the surface by the carboxylic acid functional group. Being that aFGF and TNF-α have an overall negative charge there may be charge repulsion between the protein and the surface. For CCL2, VEGF, and KC/GRO the overall positive charge may introduce charge attraction between the protein and the surface. This could lead to the larger increase in RR due to the attractive force between CCL2, VEGF, and KC/GRO.

Conclusions

This chapter shows successful attachment of 4HBA polymers onto flat sheet and microdialysis membranes using both XPS and ATR-FTIR data. BSA adsorption onto PES flat sheet shows an initial increase followed by a decrease in BSA adsorption that becomes significant at 24 hours. For lysozyme the adsorption increased upon addition of 4HBA polymers onto the surface. RR experiments using FITC-labeled dextrans showed a decrease in RR for the 24 hour reaction time of approximately 70% and a slight decrease for the 2 hour reaction time. The RR experiment for lysozyme showed no significant difference for the 2 hour modification time but was not detectable for the 24 hour modification time. For CCL2, VEGF, and KC/GRO the 2 hour reaction time showed a two to three fold increase in RR for the 2 hour 4HBA modification.

CHAPTER 3. COMPARISON OF PROTEIN ADSORPTION METHODS

Introduction

Many researchers are quantifying protein absorption onto surfaces to improve implantable devices as well as membrane purification devices. Nonspecific adsorption of proteins can lead to reduced recovery across the membrane surface, fouling of the device and inaccurate measurements.[62-64] Protein adsorption is a commonly measured parameter to determine the effectiveness of their device or treatment, but many different methods are used to determine the amount of protein adsorbed.[137] When making a comparison between different modifications to a surface, one must consider the fact that protein adsorption may be measured using different methods. This can make comparing reported results from different methods difficult.

Materials and Methods

Materials

Bovine Serum Albumin fraction V, was purchased from Rockland (Pottstown, PA) and was certified immunoglobulin and protease free. Lysozyme was purchased from MP biomedicals (Solon, OH). 100 kDa PES flat sheet membranes (UE50) were purchased from Sterlitech (Kent, WA). Fluorescein isothiocyanate isomer 1 was purchased from Alfa Aesar (Haverhill, MA). Dimethyl sulfoxide was purchased from Electron Microscopy Sciences (Hatfield, PA). Sodium hydroxide was purchased from Mallinckrodt Chemicals (St. Louis, MO). Sodium dodecyl sulfate was purchased from J. T. Baker (Phillipsburg, NJ). Dibasic sodium phosphate (ACS grade) was purchased from EMP (Howell, NJ). Sodium chloride

bioXtra grade, potassium chloride (99.0%), and monobasic potassium phosphate (ACS grade) where purchased from Sigma Aldrich (St. Louis, MO).

Protein Adsorption Measured by Absorbance at 280 nm and BCA Assay

PES flat sheet membranes of approximately 25 cm^2 were cut into pieces of approximately 1 cm^2 and placed in a solution containing either 0.5 mg/mL or 0.25 mg/mL of BSA or lysozyme in PBS (137 mM NaCl, 2.7 mM KCl, 10.1 mM Na$_2$HPO$_4$, 1.8 mM KH$_2$PO$_4$) pH 7.4. The solution was placed on a plate shaker and samples were then collected from the solution after 2, 24, 48 and 72 hours. Then, an absorbance value at 280 nm was measured and samples were also analyzed using a standard BCA assay.[130]

Protein Adsorption Measured by Removal with SDS and 0.05 M Sodium Hydroxide

PES flat sheet membranes of approximately 5 cm^2 were cut into pieces of approximately 1 cm^2 and placed in a solution containing 4.5 mg/mL of either BSA or lysozyme in PBS pH 7.4. The solution was placed on a plate shaker and the membranes were removed from the solution after 2, 24, 48 and 72 hours and placed in a solution containing 2 wt % SDS and 0.05 M NaOH for 2 hours.[87] An aliquot was then removed and an absorbance value at 280 nm was measured. This value was then compared to a calibration curve of known BSA and lysozyme concentrations in 2 wt% SDS and 0.05 M NaOH.

Protein Adsorption Measured using FITC-labeled Proteins

FITC-Labeling BSA and Lysozyme

FITC-labeling of both BSA and lysozyme was performed by placing 1 mg of FITC into 10 μL of DMSO, and dissolving 10 mg of BSA or lysozyme into 990 μL of 0.1 M phosphate at pH 8.0. These two solutions were then combined and incubated at 37°C for 2 hours. The solution was then filtered using a NAP-25 Sephedex G-25 column to separate the FITC-labeled

protein and the free FITC. The concentration of FITC labeled protein was determined based on the absorbance at 280 nm.

Protein Adsorption Measurements

For the FITC-BSA adsorption experiment PES flat sheet membranes were placed in a solution containing 74 µg/mL of FITC-BSA in PBS pH 7.4 and allowed to incubate for 2, 24, 48 or 72 hours. Then, the solution was removed and the fluorescence intensity measured using an excitation wavelength was 485 nm and the emission was measured from 500-650 nm. The emission maxima for FITC-BSA after incubation with the PES membranes were between 517 nm and 520 nm. For FITC-lysozyme, the membranes were placed in a solution containing 5.5 µg/mL of FITC-lysozyme in PBS pH 7.4. The emission maxima were between 515 nm and 517 nm for FITC-lysozyme after incubation with the membrane. To determine the concentration a calibration curve was made for both FITC-BSA and FITC-lysozyme from the stock solutions above. The concentration in µg/mL was then converted to µg/cm^2 based on the sum of the surface areas of the membrane pieces and the volume of the solution.

Results and Discussion

Protein Adsorption Measured by Absorbance at 280 nm and BCA Assay

Initially an experiment was performed using a surface areas differing by tenfold (approximately 1 cm^2 and 10 cm^2). The difference in concentration between the solution with the membrane and without the membrane was non-detectable for both the 280 nm, and BCA assay detection methods using incubation times of 2, 24, and 48 hours. To combat the issue of not being able to detect the difference in concentration between the solution with the membrane and without the membrane, the total surface area was increased to approximately 25 cm^2. Two aliquots of the solution (with and without membranes) were used for the BCA and absorbance at

280 nm detection methods. The membranes were also incubated in a solution containing either

0.5 mg/mL or 0.25 mg/mL of BSA or lysozyme. A comparison between the two methods is

shown in Table 7 and 8 for BSA and lysozyme.

Table 7. Comparison of BCA and 280 nm for BSA (0.50 mg/mL, 0.25 mg/mL). Symbol indicates significantly different at the 95% confidence level as compared to ND(*) and 24 hour time point (#).

Detection Method	Concentration	2 hours ($\mu g/cm^2$)	24 hours ($\mu g/cm^2$)	48 hours ($\mu g/cm^2$)	72 hours ($\mu g/cm^2$)
Absorbance at 280 nm	0.50 mg/mL	ND	22.88±11.90*	43.96±21.97*	ND
	0.25 mg/mL	ND	16.44±3.38*	40.22±4.51*#	32.35±1.66*#
BCA	0.50 mg/mL	ND	ND	4.49 ±1.69*	3.80±1.95*
	0.25 mg/mL	ND	ND	ND	3.32±1.48*

For BSA protein adsorption measured using the detection method of absorbance at 280

nm; there was no significant difference between amount of protein adsorbed per unit surface area

for the 24 hour and 48 hour incubation time. There was also no significant difference at the 72

hour incubation time for the BCA detection method. For the 72 hour incubation time, the

amount of protein adsorbed measured by the absorbance change at 280 nm was non-detectable

for the BSA concentration of 0.5 mg/mL, but it was detectable for the 0.25 mg/mL

concentration. For the BCA detection method the amount of protein adsorbed onto the surface

was detectable for the 0.5 mg/mL BSA concentration but non-detectable for the 0.25 mg/mL

BSA concentration. The 2 hour incubation showed non-detectable amounts of protein adsorbed

for both the absorbance at 280 nm and BCA detection methods. The 24 hour incubation time

also showed a non-detectable amount of protein adsorbed using the BCA method but showed

detectable amounts using the absorbance at 280 nm. Between the absorbance at 280 nm and

BCA detection methods at the 48 hour incubation time using the 0.50 mg/mL concentration of

BSA was not significantly different. At the 72 hour incubation time the methods were compared

using the 0.25 mg/mL concentration and showed a significant difference between the two

methods. As can be seen in Table 7 incubation time affects protein adsorption measurements as

well as the concentration of the protein used. Also, protein adsorption calculated using the

absorbance at 280 nm is significantly larger than that calculated from the same solution using the

BCA method. This could be due to these methods measuring different properties of the

molecules and possible interference in measuring the absorbance at 280 nm. The difference

method using the absorbance at 280 nm uses the intrinsic absorbance from aromatic amino acids

present in the protein, mostly tyrosine and tryptophan.[129] The BCA assay is a colorimetric assay

that uses the reduction of Cu^{2+} to Cu^{1+} by proteins in an alkaline medium with detection of the

Cu^{1+} by bicinchoninic acid.[130]

Table 8. Comparison of BCA and 280 nm for Lysozyme (0.50 mg/mL, 0.25 mg/mL). * indicates difference as compared to ND.

Detection Method	Concentration	2 hours ($\mu g/cm^2$)	24 hours ($\mu g/cm^2$)	48 hours ($\mu g/cm^2$)	72 hours ($\mu g/cm^2$)
Absorbance at 280 nm	0.5 mg/mL	ND	ND	16.60±6.21*	12.39±3.23*
	0.25 mg/mL	ND	5.13±3.50*	18.94±2.45*	16.84±12.46*
BCA	0.5 mg/mL	ND	ND	ND	9.23±4.51*
	0.25 mg/mL	ND	3.33±1.50*	4.99±2.56*	4.90±1.45*

For lysozyme (Table 8), there is no significant difference between the 48 hour and 72

hour incubation period for absorbance at 280 nm and for 72 hours BCA detection method. Since

there was no significant difference between the concentrations of lysozyme for the BCA and

absorbance 280 nm detection methods individually, the data was pooled to compare the protein

adsorbed using the two detection methods. There was found to be no significant difference

between the BCA and 280 nm detection methods at the 72 hour time point; data was pooled for

the comparison of methods. For 24 hour and 48 hour time points, the data for the 0.25 mg/mL

concentration was used for comparison and showed no significant difference in the methods for

the 24 hour incubation time, but at the 48 hour incubation time the difference is significant. For

lysozyme for the absorbance at 280 nm and BCA assay 72 hours of incubation in necessary to

detect protein adsorption. Lysozyme protein adsorption determined using the BCA and

absorbance at 280 nm detection method also showed different protein adsorption values for

different incubation times as well as different concentrations. This again could be due to the

different properties of the molecule and possible interference using the absorbance at 280 nm.

Comparison of Protein Adsorption Methods using Detection Methods of Absorbance at 280

nm, BCA Assay, FITC-Labeled Proteins, and a Removal Method using SDS and NaOH

To compare with the removal method using SDS and NaOH, and FITC-labeling, the 0.25

mg/mL protein concentration was used for the BCA and absorbance at 280 nm detection

methods. Table 9 shows the comparison of the different methods using BSA. For the BCA assay

detection method the protein adsorption, is non-detectable until 72 hours of incubation with the

protein solution. Table 10 shows a comparison of different detection methods for lysozyme.

The amount of protein adsorbed was non-detectable for the 2 hour incubation time for the

absorbance at 280 nm and BCA detection methods.

A comparison between the different detection methods for each incubation was

performed. For the 2 hour incubation time, the BCA and absorbance at 280 nm methods showed

non-detectable amount of BSA adsorbed on the surface. For the 24 hour incubation time, the

removal method with SDS and NaOH showed significantly different protein adsorption than the

other three methods (absorbance at 280 nm, BCA, and FITC-BSA) and also the BCA detection

method showed non-detectable concentration of BSA adsorption. For the 48 hour incubation

time, the FITC-BSA method was significantly different compared to the absorbance at 280 nm and removal method with SDS and NaOH. Also, the removal method with SDS and NaOH was significantly different than the absorbance at 280 nm detection method. For the 72 hour incubation period, the removal method with SDS and NaOH was significantly different than the other three detection methods; the absorbance at 280 nm was significantly different than the BCA, and FITC-BSA detection methods.

Next a comparison was made for each method within each incubation time. For the removal method with SDS and NaOH, the 2 hour incubation time was significantly different than the other three incubation times. The absorbance at 280 nm detection method showed a significant difference between the 24 hour incubation time and the 48 and 72 hour incubation times. At the 2 hour incubation time, protein adsorption was non-detectable for the absorbance at 280 nm detection method. For the BCA assay detection method, the 72 hour incubation was the only incubation time to show detectable protein adsorption. The FITC-BSA detection method showed a significant difference between the 2 hour and 24 hour incubation time, the 24 hour and 48 hour incubation time, and the 72 hour incubation time with the 2, 24, and 48 hour incubation times.

For lysozyme a comparison was made between each detection method within each incubation time. For the 2 hour incubation time, the removal method with SDS and NaOH and FITC-lysozyme were significantly different, and for the absorbance at 280 nm and BCA assay showed non-detectable values of protein adsorbed onto the surface.

Table 9. Comparison of methods to measure BSA adsorption at various time points using the protein adsorption methods by difference using detection methods of absorbance at 280 nm, BCA assay, and FITC-labeled BSA methods and removal method using SDS and NaOH. SDS (*) 280 nm (#), BCA (^), and FITC-BSA(~)indicates significantly different at the 95% confidence level compared to detection listed next to symbol. ND=not detected.

Method	2 hours ($\mu g/cm^2$)	24 hours ($\mu g/cm^2$)	48 hours ($\mu g/cm^2$)	72 hours ($\mu g/cm^2$)
SDS/NaOH	12.27±2.83~	89.07±26.46#~	69.07±2.21~	73.01±15.05#^~
280 nm	ND	16.44±3.38*	40.22±4.51*~	32.35±1.66*^
BCA Assay	ND	ND	ND	3.32±1.48*#
FITC-BSA	5.70±0.41*	7.90±0.14*	6.74±0.66*	9.15±0.10*#

Table 10. Comparison of methods to measure lysozyme adsorption at various time points using the protein adsorption methods by difference using detection methods of absorbance at 280 nm, BCA assay, and FITC-labeled BSA methods and removal method using SDS and NaOH. SDS (*) 280 nm (#), BCA (^), and FITC-lysozyme(~) indicates significantly different at the 95% confidence level compared to detection listed next to symbol. ND=not detected.

Method	2 hours ($\mu g/cm^2$)	24 hours ($\mu g/cm^2$)	48 hours ($\mu g/cm^2$)	72 hours ($\mu g/cm^2$)
SDS/NaOH	34.05±6.43~	15.25±5.20#^~	17.70±2.73^~	20.59±4.00~
280 nm	ND	5.13±3.50*	18.94±2.45^~	16.84±12.46
BCA Assay	ND	3.33±1.50*	4.99±2.56*#	4.90±1.45
FITC-Lys	0.33±0.35*	0.61±0.14*	0.36±0.10*#	0.72±0.13*

Then, for the 24 hour incubation time there was a significant difference between the SDS and NaOH removal method compared to the other three detection methods (BCA assay, absorbance at 280 nm, and FITC-lysozyme). For the 48 hour incubation time, the absorbance at 280 nm was significantly different than the BCA assay and FITC-lysozyme detection methods, and the removal method with SDS and NaOH was significantly different than the BCA assay and FITC-lysozyme detection methods. The 72 hour incubation time showed a significant difference between the removal method with SDS and NaOH and FITC-lysozyme.

Next a comparison was made between incubation time for each method. For the absorbance at 280 nm and the BCA detection methods the 2 hour incubation time was

significantly different than the 24, 48 and 72 hour incubation time. Then, for FITC-lysozyme, 2

hour and 72 hour incubation times were significantly different; for the removal method with SDS

and NaOH the 2 hour incubation time and the 24 and 48 hour incubation times were significantly

different.

The absorbance at 280 nm and removal with NaOH and SDS showed significantly higher

protein adsorption than the BCA and FITC-labeled protein detection methods. This could be due

to the SDS/NaOH removal method using the absorbance at 280 nm as the detection method to

quantify protein adsorption. The absorbance at 280 nm could have interference from other

molecules in the solution. The FITC-labeled protein and removal method with NaOH and SDS

showed detectable protein adsorption values for all incubation times. Being that the removal

method with SDS and NaOH is dependent on the interactions between the surface and the

protein the removal with SDS and NaOH may become more or less effective. This can become

an issue when comparing a modified surface to an unmodified surface especially if the

modification is reducing nonspecific adsorption. This can falsely lead to an increase in protein

adsorption when actually the removal was more effective for one surface compared to another.

Conclusions

When comparing protein adsorption values reported in the literature, it is necessary to

consider what methods they used to determine protein adsorption. Different methods, even

when analyzing the same sample, can give significantly different protein adsorption values this is

shown, in Table 7 and 8, that the BCA method and the absorbance at 280 nm method for

lysozyme and BSA. Incubation time and detection methods can also be a factor in comparing

protein adsorption values.

CHAPTER 4. CHARACTERIZATION OF LACCASE REACTION WITH 4-HYDROXYBENZOIC ACID

Introduction

Determination of the structure and molecular weight distribution of the polymer that is added to the PES membrane surface is important to understanding the protein adsorption properties of the polymer.   Understanding of the structure of the polymer such as the structure of the chains in terms of branching, the size, and molecular weight distribution can give insight about the transport across the membrane. Others have reported using gel permeation chromatography the number average molecular weight (Mn) of 8,500 Da and a weight average molecular weight (Mw) of 17,550 Da for a 4 hour reaction time on the reaction of 4HBA with laccase, *Trametes villosa*. This is a different species than the *Trametes versicolor* enzyme that is used in this dissertation.[93] The polymerization reaction between laccase from *Trametes versicolor,* 3-chloro-4-hydroxybenzic acid (3Cl4HBA) and 4HBA were characterized to determine the distributions of molecular weights present at different polymerization times. This information provides insight into the modification that is occurring on the PES membrane surface.

Materials and Methods

Materials

Laccase form *Trametes versicolor*, sodium acetate, fluorescein isothiocyanate dextran 4,000, and methyl orange were purchased from Sigma Aldrich (St. Louis, MO), 4-hydroxybenzoic acid was purchased from TCI (Portland, OR). 3-chloro-4-hydroxybenzoic acid, and 2-5-dihydroxybenzoic acid was purchased from Alfa Aesar (Haverhill, MA). HPLC grade

methanol and water were purchased from Fisher Scientific (Waltham, MA). Glacial acetic acid was purchased from VWR international (Radnor, PA). NAP-25 Sephedex G-25 column were purchased from GE healthcare (Chicago, IL). Amicon Ultra centrifugal filters of 3, 10, and 50 kDa molecular weight cut-off were purchased from EMD Millipore (Billerica, MA).

HPLC-UV Experiment to Separate Monomer from Polymer

An initial experiment was performed to see if using high performance liquid chromatography (HPLC) with an ultraviolet (UV) detector, the monomer (4HBA or 3Cl4HBA) could be separated from any formed polymer. First the reaction of 28.8 mM 3Cl4HBA and 4HBA in the presence of 0.5 U/mL of laccase in sodium acetate buffer pH 5.0 was allowed to react for 1 and 2 hours. After the specified reaction time, 2 mL of the 10 mL total sample was then centrifuged using a bench top centrifuge for 2 minutes. The precipitate was then collected and dissolved in 500 µL of 75% methanol/25% water and half of this sample was then filtered through a 0.2 µm syringe filter. Then, the samples were analyzed using the HPLC-UV using a C18 5 µm column, solvent of 65% methanol/35% water at a flow rate on 1 mL/min for 20 minutes, at a wavelength of 254 nm.

MALDI-TOF

To further analyze the polymer a polymerization solution with 0.5 U/mL of laccase and 28.8 mM 4HBA in sodium acetate pH 5 in a total volume of 2 mL was made. Then, a 90 µL aliquot of the solution was added every 15 minutes to a conical tube containing 10 µL of 10% acetic acid to reduce the pH to 2 and halt the reaction for a total of 3 hours. The samples were then filtered through a 10 kDa molecular weight cut-off centrifugal filter to remove the laccase enzyme. Each sample was then diluted by 50% with 1 M 2,5-dihydroxybenzoic acid in water and then spotted on a MALDI plate in triplicate.

Separation of Polymer from Monomer using Molecular Weight Cut-Off Filters and

Analyzing the Effluent using HPLC

To determine the molecular weight of the polymer, a separation technique was performed using centrifugal filters with Amicon Ultra 3, 10 and 50 kDa molecular weight cut-off. This was in order to see if the polymer would be excluded by one of these MWCO filters and to give an approximate molecular weight range of the synthesized polymer. The filtrate collected was then analyzed on the HPLC-UV. A modification solution containing 28.8 mM 4HBA and 0.5 U/mL of laccase was allowed to react for 24 hours. Then, 500 μL samples were collected and placed in either a 3, 10 or 50 kDa MWCO centrifugal filter and centrifuged at 14,000 x g for 30 minutes. The filter was then inverted and placed in a new microcentrifuge tube which was centrifuged at 1,000 x g for 2 minutes. The samples where then diluted 1 to 100 in 50% methanol/water and were injected onto the HPLC-UV with a mobile phase of 50% acetonitrile/water and a flow rate of 1 mL/min.

Gel Permeation Chromatography (GPC) Separation of 4HBA Polymer Solution

GPC was performed to gain a better understanding of the molecular weight distribution of the polymer present. This experiment was performed on a reaction mixture that was allowed to react for 3 days. The 4HBA precipitate solution was made by taking 2 mL of the polymerization solution and centrifuging for 8 minutes at 13,500 rpm. The solution was decanted and the precipitate was reconstituted in 500 μL of sodium acetate pH 5.0 for each 1 mL aliquot, and then the two aliquots were combined. Then the NAP-25 Sephedex G-25 column (exclusion limit of 5,000 Da) was conditioned with 4 mL of 0.1 M sodium acetate pH 5.0 and either 1 mL of the 4HBA polymer solution or the reconstituted precipitate was loaded onto the column. Then, 0.1 M sodium acetate pH 5.0 was added to the column to continue the flow and

samples were collected in 1 minute intervals, equaling a sample volume of approximately 1.5 mL per minute, for a total of 21 minutes for the 4HBA precipitate solution and for 15 minutes for the 4HBA polymerization solution.

<u>HPLC-UV Analysis of GPC Effluent</u>

After performing GPC above the experiment was repeated and samples were collected every 15 seconds using the method described above. Samples 4 (4.25 minutes), 5 (4.5 minutes), 14 (7.25 minutes), 15 (7.5 minutes), and 16 (7.75 minutes) at the apex of the two peaks were selected for HPLC-UV analysis. Each sample was diluted 1 to 10 with acetonitrile. Then, 20 μL samples were in injected onto the column with a mobile phase of 50/50 acetonitrile/water at a flow rate of 1.5 mL/min. The UV detector was set at 254 nm using a Restek Ultra C18 5 μm column.

Calibration of GPC with Methyl Orange and FITC-4

This experiment was performed using the reaction mixture of 28.8 mM 4HBA with 0.5 U/mL of laccase from *Trametes versicolor* after 24 hours. After the NAP-25 Sephedex G-25 column was conditioned with 4 mL of 0.1 M sodium acetate pH 5.0, 1 mL of the 4HBA polymer solution was loaded onto the column. Then, 0.1 M sodium acetate pH 5.0 was loaded onto the column, and samples were collected in 30 second intervals for a total of 25 minutes. Then, the absorbance values of the samples were measured at 280 nm and 250 nm. Next solutions of fluorescein isothiocyanate (FITC-4) (4,389 Da) and methyl orange (327 Da) were loaded onto the column, and samples were collected using the procedure described above. The absorbance measurements were made at 460 nm and 494 nm for methyl orange and FITC-4 solutions.

GPC of 4-Hydroxybenzoic Acid Solution

The purpose of this experiment was to determine the molecular weight distribution of the 4HBA polymer formed in solution. This was done using a GPC column with an exclusion limit of 5,000 Da. This experiment was performed using the reaction mixture of 28.8 mM 4HBA with 0.5 U/mL of laccase from *Trametes versicolor* after 2 and 24 hours. After the NAP-25, Sephedex G-25 column was condition with 4 mL of 0.1 M sodium acetate pH 5.0, 1 mL of the 4HBA polymer solution was loaded onto the column. Then, 0.1 M sodium acetate pH 5.0 was loaded onto the column, and samples were collected in 30 second intervals for a total of 12.5 minutes. The absorbance values of the samples were measured at 280 nm and 250 nm. Also, a solution of 0.6 mg/mL of 4HBA (monomer) was analyzed.

Direct Infusion-Mass Spectrometry Methods

Three groups of samples were prepared, one with a buffer of 0.1 M sodium acetate pH 5.0, one with 0.1 M ammonium acetate pH 5.0, and one prepared with water. Also 28.8 mM 4HBA was made in each one of the solvents and another with 28.8 mM 4HBA and 0.5 U/mL laccase. First, the 4HBA and the 4HBA with laccase solutions, and a solution containing the solvent (blank) were passed through a NAP-25 column with the corresponding solvent and samples were collected from minute 5 to minute 10. The samples were then diluted 1,000 fold with HPLC grade water. These samples were then analyzed using direct infusion at a flow rate of 0.05 mL/min into an electrospray quadrupole ion trap mass spectrometer with a solvent of methanol with 0.1% formic acid.

Results and Discussion

HPLC-UV Experiment to Separate Monomer from Polymer

To detect polymer formation an experiment was designed to analyze the monomer and the polymerization solution after 1 and 2 hour reaction times. The samples collected were centrifuged and precipitate collected. The precipitate was then diluted in the mobile phase (75% methanol/water) was filtered through a 0.2 μm filter. Both of these samples were then analyzed on the HPLC-UV. In Figure 21, the results for the reaction with 4HBA are shown, and in Figure 21 the results for the reaction with 3Cl4HBA are shown. Both reaction mixtures show the presence of an initial peak at approximately 2.5 to 3 minutes which contains the monomer and possibly polymers that retain on the column similar to the monomer. This is confirmed by the retention time being similar to the monomer (4HBA, 3Cl4HBA) shown below. The next peak at approximately 8 minutes for the 1 hour reaction and 11 minutes for the 2 hour reaction is the polymer. Further analysis on these peaks was performed to confirm the identity of the first peak as the monomer and identify the molecular weight of the polymer using MALDI-TOF.
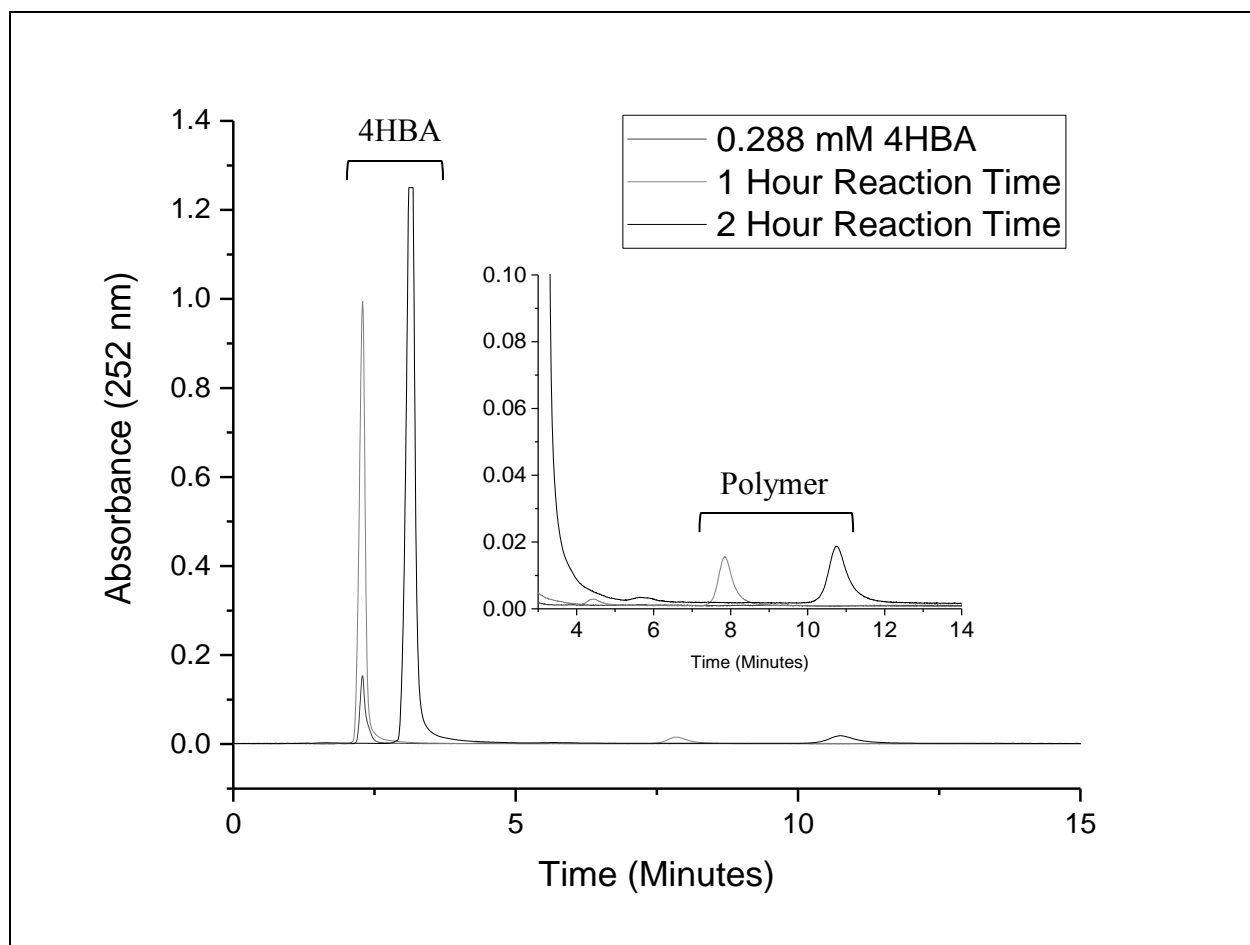
Figure 21. HPLC results for 4-hydroxybenzoic acid with laccase for a 1 and 2 hour reaction times as well as a solution of 4-hydroxybenzoic acid (0.288 mM 4HBA).
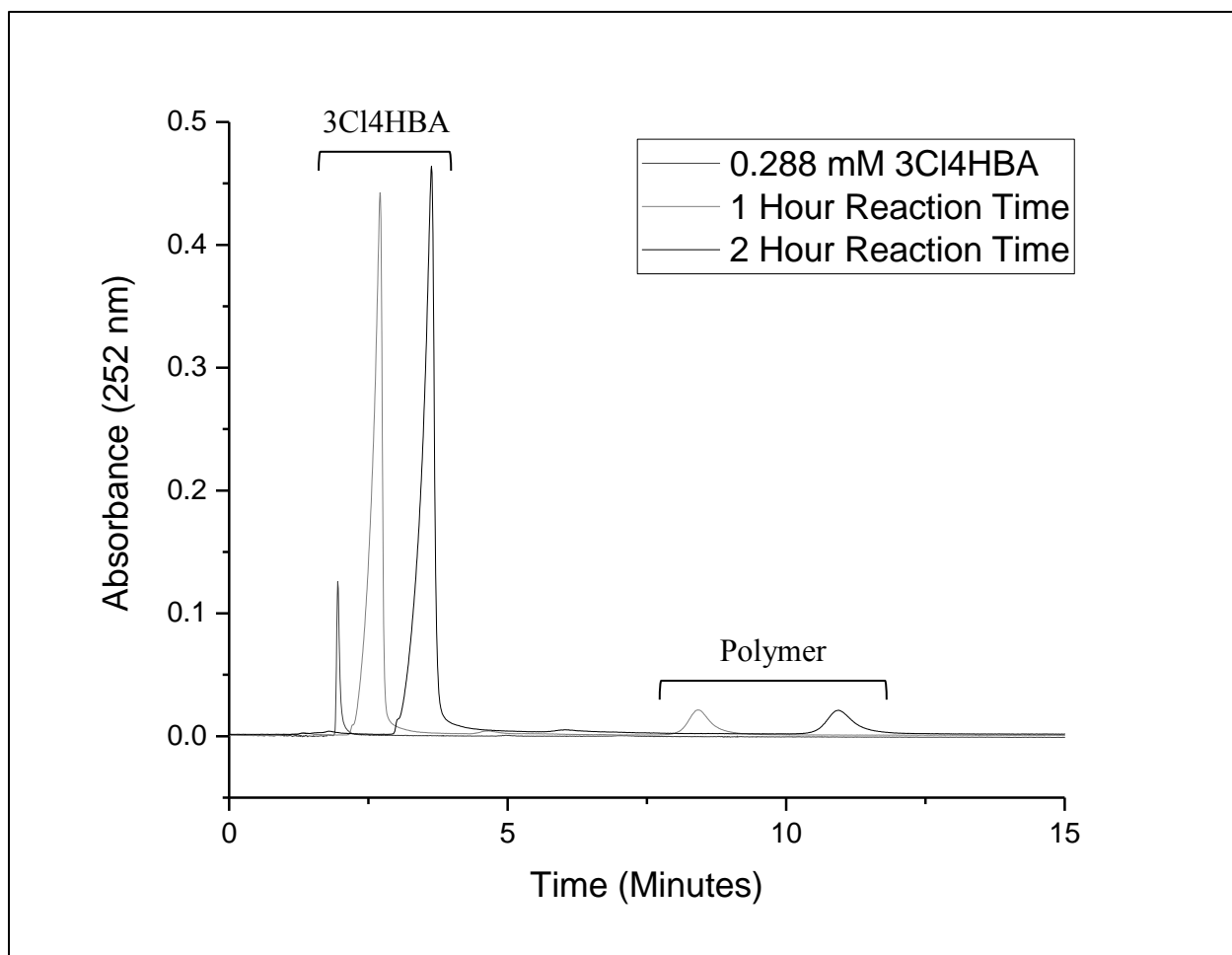
Figure 22. HPLC results for 3-chloro-4-hydroxybenzoic acid with laccase for 1 and 2 hour reaction times, and a solution of 3-chloro-4-hydroxybenzoic acid (0.288 mM 3Cl4HBA).

MALDI-TOF to Determine Polymer Characteristics

Analysis on the 4HBA modification solution and the precipitate formed in the

polymerization reaction was analyzed using MALDI-TOF mass spectrometry to determine the

molecular weight of the polymer. Being that the monomer (4HBA) is very similar in structure to

the matrix 2,5-dihydroxybenzoic acid, the 4HBA was not distinguishable from the multimers

formed from the matrix. This also made it difficult to determine what was 4HBA polymer as

well.

Separation of Polymer from Monomer using Molecular Weight Cut-Off Filters and

Analyzing the Effluent using HPLC

Next an experiment was designed to separate the polymer from the monomer using 3, 10,

and 50 kDa molecular weight centrifuge filters; based on the presence of the polymer one could

determine a molecular weight range of the polymer. The results from this experiment, in Figure

23, show no significant change in the retention time; although, the intensity increased with

increasing molecular weight cut-off. This could indicate that more of the polymer is allowed

through the 50 kDa filter than the 10 and 3 kDa filters, showing that some of the polymer is

being excluded by the filter; although, not all of the polymer is excluded.
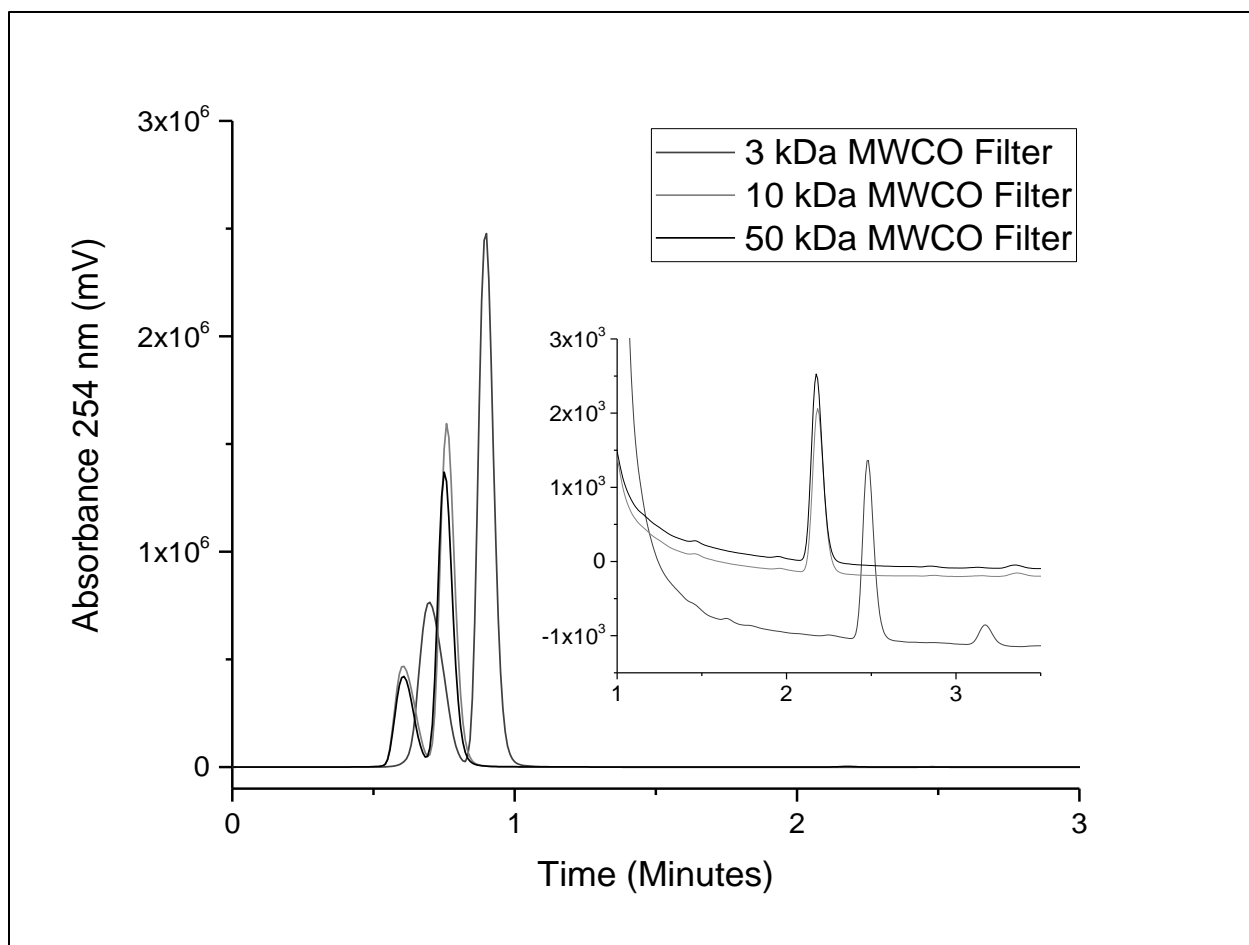
Figure 23. HPLC results for 4HBA polymerization solution concentrate solutions collected from 3, 10, and 50 kDa molecular weight centrifugal filters. The inset is the HPLC chromatogram from 1 to 3.5 minutes.

Gel Permeation Chromatography (GPC) Separation of 4HBA Modification Solution

       To further characterize the size distribution of the polymer formed when 4HBA reacts with laccase; the reaction mixture was passed through a gel permeation chromatography (GPC) column. GPC is a technique that separates molecules based on their size, as compared to reversed phase HPLC with a C18 column which separates molecules by their polarity. With proper calibration, this method can be used to determine the number average and weight average molecular weights as well as the polydispersity. The purpose of this experiment was to separate the polymer formed from the monomer. Two different samples were analyzed using at NAP-25 Sephedex G-25 GPC column: 4HBA polymer solution (Figure 24) and the reconstituted precipitate (Figure 25).

       The conclusions from this experiment are that for the polymerization solutions (Figure 24) there are 2 regions of polymer of different molecular weight which can be seen by the two peaks at the 250 nm wavelength. Also, there is a peak shown by the absorbance at 280 nm that elutes between these 2 peaks at 250 nm. The NAP-25 column has an exclusion limit of 5 kDa. Considering the enzyme is 55 kDa; the enzyme itself is more than likely not eluting at minute 6. This peak could possibly be polymer forming that absorbs at 280 nm. For the reconstitute precipitate (Figure 25), there is only one peak present between minute 4 and minute 9 at 250 nm as compared to the 4HBA polymerization solution that has 2 peaks present in that time frame. This difference could be due to the decrease in the intensity of the peak for the precipitate sample or an increase in the species that is eluting at the 7 minute time point.
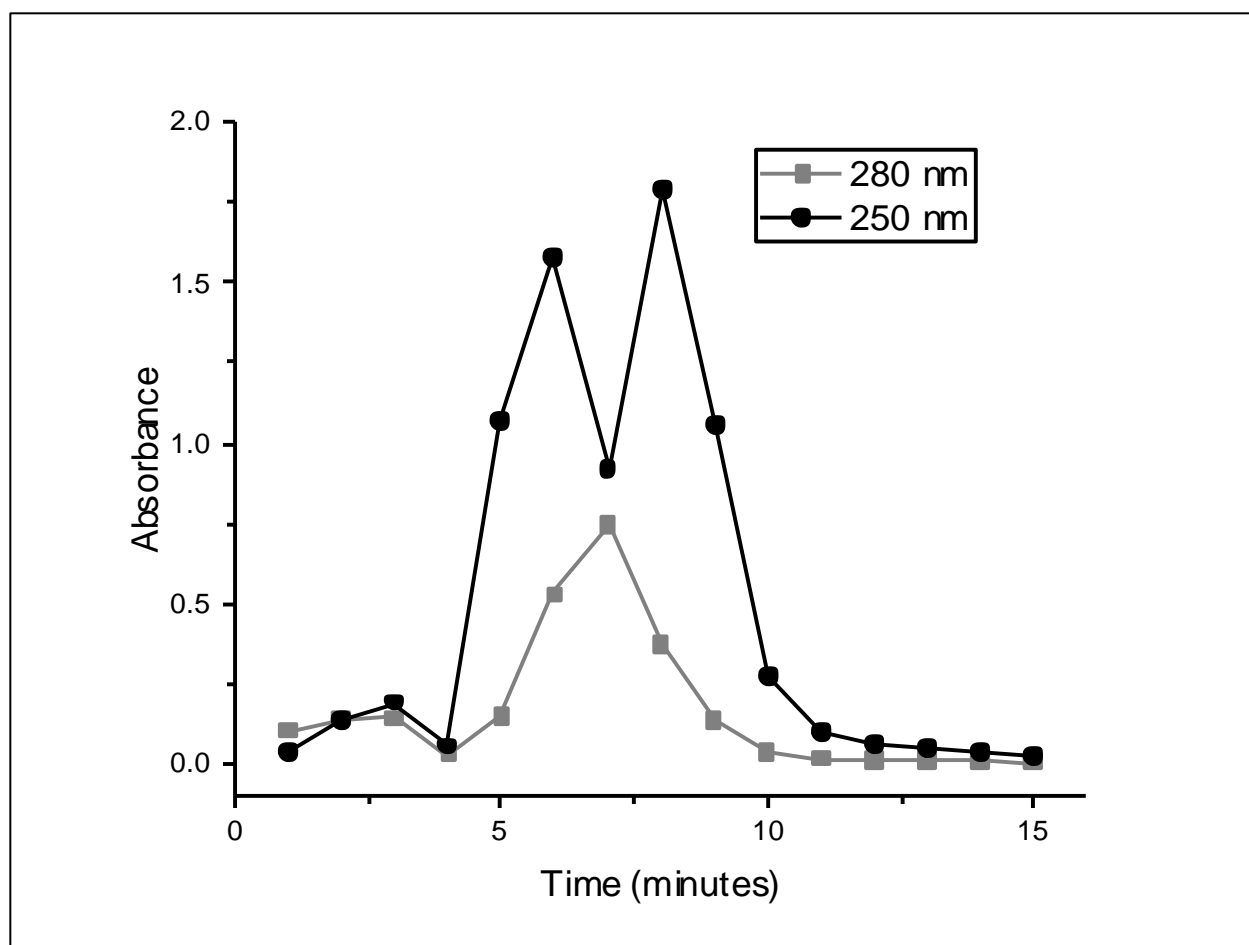
Figure 24. Absorbance values for aliquots collected every minute for 15 minutes from a NAP-25, Sephedex G-25 column loaded with 1 mL of the polymerization solution. Absorbance at 280 nm and 250 nm were measured.
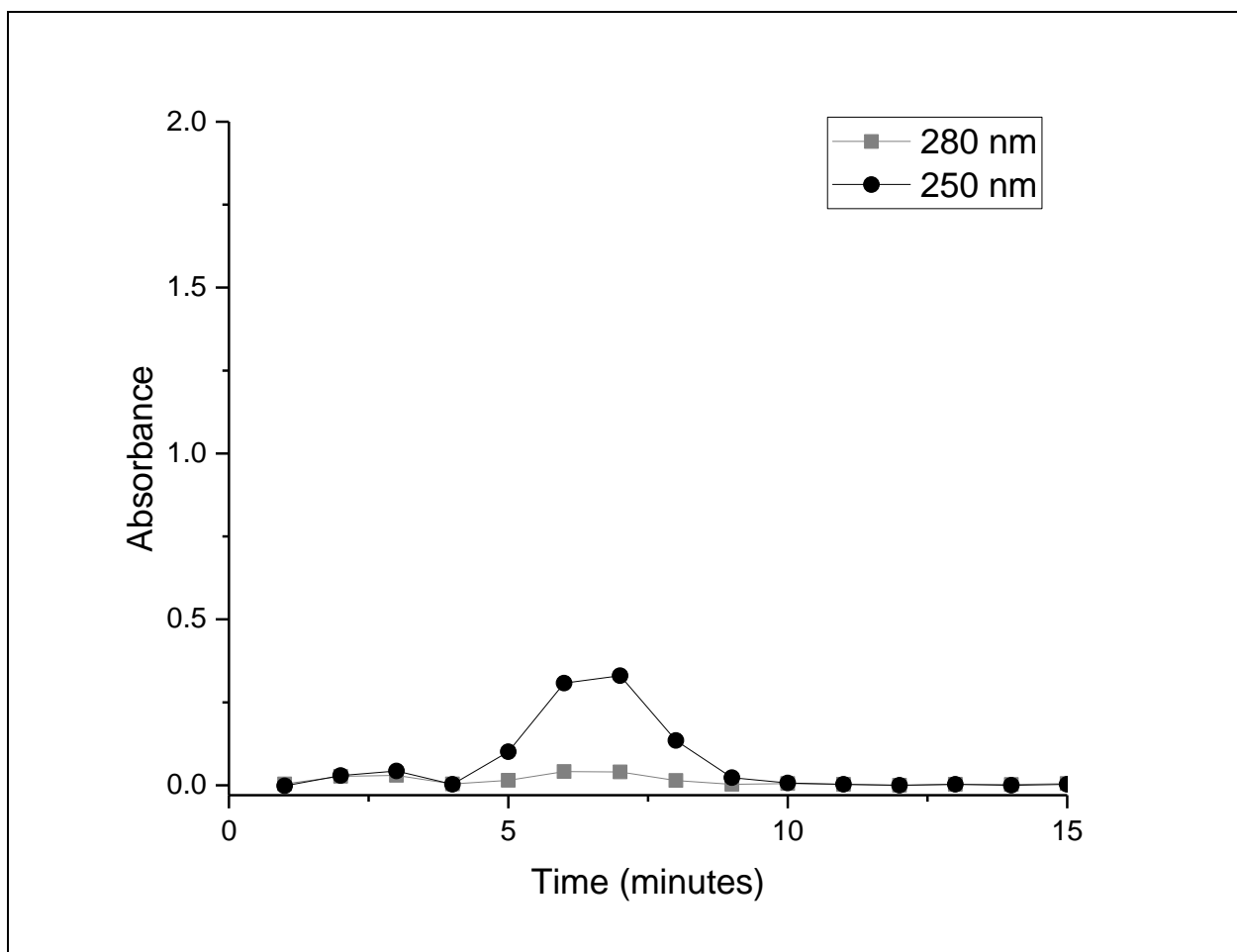
Figure 25. Absorbance values for aliquots collected every minute for 21 minutes from a NAP-25, Sephedex G-25 column loaded with 1 mL of the reconstituted precipitate.

To further analyze the fractions collected with GPC, HPLC analysis was performed. This was in order to see if the initial peak for 4HBA decreased and the suspected polymer peak increased with increasing elution time on the GPC column.

Table 11. HPLC-UV analysis of GPC fractions showing retention time and peak area at an absorbance value of 254 nm.

Fraction (time)	Peak 1		Peak 2	
	Retention Time (minutes)	Peak Area	Retention Time (minutes)	Peak Area
4 (4.25 minutes)	0.406	2,138,076	1.382	61,846
5 (4.5 minutes)	0.408	4,022,054	1.398	42,172
14 (7.25 minutes)	0.432	3,136,303	1.407	52,218
15 (7.5 minutes)	0.421	2,239,927	1.397	82,700
16 (7.75 minutes)	0.417	1,578,258	1.398	80,093

The results from this experiment (Table 11) show the presence of a peak at approximately 0.4 minutes and a smaller peak at approximately 1.4 minutes. Considering that samples 4-5 and 14-16 were from two different regions in the GPC experiment shown in Figure 24, but eluted at the same time for the HPLC experiment, indicates that the two sets of polymers are of very similar chemical structure but are different in size. For the initial peak, there is an initial increase in the area followed by a decrease in area after fraction 5. This indicates that there is more monomer and/or small polymer in the initial samples. For the second peak the area for the later fractions (15, 16) is larger than the initial samples (4, 5) this indicates that there an increase in larger polymer in the later samples than the initial samples. This could be an indication that the polymer is not following size exclusion behavior because larger polymer should elute (in earlier fractions) before smaller polymer. In this experiment, the opposite is observed because the smaller polymer elutes in earlier fractions than does the larger polymer. This could be due to the branched nature of the polymer becoming trapped in the column material leading to a longer retention time.

Calibration of GPC with Methyl Orange and FITC-4

The experiment was then repeated with a 24 hour polymerization reaction with methyl orange and FITC-4 used to calibrate the GPC column. The results from this experiment are shown in Figure 26. The conclusion from this experiment is that the 24 hour polymerization solution has a similar GPC elution profile to the 3 day polymerization solution. Also from this experiment, the polymers formed in solution are between the molecular weights of 4,389 Da (FITC-4) and 327 Da (methyl orange).
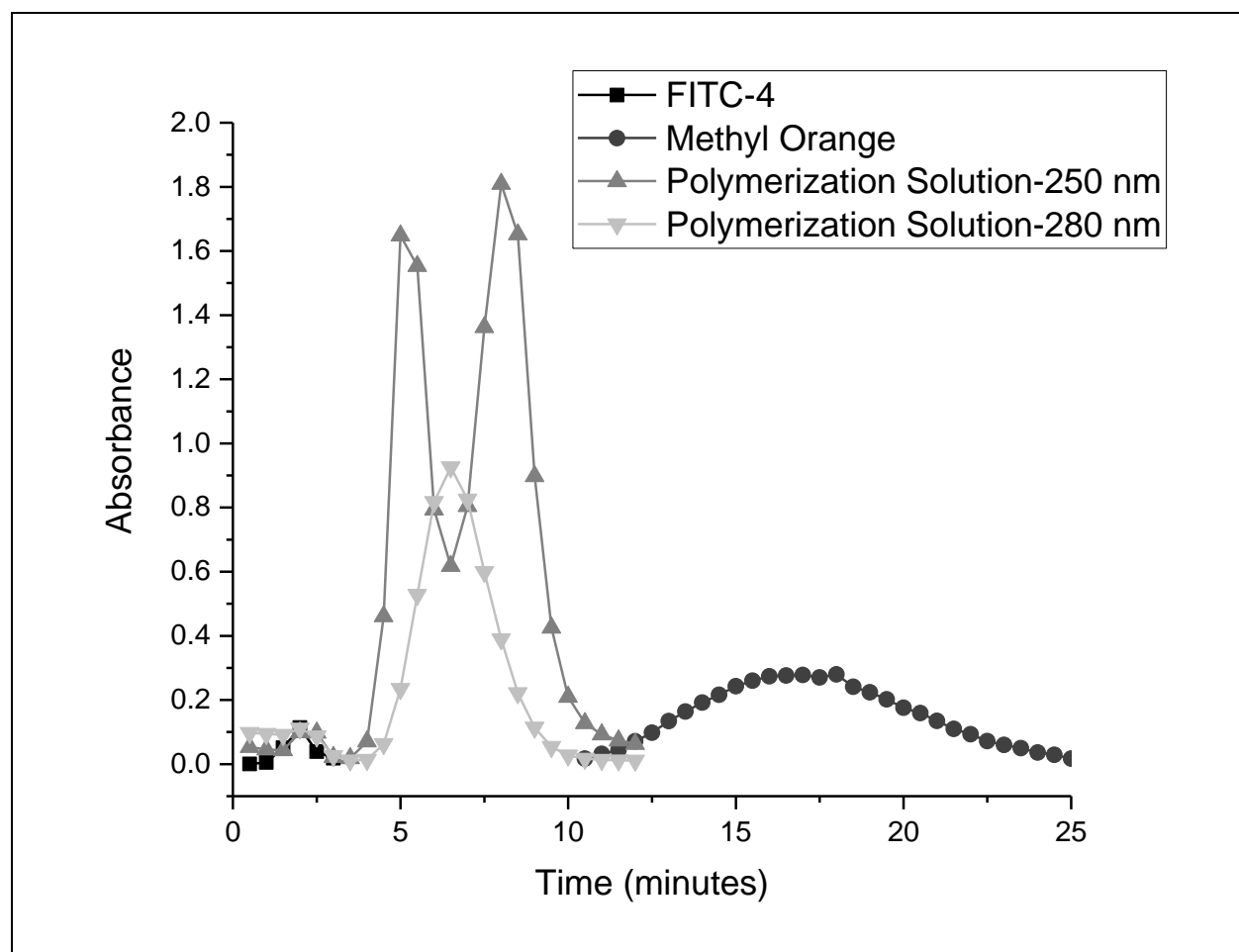
Figure 26. Gel permeation chromatography experiment performed using a NAP-25 Sephadex G-25 column (exclusion limit of 5 kDa) for 24 hour 4HBA polymer solution, methyl orange solution, and FITC-4 solution.

GPC of 4-Hydroxybenzoic Acid Solution

  In this experiment the monomer (4HBA) and laccase solutions were loaded onto the column to look at their elution behavior compared to the polymer. As shown in Figure 27 and 28 the laccase solution is not of sufficient concentration to absorb at 280 nm and shows no observable peaks that would interfere with the peaks observed for the monomer (4HBA) or the polymer. Also the monomer elutes as the first peak which shows that the 4HBA polymers do not follow size exclusion behavior because the smaller species, the monomer, elutes first. This information makes it difficult to predict the molecular weight of the polymer using this method. Typically for SEC the larger molecules elute first followed by the smaller molecules. This could be due to the highly branched nature of this polymer which can lead to abnormal SEC elution behavior due to large molecules spending too much time diffusing in and out of the column packing creating an Argentinean bolas effect (entanglement of a part of the macromolecule in the column packing) and sieving in the voids between packing spheres.[114] In order to further understand the molecular weights present in the solution samples were analyzed using direct infusion-MS.
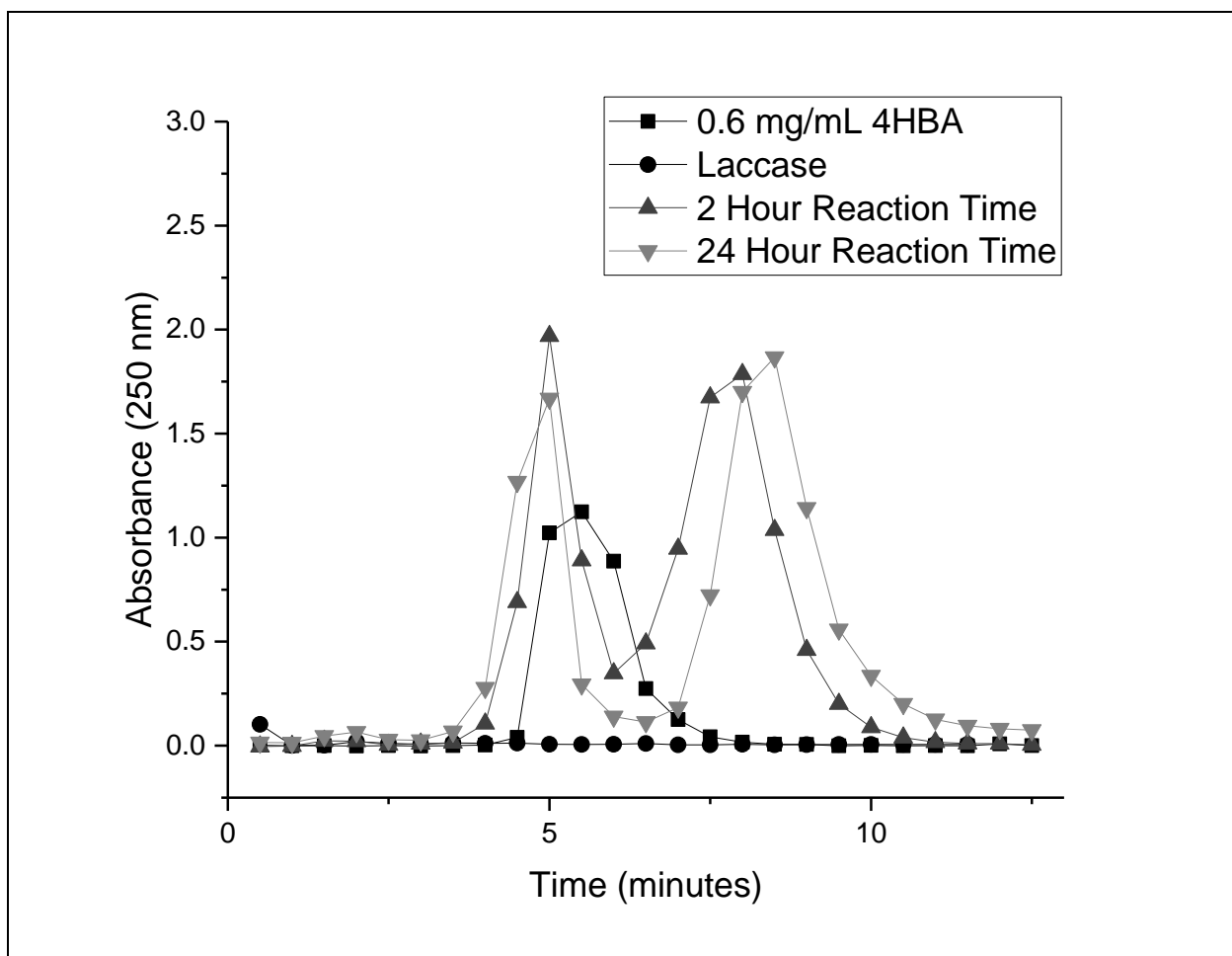
Figure 27. Gel permeation chromatography experiment performed using a Sephadex G-25 column (exclusion limit of 5 kDa) for 2 and 24 hour 4HBA polymer solution reaction times 4-hydroxybenzoic acid, and laccase at 250 nm.
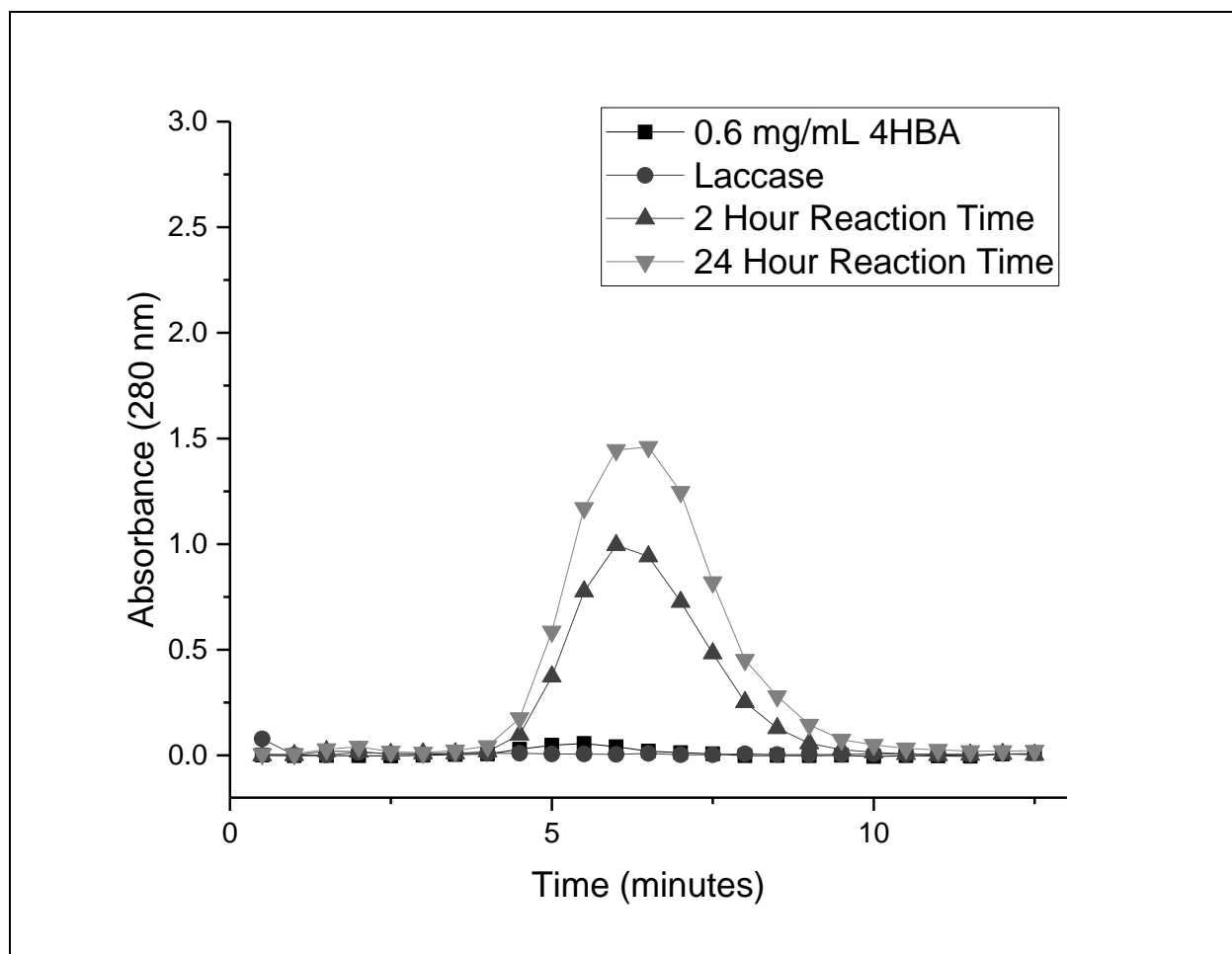
Figure 28. Gel permeation chromatography experiment performed using a Sephadex G-25 column (exclusion limit of 5 kDa) for 2 and 24 hour 4HBA polymer solution reaction times, 4-hydroxybenzoic acid, and laccase at 280 nm.

Direct Infusion-Mass Spectrometry Experiment

For the direct infusion mass spectrometry experiments, three different sample solutions were used: water, 0.1 M sodium acetate buffer pH 5.0 and 0.1 M ammonium acetate buffer pH 5.0. Sodium acetate and ammonium acetate at pH 5.0 were chosen due to the conditions required for the polymerization reaction to occur and water was chosen to eliminate the salt interference for the monomer solution even though the polymerization reaction does not occur in water. These solutions were then passed through the GPC column and analyze in the mass spectrometer. The results from this experiment were inconclusive due to high background noise from the blank samples shown in Figure 29 (A), 30 (A), and 31 (A). For the solutions containing 4HBA (Figure 29 (B, C), 30 (B, C), and 31 (B, C)) a peak corresponding to phenol (m/z 92.6) could be observed. This is from the decarboxylation of 4HBA in the ESI source. The ammonium acetate buffer shows the least background. Polymer formation could not be detected in the 4HBA and laccase solutions as there were no peaks present in significant quantity that were not present in the background or the 4HBA solution. This could be due to polymerization of the monomer in the ESI ionization source.[138] Also for the polymerization solution the formation of a large amount of small concentrations of a heterogeneous mixture of polymers could be a reason for not detecting the polymer formation using mass spectrometry.
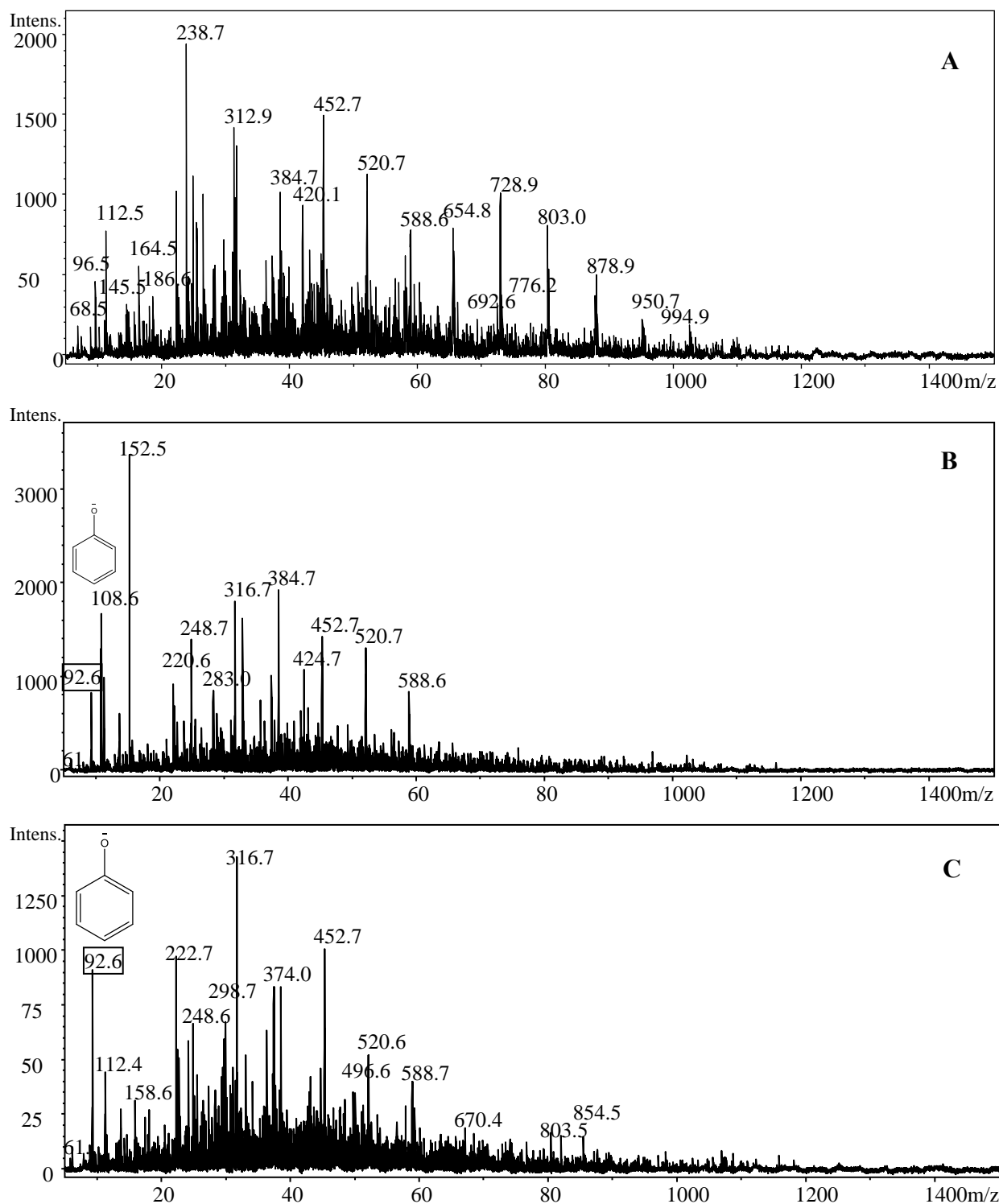
Figure 29. Mass spectra using direct infusion of fractions collected from GPC column containing (A) sodium acetate pH 5, (B) 4HBA in sodium acetate pH 5.0, and (C) 4HBA, and laccase in sodium acetate pH 5.0.
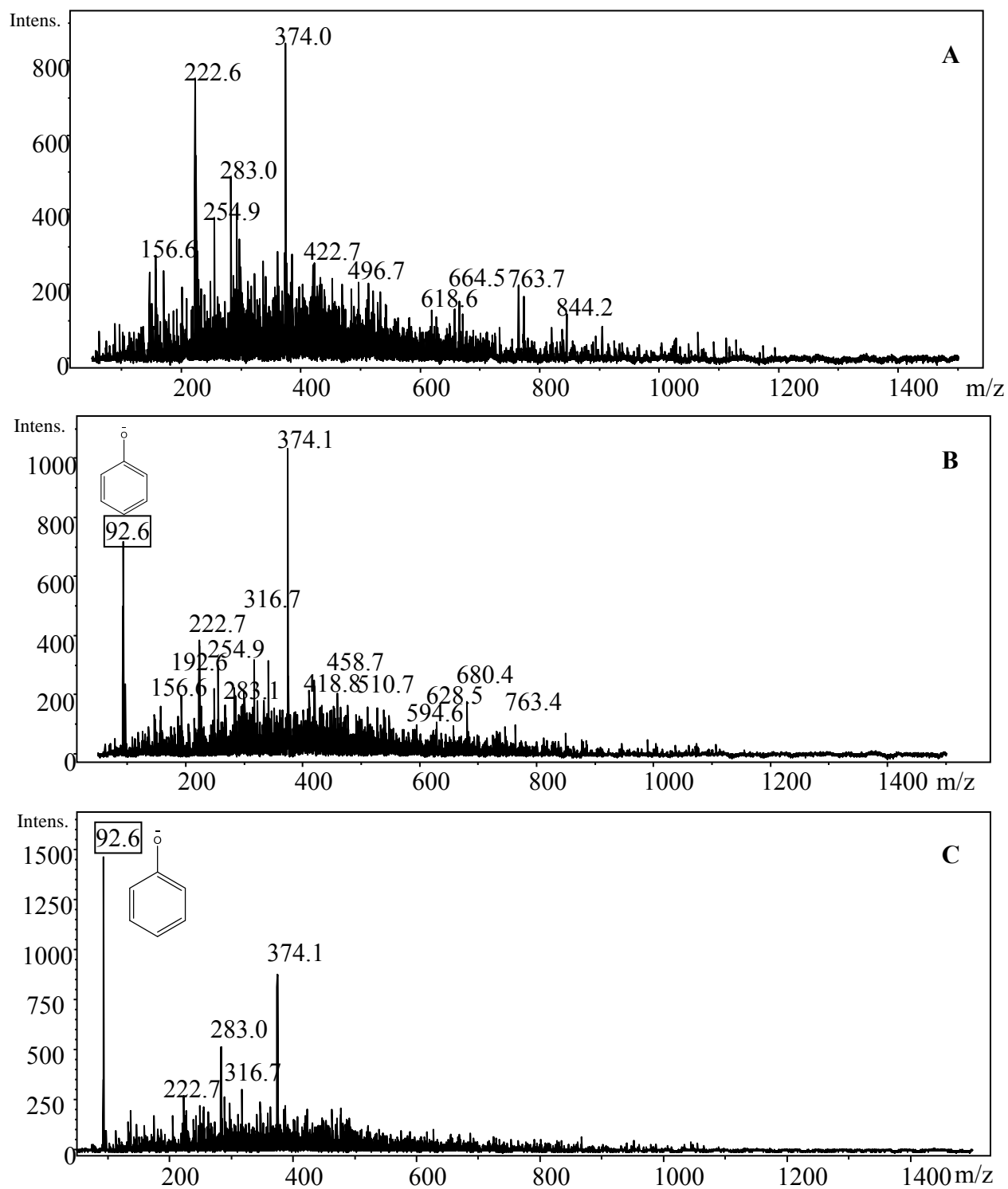
Figure 30. Mass spectra using direct infusion of fractions collected from GPC column containing (A) water, (B) 4HBA in water, and (C) 4HBA, and laccase in water.

97
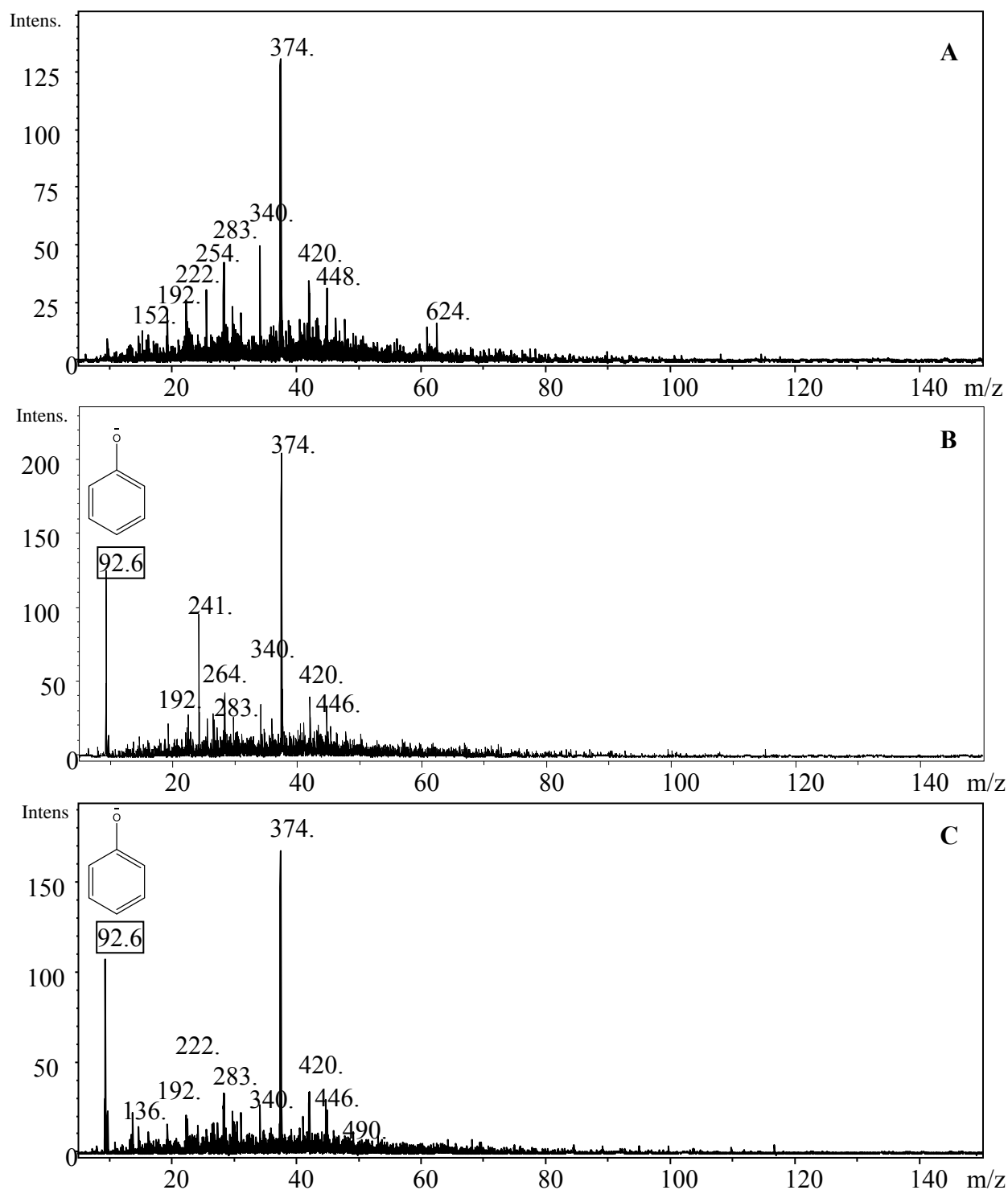
Figure 31. Mass spectra using direct infusion of fractions collected from GPC column containing (A) ammonium acetate pH 5.0, (B) 4HBA in ammonium acetate pH 5.0, and (C) 4HBA, and laccase in ammonium acetate pH 5.0.

Conclusions

From the GPC experiment the monomer and the polymer were able to be observed using UV absorbance at 250 nm and 280 nm. It could also be concluded that the 4HBA monomer and polymer does not follow size exclusion behavior in that the monomer elutes before the polymer. Further analysis needs to be performed in order to understand the polymer's distribution. Laccase *Trametes versicolor*, might require a size exclusion column which was used with laccase, *Trametes villosa*.[93]

CHAPTER 5. MODIFICATION OF PES FLAT SHEETS AND MICRODIALYSIS MEMBRANES WITH HEPARIN TO IMPROVE RELATIVE RECOVERY

Introduction

Microdialysis is a frequently used sampling technique to collect analytes from the extracellular fluid space within an organism. Researchers are interested in the proteins found in the extracellular fluid space but one of the challenges to analyzing proteins is their low concentration and their low RR which makes them difficult to detect. One method that has been previously used to increase the RR is to add a capture agent for the protein of interest into the perfusion fluid. Heparin is an affinity agent that is known to bind a wide variety of proteins, including growth factors such as aFGF, VEGF and TGF-β.[44] Heparin is also known to bind to IL-8, CCL2, MIP-1, RANTES and TNF-α with nM affinity.[45-48] This chapter focuses on the characterization of the heparin modification on PES flat sheets and hollow fibers using the following reaction scheme (Figure 32), as well as the RR of three heparin binding proteins.
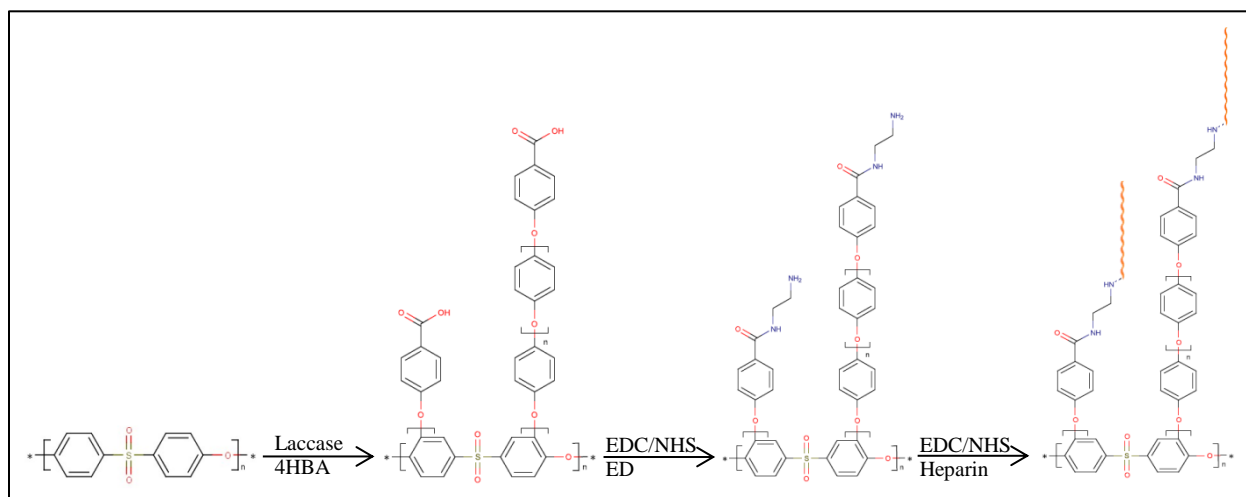
Figure 32. Reaction scheme for attachment of heparin onto PES membrane surface.

Materials and Methods

Materials

Laccase form *Trametes versicolor*, sodium acetate, heparin sodium salt from porcine intestinal mucosa, fluorescein isothiocyanate dextran 4,000, fluorescein isothiocyanate dextran 10,000, ethylenediamine dihydrochloride and methyl orange were purchased from Sigma Aldrich (St. Louis, MO); 4-hydroxybenzoic acid was purchased from TCI (Portland, OR). 3-chloro-4-hydroxybenzoic acid and 2-5-dihydroxybenzoic acid was purchased from Alfa Aesar (Haverhill, MA). Sulfo-NHS premium grade, and HPLC grade methanol and water were purchased from Fisher Scientific (Waltham, MA). Glacial acetic acid was purchased from VWR international (Radnor, PA). NAP-25 Sephedex G-25 columns were purchased from GE healthcare (Chicago, IL). Bovine Serum Albumin fraction V was purchased from Rockland (Pottstown, PA) and was certified immunoglobulin and protease free. Lysozyme was purchased from MP biomedicals (Solon, OH). The 100 kDa PES flat sheet membranes (UE50) were purchased from Sterlitech (Kent, WA). Fluorescein isothiocyanate isomer 1 was purchased from Alfa Aesar (Haverhill, MA). Dibasic sodium phosphate (ACS grade) was purchased from EMP (Howell, NJ). Sodium chloride bioXtra grade, potassium chloride (99.0%), and monobasic potassium phosphate (ACS grade) where purchased from Sigma Aldrich (St. Louis, MO). CMA 20 microdialysis probes were purchased from Harvard Apparatus (Holliston, MA). CCL2 optiEIA ELISA kit was purchased from BD bioscience (San Jose, CA). Recombinant rat KC/GRO, and mouse aFGF, and VEGF Duo set ELISA kits were purchased from R&D systems (Minneapolis, MN). Recombinant mouse FGF1 was purchased from Sino Biologicals (Beijing, China) and recombinant mouse VEGF was purchased from Life Technologies (Carlsbad, CA). EDAC-HCl was purchased from Amresco (Dallas, TX).

Modification to PES Flat Sheets for XPS and ATR-FTIR Analysis

Initially, the heparin modification procedure was performed on PES flat sheets due to the ease of analysis using ATR-FTIR and cost effectiveness compared to microdialysis probes. Modification of the 100 kDa PES flat sheets were performed using the procedure described in Chapter 4. Briefly, membranes were allowed to react in the 4HBA polymerization solution for 1, 2, 3 and 4 days and then were placed in a solution of 0.1 M sodium acetate pH 5.0 overnight to wash the membranes. These membranes were then analyzed with ATR-FTIR. These membranes were then modified with ethylenediamine (ED) in order to attach a primary amine to the surface of the carboxyl-functionalized membranes. This was done by first adding 10 mg of 1-ethyl-3-(3-dimethylaminopropyl) carbodimide (EDC) to a 30 mL solution of 0.1 M MES buffer at pH 5.5 with the flat sheet membranes. Then 28 mg of sulfo-NHS (N-hydroxysuccinimide) was added to this solution. This mixture was allowed to react for 30 minutes at room temperature. Next, the membranes were removed from this solution, placed in a solution containing 60 mg of ED in 30 mL of PBS (137 mM NaCl, 10 mM phosphate, 2.7 mM KCl) at pH 7.4 and allowed to react for 24 hours at room temperature. The membranes were then placed in a solution of PBS pH 7.4 overnight at room temperature.

To heparin modify the ED modified membranes; the membranes were placed in a solution containing 27 mg of EDC and 65 mg of sulfo-NHS in 30 mL 0.1 M MES buffer pH 5.5 for 30 minutes. Then, the membranes were placed in a solution containing 30 mg of heparin in 30 mL of PBS pH 7.4 for 24 hours. Later, the membranes were removed from the solution and rinsed overnight in PBS pH 7.4. After each modification step the PES flat sheets were placed in a desiccator and analyzed using ATR-FTIR.

Protein Adsorption to Heparin Modified Membranes

Protein adsorption was measured to determine if the addition of heparin onto the membrane surface would reduce protein adsorption of BSA and lysozyme. In order to test the protein adsorption, BSA and lysozyme were FITC-labeled. FITC-BSA and FITC-lysozyme were made using the procedure described in Chapter 2. PES flat sheet membranes were initially reacted with 4HBA for 0, 1, 8, 12 and 24 hours using the procedure described in Chapter 2. After the modification of the membranes with ED, the membranes reacted with heparin described above, then the membranes were placed in a solution of FITC-BSA or FITC-lysozyme. The concentration was compared with a solution that only contained FITC-BSA or FITC-lysozyme; based on the difference in fluorescence, the concentration adsorbed onto the surface was calculated and converted to protein adsorbed per unit area using Equation 12 in Chapter 2.

Equilibrium Dialysis Experiments

Following ATR-FTIR and XPS data (which confirmed the attachment of heparin), equilibrium dialysis experiments were performed. These experiments were performed using an equilibrium dialysis chamber with a 1, 2, 3 and 4 day 4HBA modified membranes with heparin attached. These experiments were performed by placing a 25 μL amount of buffer (PBS + 0.1% (w/v) BSA) in one chamber, either the PET side or PES side of the membrane and then placing 4 ng/mL of CCL2 in the opposite chamber. The samples were then collected after 24 hours, and then each side was incubated in a solution of 2 M NaCl in PBS at pH 7.4 for 30 seconds, 1 minute, 1 hour and 24 hours. The concentration was then increased to 112 ng/mL to increase the likelihood of detecting CCL2 on both sides of the chamber.

Nonspecific Adsorption of BSA to the Equilibrium Dialysis Chamber

To better understand the reasoning behind the sample loss observed in the CCL2 experiment above, the amount of BSA that nonspecifically adsorbed to the equilibrium dialysis surface was calculated. In this experiment, a solution of 0.25 mg/mL of BSA was placed in the equilibrium dialysis chamber with no membrane and allowed to incubate for 24 hours. The solution was then removed and the concentration was determined using a standard bicinchoninic acid (BCA) assay and compared to the initial solution.

FITC-10 and Methyl Orange Equilibrium Dialysis Experiment

To test the equilibrium dialysis chamber and the membranes with a simpler system, FITC-10 equilibrium dialysis experiments were performed. This was done by placing a 100 kDa PES flat sheet that had been soaked overnight in PBS pH 7.4 into the chamber. One side of the chamber contained 25 μL of 1.2 mM FITC-10 and PBS was placed on the PES side of the membrane. A 2 μL sample was collected from each side and from the stock solution at approximate times of 1, 3, 7 and 22 hours. These samples were then analyzed by measuring the absorbance at 492 nm.

Since 90 to 95% of the FITC-10 solution adsorbed onto the membrane, this experiment was repeated with a 300 kDa PES flat sheet with methyl orange. Methyl orange has a molecular weight of 327 Da. A 5 mM methyl orange solution was placed on the PET side of the membrane and then PBS pH 7.4 was placed on the PES side of the membrane. Then, 2 μL samples were collected from each side at 1, 2, 5 and 24 hours and absorbance values measured at 460 nm.

Attachment of Heparin to Microdialysis Membranes

After confirming the attachment of heparin to PES flat sheet membranes the method was applied to the modification of microdialysis membranes. The modification of PES microdialysis

membranes was performed by first attaching 4HBA polymers onto the surface using the method described in chapter 2. Briefly this was performed by perfusing a solution containing 28.8 mM of 4HBA and 0.5 U/mL of laccase from *Trametes versicolor* that was dissolved in 0.1 M sodium acetate buffer pH 5.0 at a flow rate of 1 µL/min for 2 hours or 24 hours. Following modification, the probe was flushed with 0.1 M sodium acetate buffer pH 5.0 overnight at a flow rate of 3 µL/min.

Then, these membranes were modified with ED in order to attach a primary amine to the surface of the carboxyl-functionalized membranes. This is in order to attach heparin using EDC/NHS chemistry. To attach ED, 2 mg of EDC was added to 200 µL of 0.1 M MES buffer at pH 5.5. Then, 5.5 mg of sulfo-NHS was added to this solution. This mixture was then perfused through the microdialysis probe for 45 minutes at 1 µL/min. Then a solution containing 10 mg of ED in PBS at pH 7.4 was perfused through the probe at 1 µL/min for 24 hours. The probe was then flushed with PBS pH 7.4 at 3 µL/min overnight.

To heparin modify the ED modified microdialysis membranes 4 mg of EDC and 12 mg of sulfo-NHS were added to 200 µL of 0.1 M MES buffer pH 5.5. This mixture was perfused through the microdialysis probe for 45 minutes at 1 µL/min. Then, a solution containing 10 mg of heparin in PBS pH 7.4 was perfused through the probe at 1 µL/min for 24 hours. The probe was then flushed with PBS pH 7.4 at 3 µL/min overnight. XPS was used to confirm the attachment of 4HBA polymers and heparin.

FITC-Dextran and Lysozyme Relative Recovery Experiments

To test how this modification affected the membrane surface a FITC-4 RR experiment was performed. CMA20 microdialysis probes were modified with 4HBA polymer for 24 hours ED, and heparin. Then, between each step FITC-4 RR was measured. The FITC-4 RR

experiment was performed by perfusing with PBS at pH 7.4 (perfusion fluid) at a flow rate of 1 μL/min through a microdialysis probe placed in a solution containing 500 μM FITC-4 in perfusion fluid. Samples were collected every 20 minutes for a total of 60 minutes, and absorbance values were measured in triplicate for each sample at 493 nm. Concentrations were determined using a calibration curve generated that day. Also FITC-4, FITC-10, and FITC-20 RR was determined for 2 hour and 24 hour 4HBA-heparin modified microdialysis membranes. Also, RR of lysozyme was performed using 500 μg/mL of lysozyme with a perfusion fluid of PBS at pH 7.4 at a flow rate of 1 μL/min. Samples were collected every 30 minutes for a total of 2 hours and were analyzed using a standard BCA assay.

KC/GRO Relative Recovery Experiment

After confirming the attachment of heparin onto microdialysis membranes the relative recovery of KC/GRO was obtained. For KC/GRO RR experiments, control and 24 hour heparin modified microdialysis probes were compared. To determine the RR the probes were placed in a solution containing 2,000 pg/mL of KC/GRO in PBS 0.1% BSA at pH 7.4. Microdialysis probes were perfused at 1 μL/min with PBS 0.1% BSA at pH 7.4 and samples were collected every hour for a total of 4 hours. The samples were then analyzed using a standard KC/GRO ELISA kit.

Heparin Binding Protein Relative Recovery Experiments

Next, RR of three heparin binding protein was determined. For these experiments, 2 hour and 24 hour 4HBA modified and heparin modified microdialysis probes, were compared with control (unmodified) microdialysis probes. To determine the RR of these analytes, the probes were placed in a solution containing 6 ng/mL of CCL2, 800 ng/mL of aFGF, or 200 ng/ml of VEGF in PBS 0.1% BSA at pH 7.4. Probes were perfused with PBS 0.1 % BSA at pH 7.4 at 1

μL/min. Samples were collected every hour for a total of 4 hours and analyzed using a standard CCL2, aFGF, or VEGF ELISAs.

Results and Discussion

ATR-FTIR Analysis of ED and Heparin Modified PES Flat Sheets

To confirm the attachment of heparin onto PES flat sheet membranes, XPS and ATR-FTIR analyses were performed. The ATR-FTIR results show the presence of a carboxylic acid functional group by the peak at approximately 3300 cm^{-1} in Figure 33(A), shown for comparison purposes from Chapter 2. Upon modification with ED as shown in Figure 33(B), there is a disappearance of the peak at approximately 3300 cm^{-1} indicating that the primary amine reacted with the carboxylic acid functional group that was present in the 4HBA modified membranes. Also, the weak peak at 3300 cm^{-1} could indicate remaining carboxylic acid or a secondary amine. In Figure 34, the PET side shows water is not present in the membrane and that ED does not react with the PET side of the membrane.

The next step was to attach heparin to the ED functionalized membranes. After modification with heparin ATR-FTIR analysis was performed on the membranes. As seen in Figure 35 there is an increase in the peak at approximately 3300 cm^{-1} indicative of the hydroxyl functional groups on heparin. This peak is not present in the ED functionalized membranes shown in Figure 33(B). Moreover, the PET side (Figure 36) shows the absence of water and that the reaction is selective for the PES side.
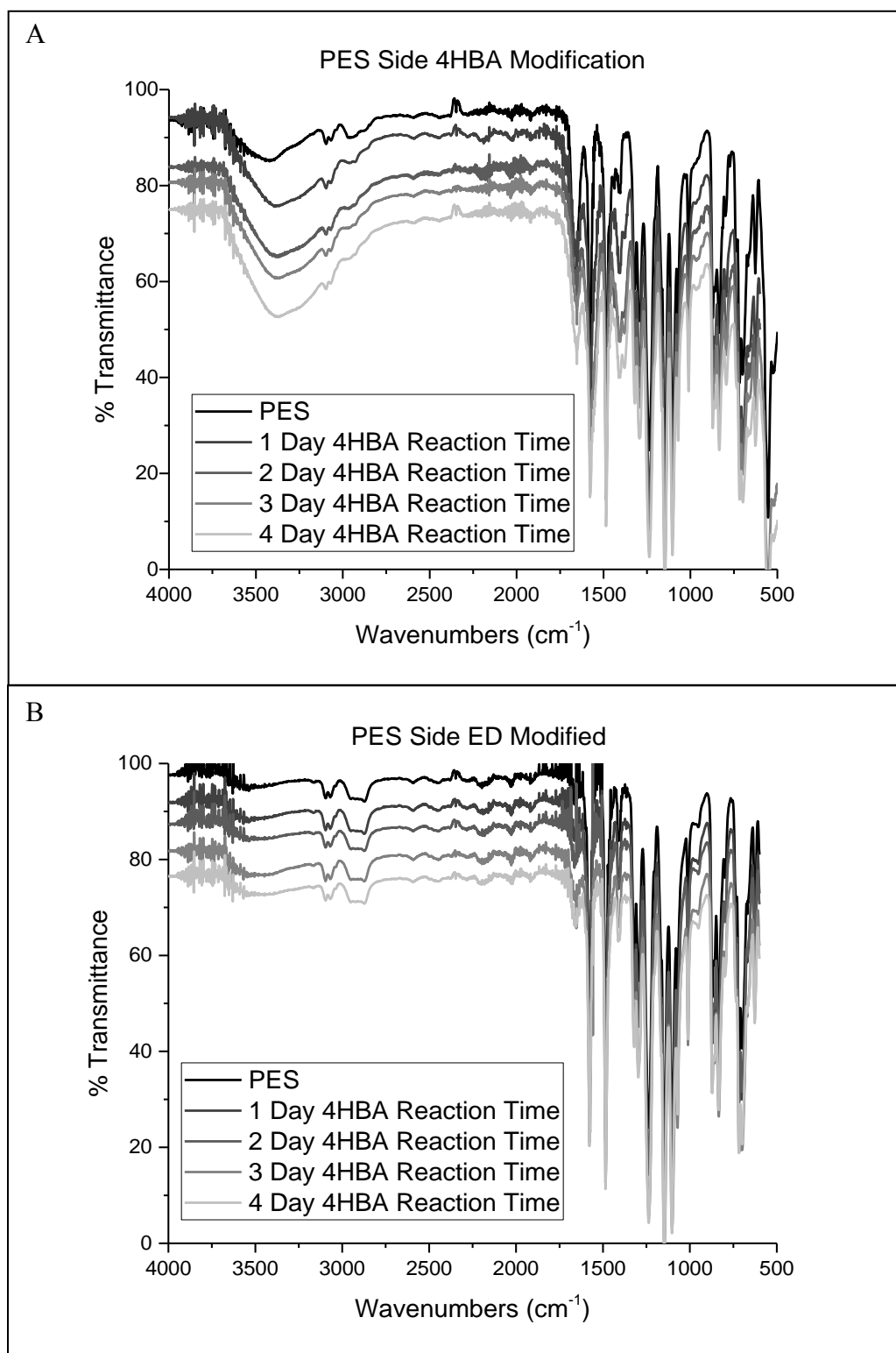
Figure 33. (A) IR spectra of the PES side of flat sheet membranes modified with 4HBA for 0 (PES), 1, 2, 3, and 4 days. (B) IR spectra of the PES side of flat sheet membrane for 0 (PES), 1, 2, 3, and 4 day modifications with 4HBA after attachment of ED.
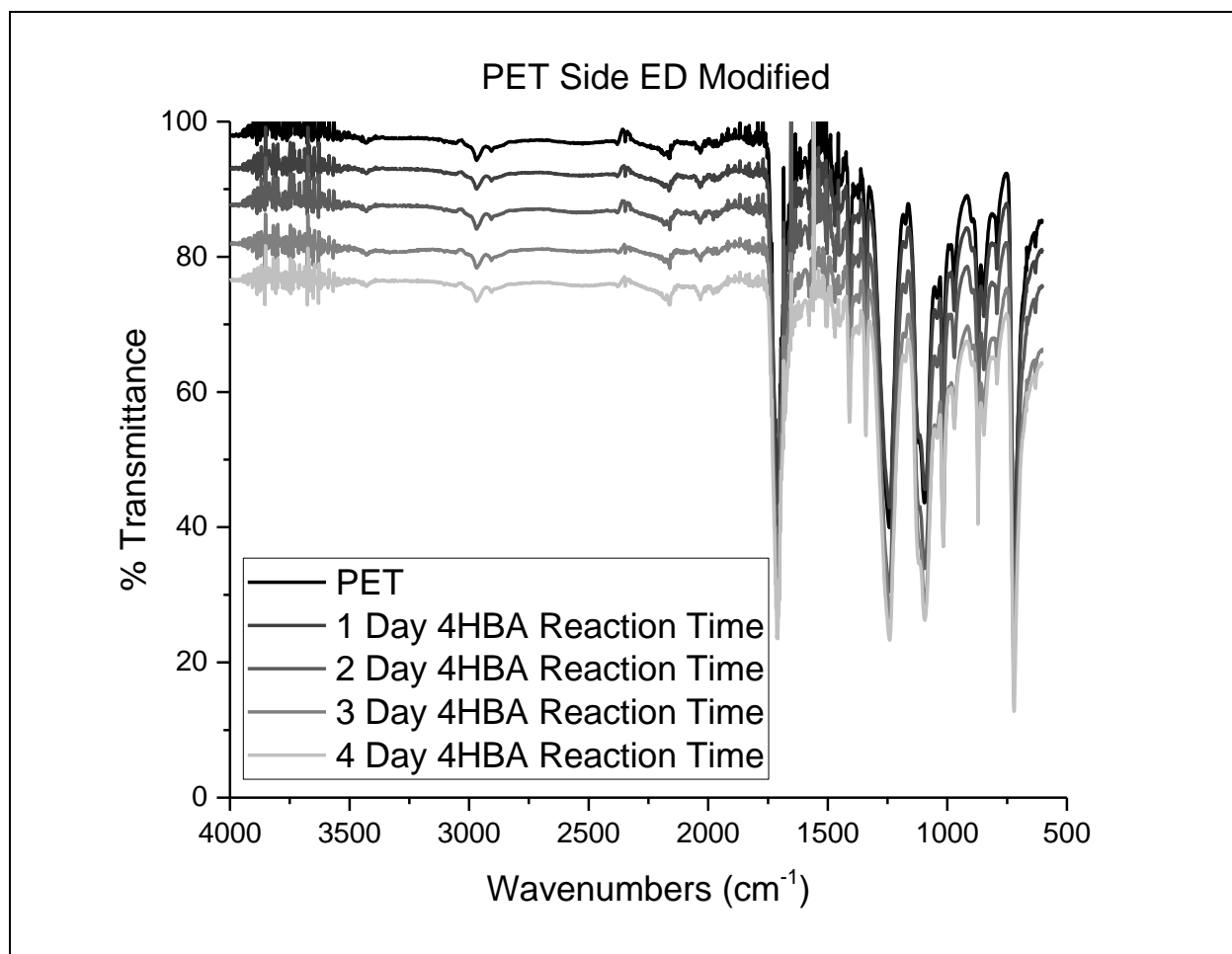
Figure 34. IR spectra of the PET side of flat sheet membrane for PES, 1 day modification, 2 day modification, 3 day modification, 4 day modification with 4HBA after attachment of ED.
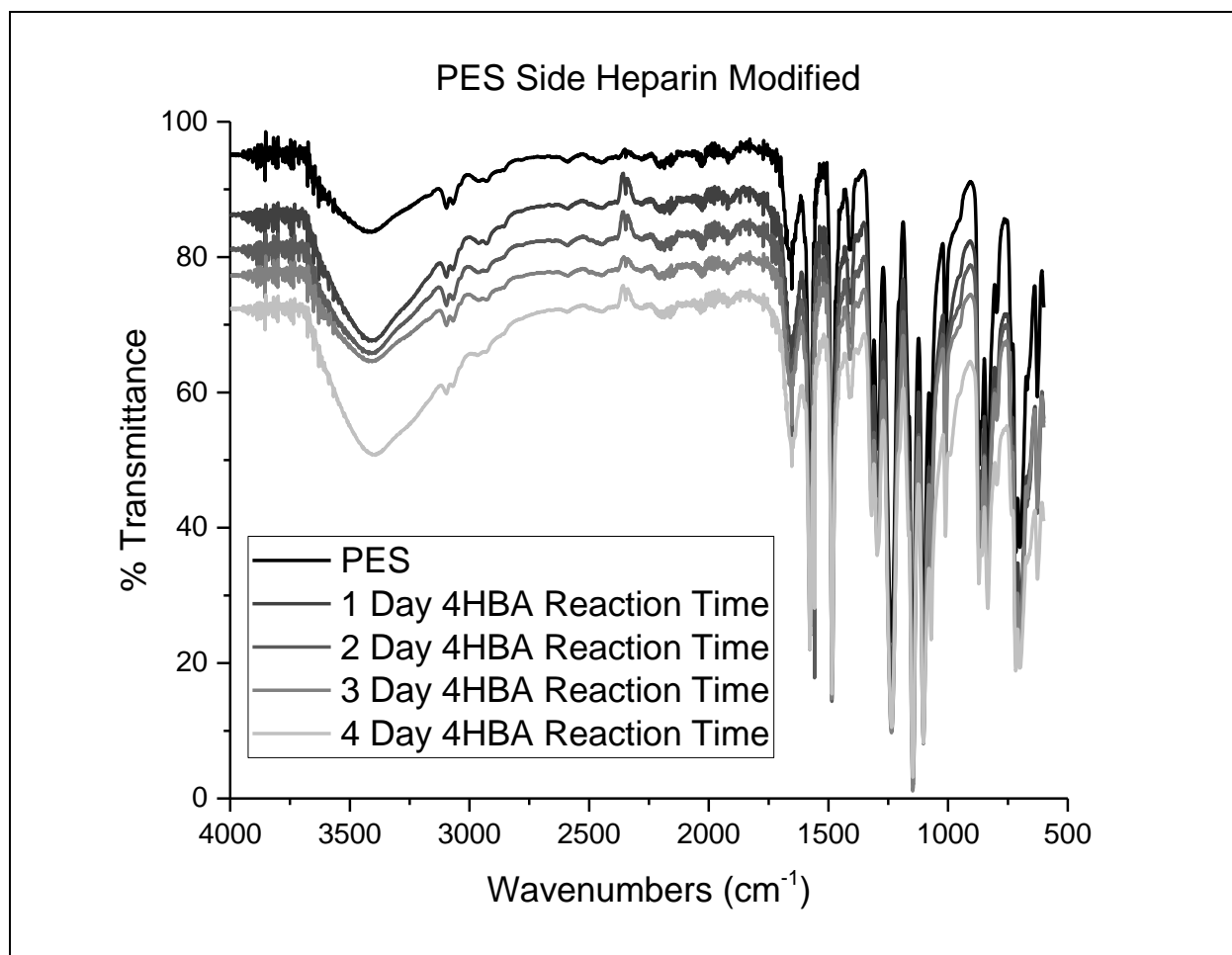
Figure 35. IR spectra of the PES side of flat sheet membranes for PES, 1 day modification, 2 day modification, 3 day modification, 4 day modification with 4HBA after attachment of heparin.
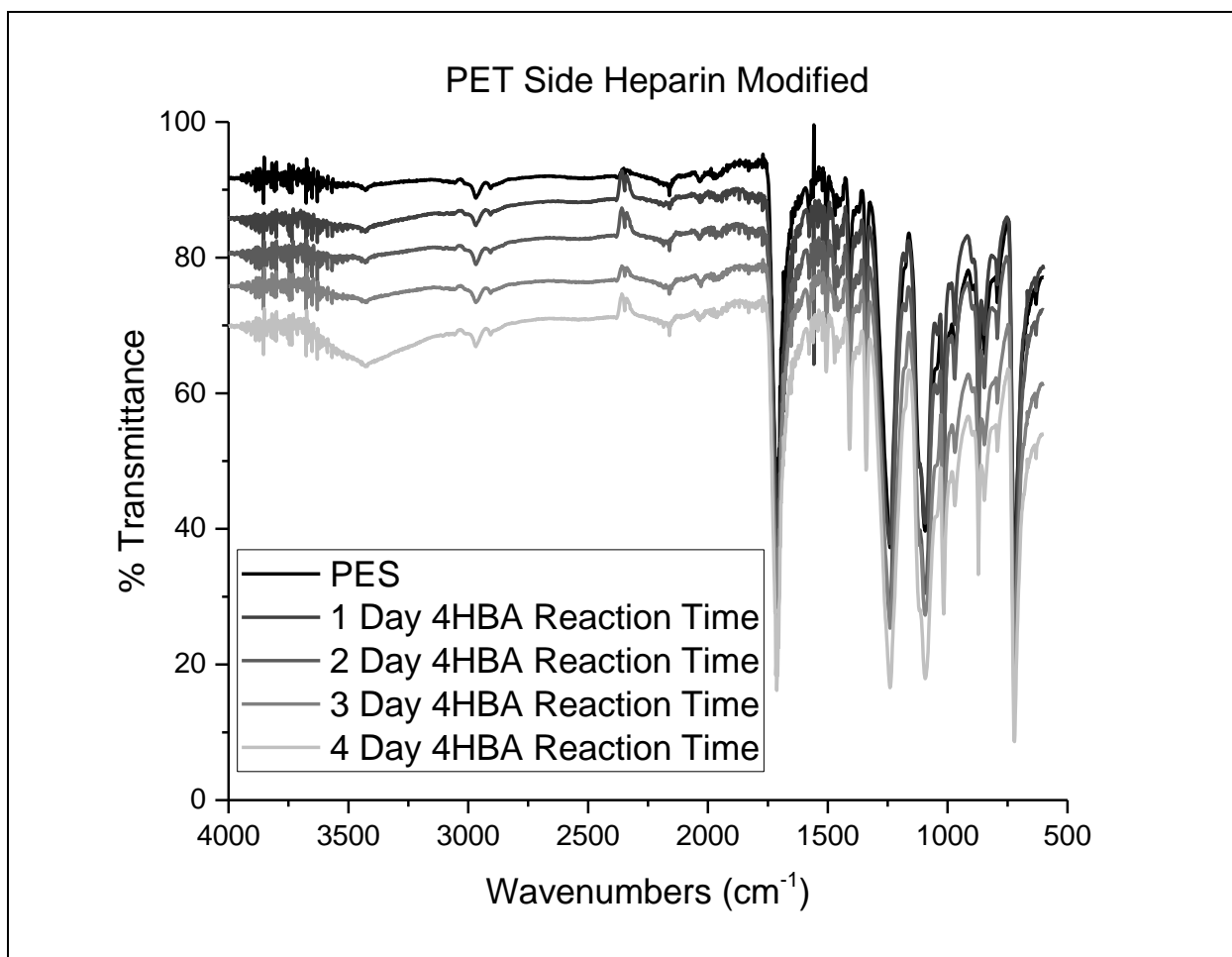
Figure 36. IR spectra of the PES side of flat sheet membranes for PET, 1 day modification, 2 day modification, 3 day modification, 4 day modification with 4HBA after attachment of heparin.

Analysis of PES Flat Sheets Modified with Heparin using XPS

The next step was to analyze the heparin modified membranes using XPS. This was done to further confirm the attachment of heparin on the membrane surface. The results from XPS analysis, shown in Table 12, show the presence of S2p in the heparin modified membranes. Since heparin is highly sulfonated, the presence of S2p indicates the presence of heparin. There is also a decrease in the presence of the C-S functional groups for the heparin modified membranes and a decrease in the C-S present in the 4HBA modified membranes. The C-S functional group is found only in the sulfone group on PES so the decrease in C-S indicates the addition of a substance onto the surface (4HBA, and heparin). There is also a significant increase in the COOH functional groups for the 4HBA modified membranes, and for the heparin modified membranes. Also, the binding energy of the COOH functional groups for the 4HBA and heparin modified membranes are different. This indicates a different chemical environment which would be expected because 4HBA and heparin have different structures. There was also no significant change in the C-H/C-C content. In addition, there was also no significant difference in the heparin modified membranes based on the length of 4HBA modification between 1 and 4 day modification.

Table 12. Three PES flat sheet membranes analyzed using XPS. Percentages are determined from the peak areas of the C1s, O1s, and S2p high resolution XPS spectra. * indicates a significant difference from the sodium acetate control, 4HBA control, and 3Cl4HBA control at the 95% confidence level using a single factor ANOVA with Bonferroni post hoc test. ND indicates not detected (<0.1 atom%). For statistical analysis ND values were replaced with the detection limit (0.1 %).

	C-C/C-H	C-O-C	C-S	O-C	O-S	COOH-4HBA	COOH-heparin	S2p	S2p
Binding Energy (eV)	284.77 ±0.027	286.25 ±0.080	288.82 ±0.097	531.73 ±0.15	533.43 ±0.14	287.45 ±0.18	287.85 ±0.14	167.67 ±0.059	168.87 ±0.068
Control	55.32 ± 3.33%	13.89 ± 0.95%	7.79 ± 0.95%	12.54 ± 0.96%	10.46 ± 1.07%	ND	ND	ND	ND
Laccase Control	47.00 ± 5.47%	23.28 ±0.89%*	8.51 ± 0.57%	14.06 ± 4.38%	7.15 ± 1.32%	ND	ND	ND	ND
4HBA Control	57.25 ± 0.78%	13.05 ± 2.97%	7.20 ± 0.79%	13.09 ± 1.43%	9.41 ± 1.40%	ND	ND	ND	ND
4HBA Modified	58.26 ± 4.34%	11.68 ± 1.41%	3.50 ± 1.10%*	14.40 ± 6.96%	3.59 ± 1.36%*	8.57 ± 0.83%*	ND	ND	ND
1 Day-4HBA-Heparin	61.27± 6.27%	8.42 ± 1.98%	ND*	16.97 ± 1.35%	2.32 ± 1.80%*	ND	5.29 ± 2.23%*	1.50 ± 0.11%*	0.92 ± 0.27%*
2 Day 4HBA-Heparin	56.50 ± 0.12%	7.82 ± 1.16%	ND*	19.51 ± 1.07%	2.07 ± 0.77%*	ND	7.33 ± 0.16%*	1.20 ± 0.18%*	0.77 ± 0.02%*
3 Day 4HBA-Heparin	57.55 ± 0.97%	7.52 ± 0.91%	ND*	18.53 ± 0.41%	3.18 ± 0.40%*	ND	5.99 ± 1.27%*	1.46 ± 0.06%*	0.87 ± 0.07%*
4 Day 4HBA-Heparin	58.64 ± 1.00%	7.14 ± 1.25%	ND*	17.38 ± 1.01%	2.89 ± 0.22%*	ND	6.63 ± 0.90%*	1.58 ± 0.04%*	0.97 ± 0.15%*

FITC-BSA and Lysozyme Adsorption

To analyze protein adsorption onto the heparin modified PES flat sheets, BSA and lysozyme adsorption were determined. This experiment was performed by using PES flat sheets that were modified with 4HBA for the specified time shown (Figure 37 and 38), and then reacted with ED and heparin. The results for FITC-lysozyme show an increase in protein adsorbed as the 4HBA modification time increased (Figure 37). This could be due to an increase in the amount of heparin on the surface and/or the increase in unreacted 4HBA on the surface. Since the protein adsorption increased with heparin modification that could indicate a charge-charge interaction between the negatively charge membrane surface with an overall positively charged for lysozyme. For FITC-BSA (Figure 38), there was no significant difference between the control membranes and the membranes modified with heparin. This shows that BSA adsorption does not decrease upon addition of heparin to the membrane surface.
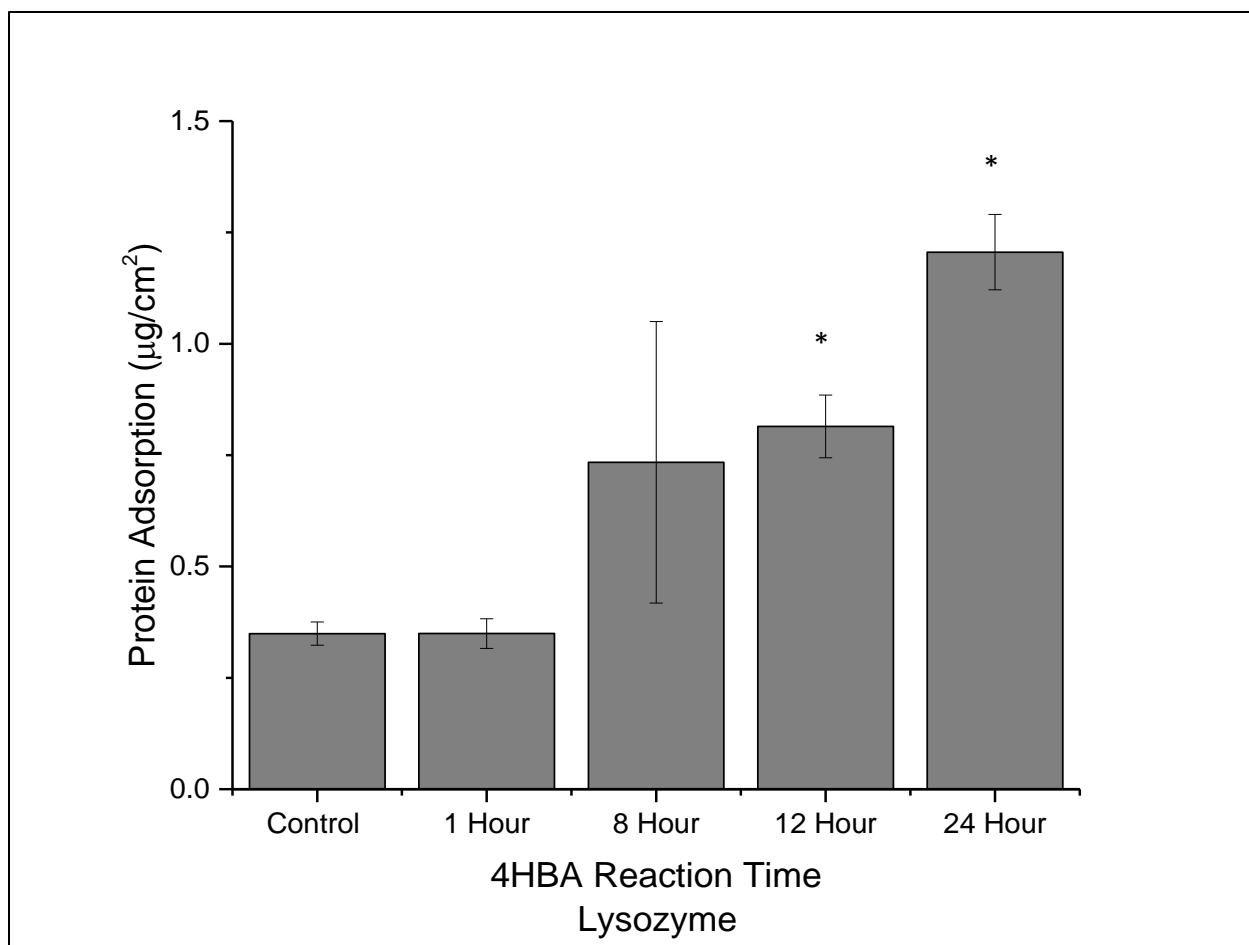
Figure 37. Lysozyme adsorption onto PES membranes modified with 4-hydroxybenzoic acid (4HBA) polymers for 1, 8, 12, and 24 hours then heparin modified compared to control PES membranes. N=3 * indicates a significant difference at the 95% confidence level compared the control using a single factor ANOVA with Bonferroni post hoc test.
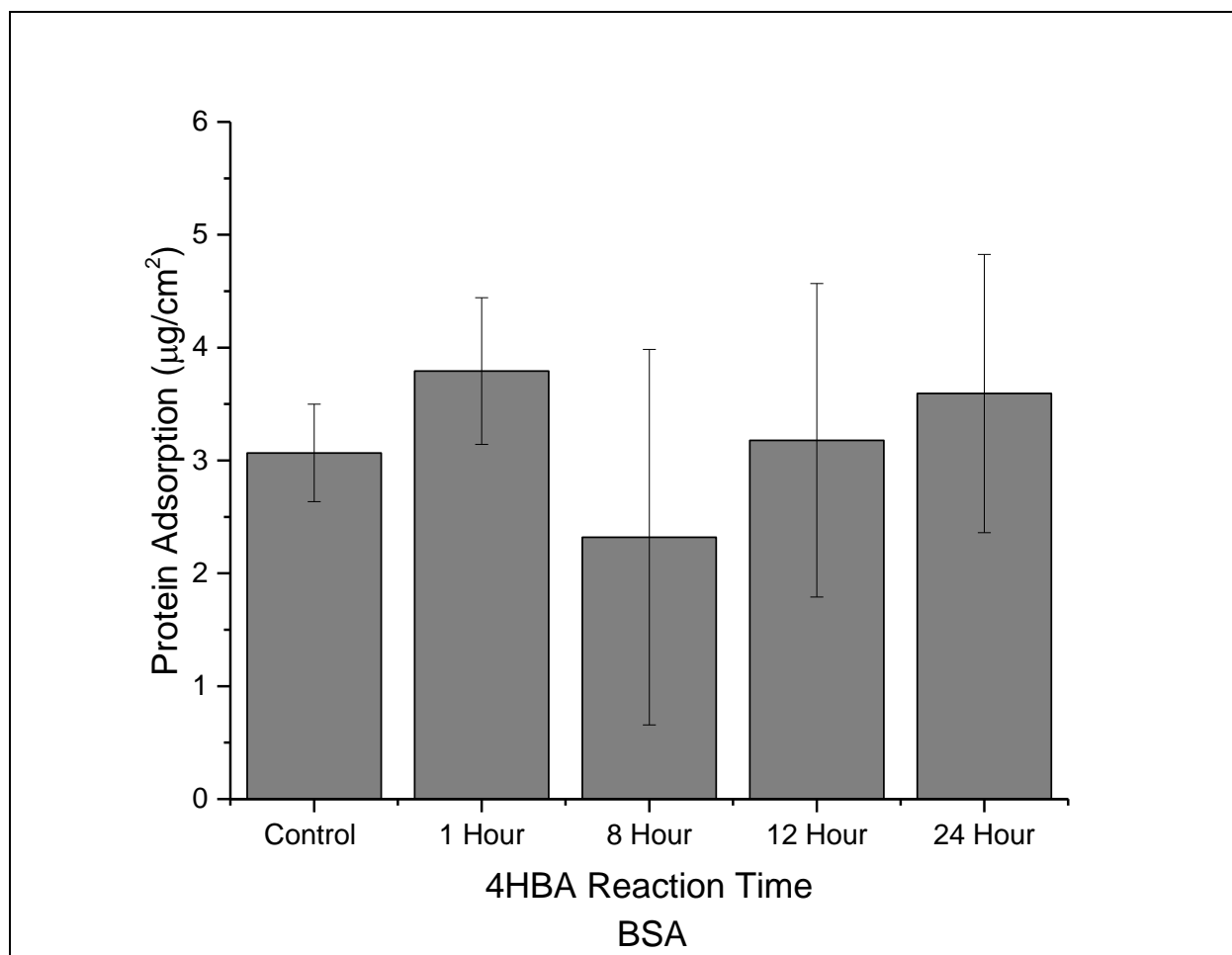
Figure 38. BSA adsorption onto PES membranes modified with 4-hydroxybenzoic acid (4HBA) polymers for 1, 8, 12, and 24 hours then heparin modified compared to control PES membranes. N=3, * indicates a significant difference at the 95% confidence level compared the control using a single factor ANOVA with Bonferroni post hoc test.

Equilibrium Dialysis Experiments

Equilibrium dialysis experiments were performed to provide a way to test the transport across the PES flat sheet membranes modified with heparin. An initial experiment was performed to test if by placing the affinity agent on the same side or opposite side of the target (CCL2), it would increase transport. The results from this experiment (Table 13) show that placing the affinity agent and the target on the same side showed a non-detectable concentration for each side of the membrane. This could be due to the binding of CCL2 to the heparin side making the levels not detectable in solution. Also, by placing the CCL2 on the PET side and the heparin modification being on the PES side, CCL2 was observed on the PET side. However, CCL2 was only detected on the heparin modification side for the 2 day 4HBA modified, heparin modified membrane. This could be due to the binding on the heparin and CCL2. The samples collected after incubation with 2 M NaCl showed non-detectable concentrations of CCL2 indicating that the bound CCL2 was not removed by the addition of NaCl.

The concentration of CCL2 was then increased to 112 ng/mL (Table 14) observable concentrations of CCL2, however when this experiment was repeated, concentrations of CCL2 were not detectable. This could be due to the binding of CCL2 to the membrane surface and blocking pores since a significant portion of the 112 ng/mL CCL2 concentration was lost to the equilibrium dialysis chamber and the membrane.

Table 13. Equilibrium dialysis experiment using 4,000 pg/mL of CCL2 placed on either the same side or opposite side of the heparin modification inside the chamber for 24 hours. Samples were then collected from each side and analyzed using a CCL2 ELISA. ND= not detected (<31 pg/mL).

Opposite Side			Same Side		
4HBA Reaction Time (Days)	Heparin PES (pg/mL)	PET with CCL2 (pg/mL)	4HBA Reaction Time (Days)	Heparin PES (pg/mL)	PET (pg/mL)
1	ND	480	1	ND	ND
2	270	1110	2	ND	ND
3	ND	450	3	ND	ND
4	ND	450	4	ND	ND
PES	ND	ND	PES	ND	ND

Table 14. Equilibrium dialysis experiment using 112 ng/mL of CCL2 placed on the opposite side of the heparin modification inside the chamber for 24 hours. Samples were then collected from each side and analyzed using a CCL2 ELISA.

4HBA Reaction Time (Days)	Heparin side (PES) (ng/mL)	PET side (ng/mL)
1	10.4	0.3
2	13.8	0.5
3	1.8	0.3
4	2.7	0.1

Nonspecific Adsorption of BSA to the Equilibrium Dialysis Chamber

BSA adsorption to the equilibrium dialysis chamber was calculated to determine to what extent protein is adsorbing onto the equilibrium dialysis chamber. The determined amount of loss of BSA to the equilibrium dialysis chamber was 0.54 $\mu g/cm^2$ this was 23% of the original BSA added to the container. Although the experiments performed with CCL2 did have a concentration of 0.1% BSA as a blocking agent, this could explain some of the loss of the analyte (CCL2).

<u>FITC-10 and Methyl Orange Equilibrium Dialysis Experiments</u>

FITC-10 and methyl orange equilibrium dialysis experiments were performed in order to provide a simpler system to better understand the sample loss that is occurring in these equilibrium dialysis experiments. The results for this experiment (Figure 39) show that compared to the starting concentration, the PET side decreases in concentration. However, the PES side did not increase as rapidly to match the decrease in concentration from the PET side. This indicates that the FITC-10 is either adsorbed onto the material and/or trapped inside the pores which can be visibly seen by a yellow color when the membrane is removed from the module.

Since FITC-10 was adsorbing to the membrane surface with the 100 kDa PES flat sheets, an experiment was performed with methyl orange with 300 kDa PES flat sheets. The data from this experiment (Figure 40) show a decrease in the concentration of the PET side compared to the starting concentration. The PES side does not show a corresponding increase in methyl orange concentration, indicating that the methyl orange is trapped inside the membrane. Although equilibrium is reached between hours 2 and 5 indicated by the absorbance values being almost identical, there is still significant loss of the methyl orange to the membrane surface which is observed by the orange color of the membrane.
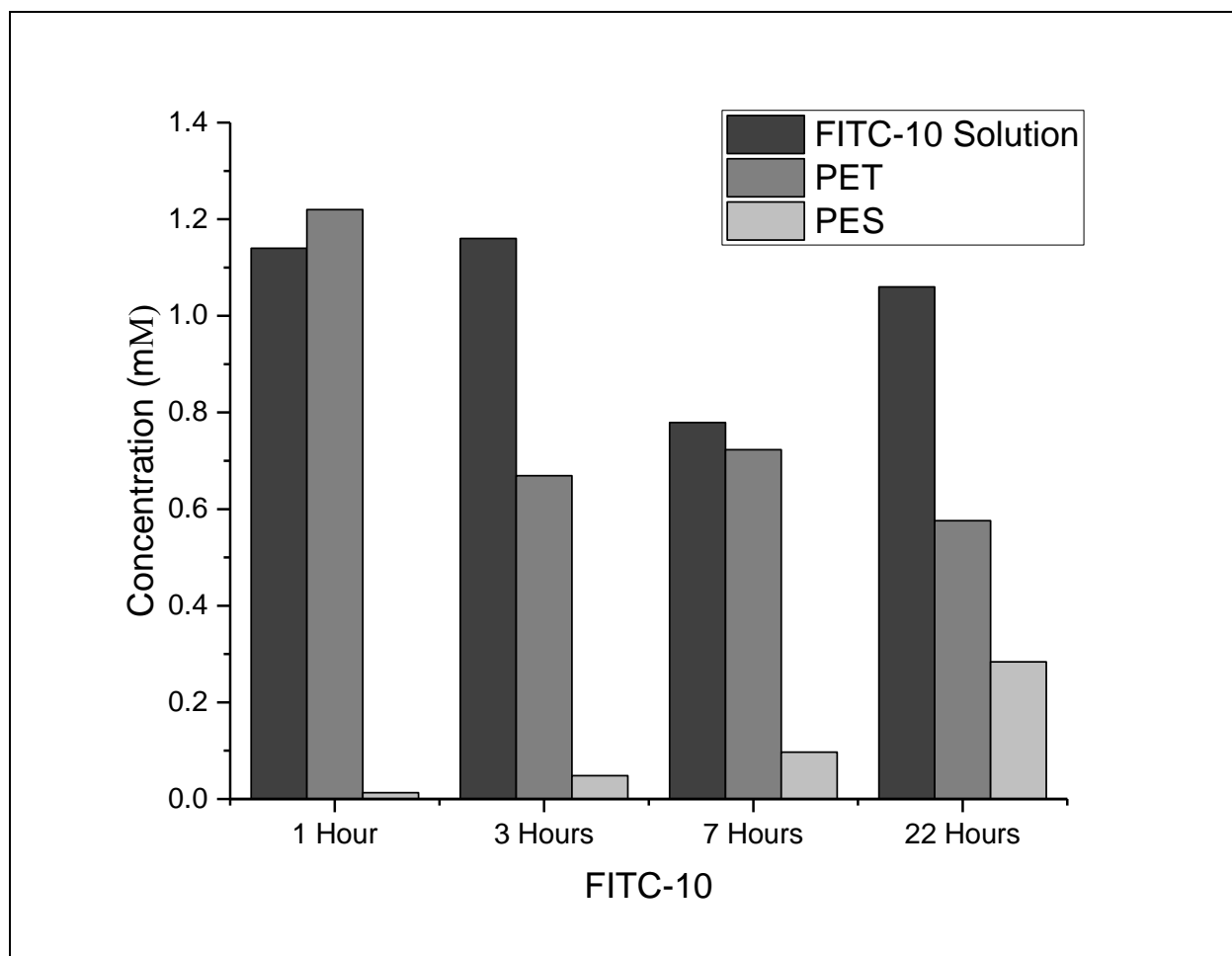
Figure 39. Equilibrium dialysis data for FITC-10 on 100 kDa PES flat sheet membranes. The side of the chamber that exposed the PES side of the membrane contained the initial FITC-10 solution labeled PES above and the side of the chamber that exposed the PET side of the membrane labeled PET above. Both sides of the chamber were analyzed.
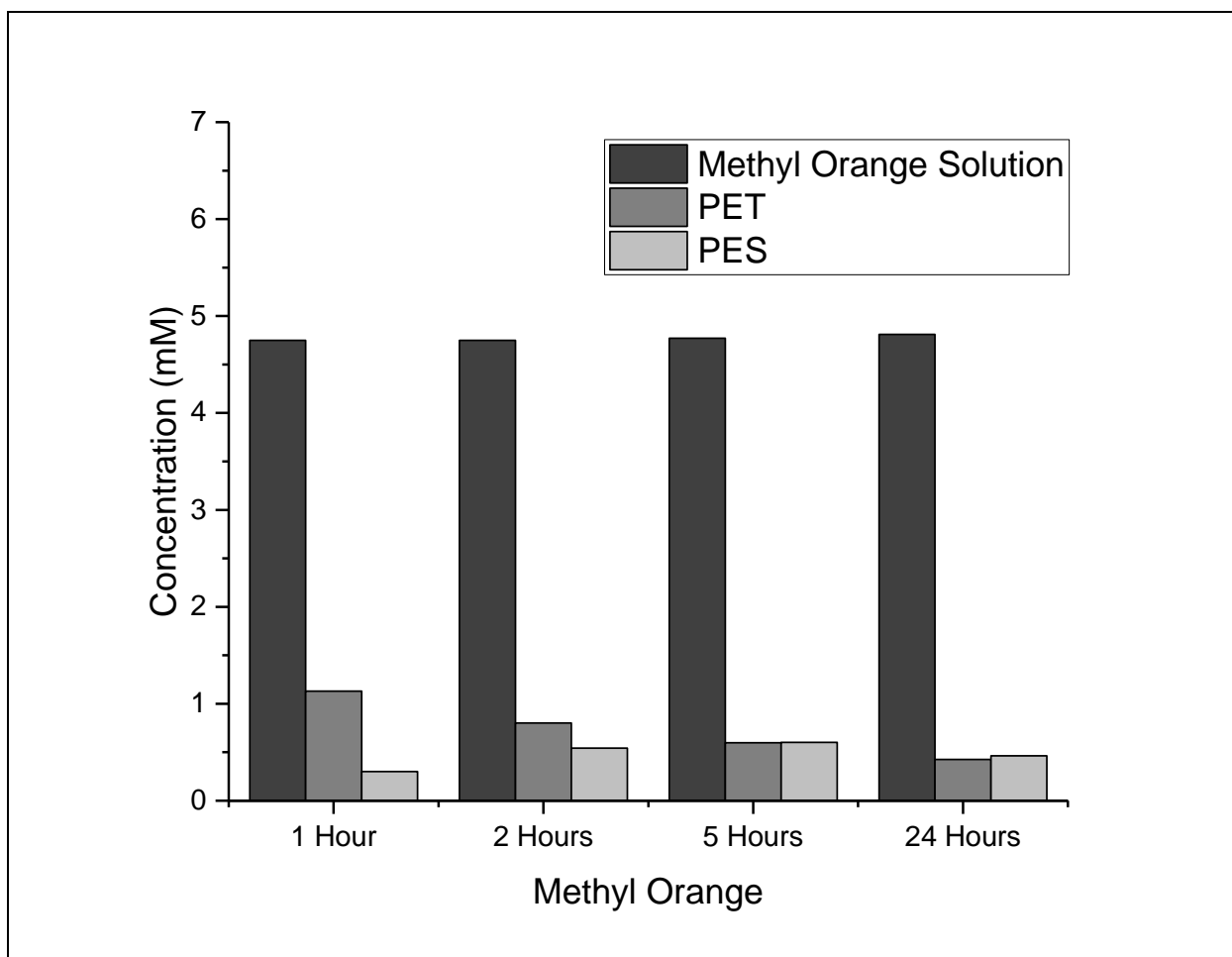
Figure 40. Equilibrium dialysis data for methyl orange for 300 kDa PES flat sheet membranes. The side of the chamber that exposed the PES side of the membrane contained the initial FITC-10 solution labeled PES above and the side of the chamber that exposed the PET side of the membrane labeled PET above. Both sides of the chamber were analyzed.

Conclusions from Equilibrium Dialysis Experiments

After confirming the attachment of heparin on the PES flat sheets but determining that transport across these flat sheets was hindered by the analyte adsorbing onto the membrane surface and/or pores, microdialysis experiments were performed. The reason for making this decision was based on previous research which showed that analytes could be collected in the dialysate using microdialysis. The overall goal of using the flat sheet membranes was to understand the chemistry to attach heparin onto the surface. This was successful in confirming the attachment of heparin onto the PES flat sheet membranes. The information provided through the equilibrium dialysis experiments could provide insight into mass transport enhancement however these membranes are typically used in pressurized systems and are rated for such systems, so it was difficult to see transport using an equilibrium dialysis chamber. Applying a pressurized system for cytokine collection would be difficult due to the increase in sample size that would be needed.

Effect of Heparin Modification of Microdialysis Membranes on Relative Recovery of Heparin Binding Proteins

After confirming the attachment of heparin to PES flat sheets, the method was applied to the membrane of microdialysis probes. To confirm the attachment of heparin to microdialysis membranes XPS analysis was performed and then the RR experiments were performed. Initially FITC-4, FITC-10, and FITC-20 were used to determine if heparin modification reduced RR significantly due to pore blockage caused by the modification. Next, RR of three heparin binding proteins (CCL2, VEGF, and aFGF) was determined as well as KC/GRO. The reason for choosing these heparin binding proteins was that CCL2 has a slow off rate compared to VEGF, and aFGF. This will test if RR enhancement is affected by the off rate.

Modification of Microdialysis Membranes with Heparin

XPS analysis was performed on microdialysis membranes in order to confirm the attachment onto the membrane surface. Results from XPS analysis, Table 15, show that the carboxylic acid functional group is found in the heparin modified membranes and not present in the control membranes. There is also a decrease in the C-S functional group to below detectable levels upon modification with heparin. Also, there is a significant increase in the percentage of sulfur 2p found in heparin modified membranes. The carboxylic acid functional group is found in both heparin and 4HBA modifications, but the increase in the amount S2p present can only come from the addition of heparin to the membrane surface which confirms the attachment of heparin to the microdialysis membrane.

Table 15. XPS data from control 4HBA and heparin modified microdialysis membranes. Percentages are determined from the peak areas of the C1s, O1s, and S2p high resolution XPS spectra. * indicates a significant difference from the control at the 95% confidence level using a single factor ANOVA with Bonferroni post hoc test. # indicates significant difference from the 4HBA modified MD membrane at the 95% confidence level. ND indicates not detected (<0.1%).

	C-C/C-H	C-O	COOH	S2p	O-C	O-S
Binding Energy (eV)	284.64 ± 0.15	285.75 ± 0.38	287.72 ± 0.35	167.89 ± 0.17	531.82 ± 0.32	533.54 ± 0.24
Control	54.65 ± 10.40%	22.54 ± 6.76%	ND	3.12 ± 1.14%#	15.14 ± 5.07%	3.15 ± 0.64%
4HBA Modified	49.83 ± 11.88%	17.68 ± 6.50%	9.73 ± 5.94%*	0.85 ± 0.18%*	14.81 ± 4.36%	ND
Heparin Modified	56.60 ± 4.66%	22.35 ± 17.93%	3.23 ± 2.86%*	2.31 ± 0.49%#	22.30 ± 11.52%	ND

FITC-Dextran and Lysozyme Relative Recovery

After confirming the attachment of heparin to microdialysis probes RR experiments were performed. First FITC-4 RR was analyzed to determine if the modification with heparin blocked pores inhibiting the RR. FITC-4 relative recovery was determined for microdialysis membranes initially, and after 4HBA, ED, and heparin modifications. This was determined to see if recovery of FITC-4 would be affected by the modification. The results from this experiment (Figure 41) show a significant decrease in the RR of FITC-4 after modification with 4HBA polymerization solution for 24 hours. The RR for FITC-4 does not change after modification with ED and heparin, indicating that after modification for 24 hours with 4HBA, that the addition of ED and heparin does not further decrease the RR of FITC-4. After testing the RR for FITC-4 with a 24 hour 4HBA modification time, the RR was analyzed with 2 hour and 24 hour 4HBA-heparin modified probes and compared to the control for FITC-4, FITC-10, and FITC-20 as well as lysozyme. For FITC-4 (Figure 42), FITC-10 (Figure 43), and FITC-20 (Figure 44), the RR was significantly lower after heparin modification compared to the control. For

FITC-4 and FITC-20 the decrease in RR for heparin modified membranes when compared to the

4HBA modification was not significantly different for the 24 hour modification time but was

significantly lower for the 2 hour modification time. For FITC-10, RR for the 2 hour 4HBA

modification time before and after heparin modification was not significantly different but FITC-

10 RR was significantly higher for the 24 hour modification time after heparin modification

compared to before heparin modification.
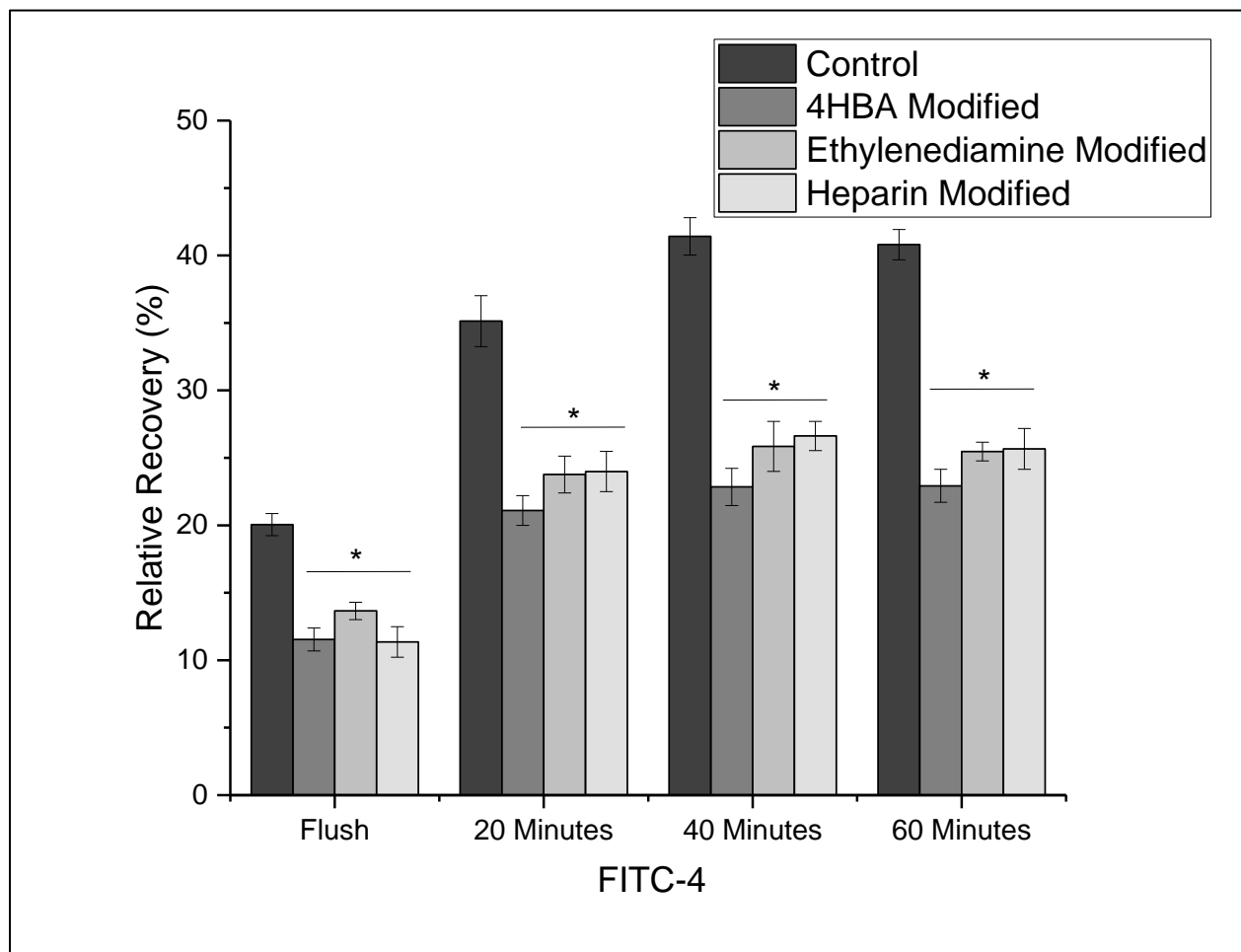
Figure 41. FITC-4 relative recovery for the same control, 24 hour 4HBA, ethylenediamine, and heparin modified microdialysis probes. N=3 *indicates a significant difference at the 95% confidence level compared the control using a two factor ANOVA with Bonferroni post hoc test.
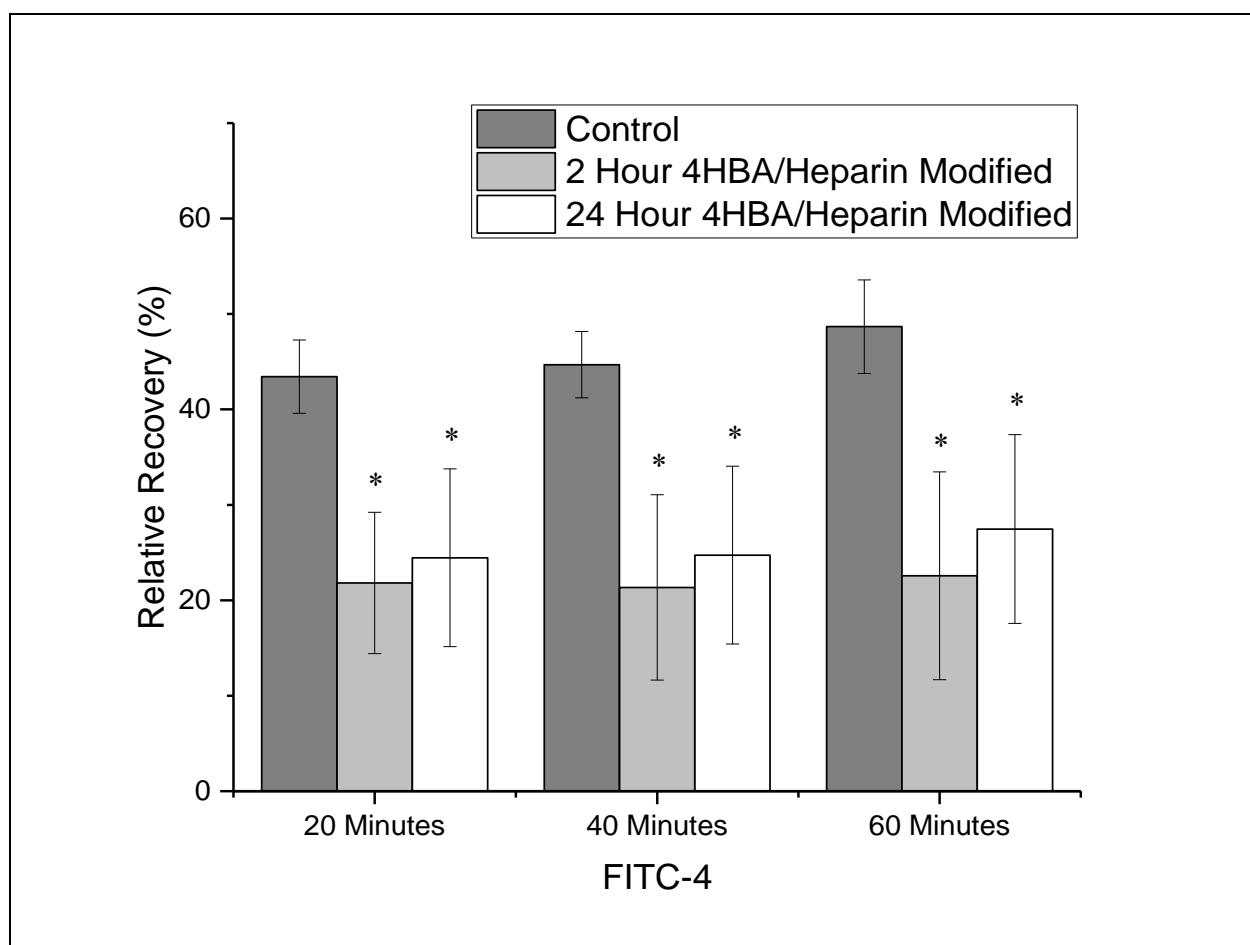
Figure 42. FITC-4 relative recovery for control, 2, and 24 hour 4HBA-heparin modified microdialysis probes. N=3, * indicate significant difference at the 95% confidence level using a two factor ANOVA with Bonferroni post hoc test.
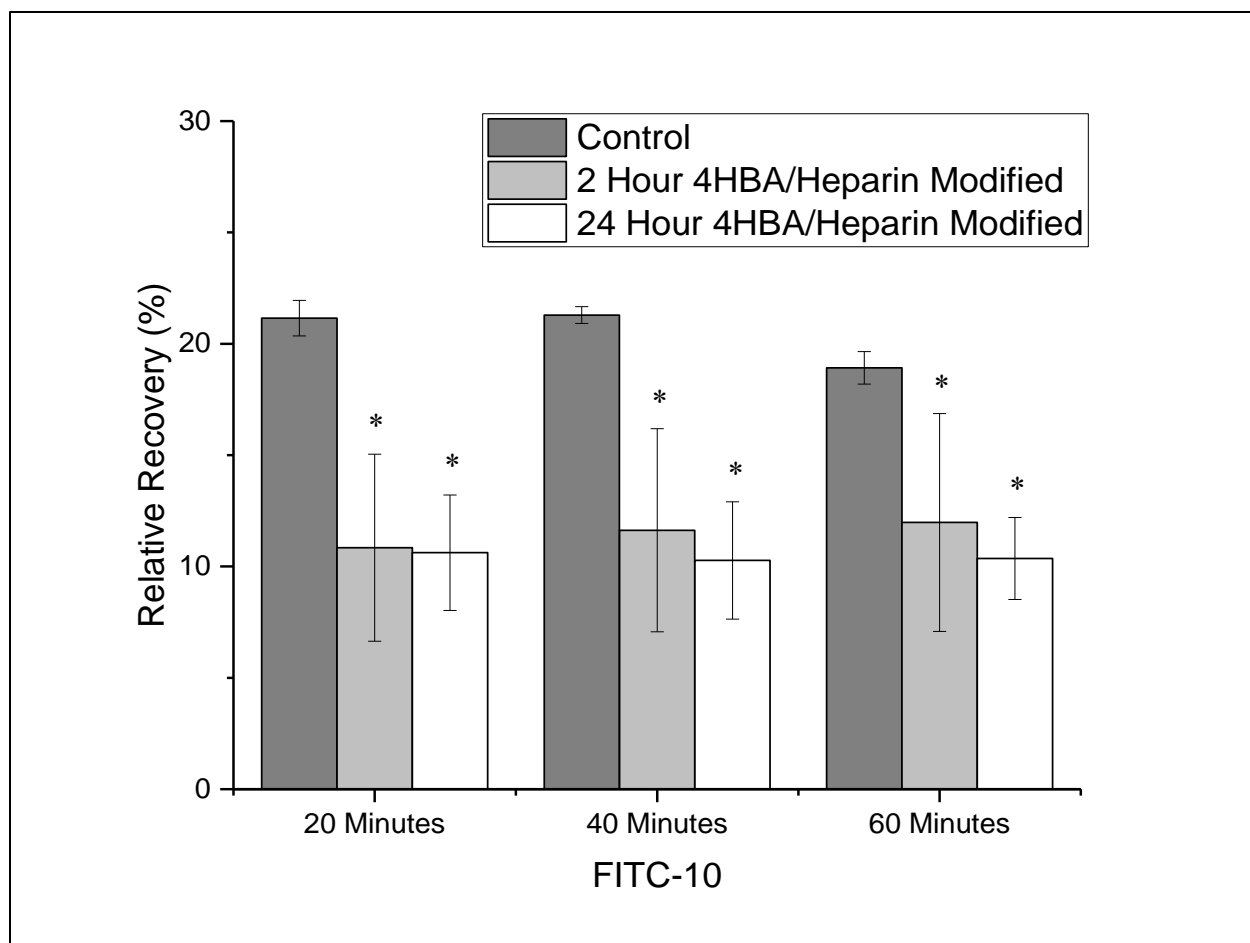
Figure 43. FITC-10 relative recovery for control, 2, and 24 hour 4HBA-heparin modified microdialysis probes. N=3, * indicate significant difference at the 95% confidence level using a two factor ANOVA with Bonferroni post hoc test.

Figure 44. FITC-20 relative recovery for control, 2, and 24 hour 4HBA-heparin modified microdialysis probes. N=3, * indicate significant difference at the 95% confidence level using a two factor ANOVA with Bonferroni post hoc test.
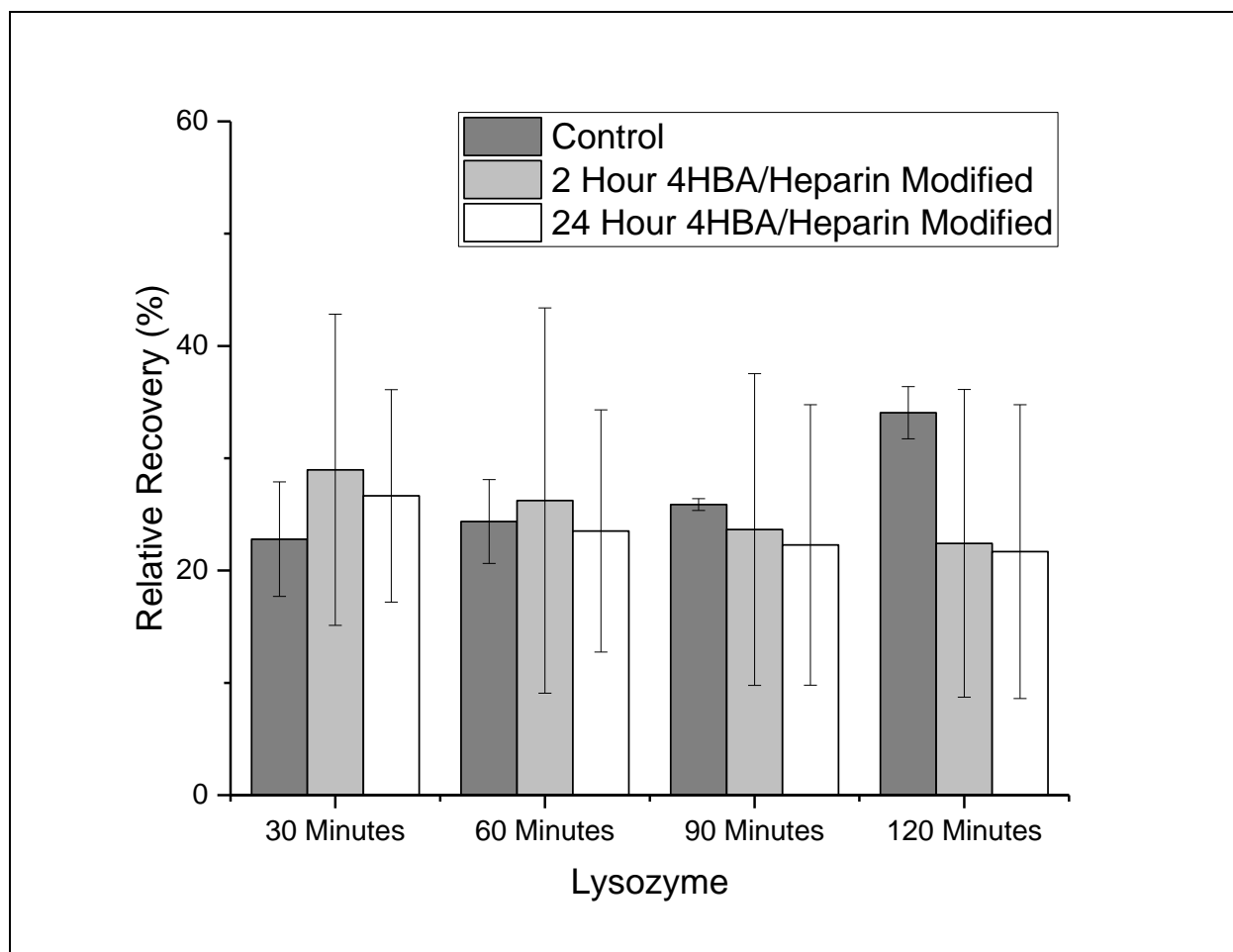
Figure 45. Lysozyme relative recovery for control, 2 hour, and 24 hour 4HBA-heparin modified microdialysis probes. Probes were placed in a solution containing 500 µg/mL of lysozyme. N=3

Lysozyme RR, shown in Figure 45, shows no significant difference between the control and after heparin modification regardless of 4HBA modification time. What is interesting about this is that for the 24 hour 4HBA modification, the RR was below the detection limit of the assay (25 µg/mL); upon modification with heparin the RR increased to a value that was not significantly different than the control RR.

Relative Recovery of KC/GRO for Control, 2 Hour and 24 Hour 4HBA-Heparin Modified Microdialysis Membranes

Next RR for KC/GRO was tested with control, 2 and 24 hour heparin modified microdialysis membranes. KC/GRO was also analyzed because the human analog of rat KC/GRO is IL-8 which is a known heparin binding protein.[139] The reason for testing this analyte was to see if RR enhancement could be observed which could be an indication of KC/GRO binding to heparin. The results for this experiment (Figure 46) show no enhancement in RR for the 24 hour 4HBA-heparin modified membranes compared to the control membranes. For the 2 hour 4HBA-heparin modified membranes relative recovery approximately doubled. This could indicate that KC/GRO is binding to the heparin modification on the membrane surface. The increase in RR could also be due to a charge-charge interaction between the negatively charge surface and KC/GRO because the results are similar to what was observed for the 2 hour 4HBA modified microdialysis membranes. This could indicate that the heparin modification is also reducing nonspecific adsorption of KC/GRO leading to an increase in RR.
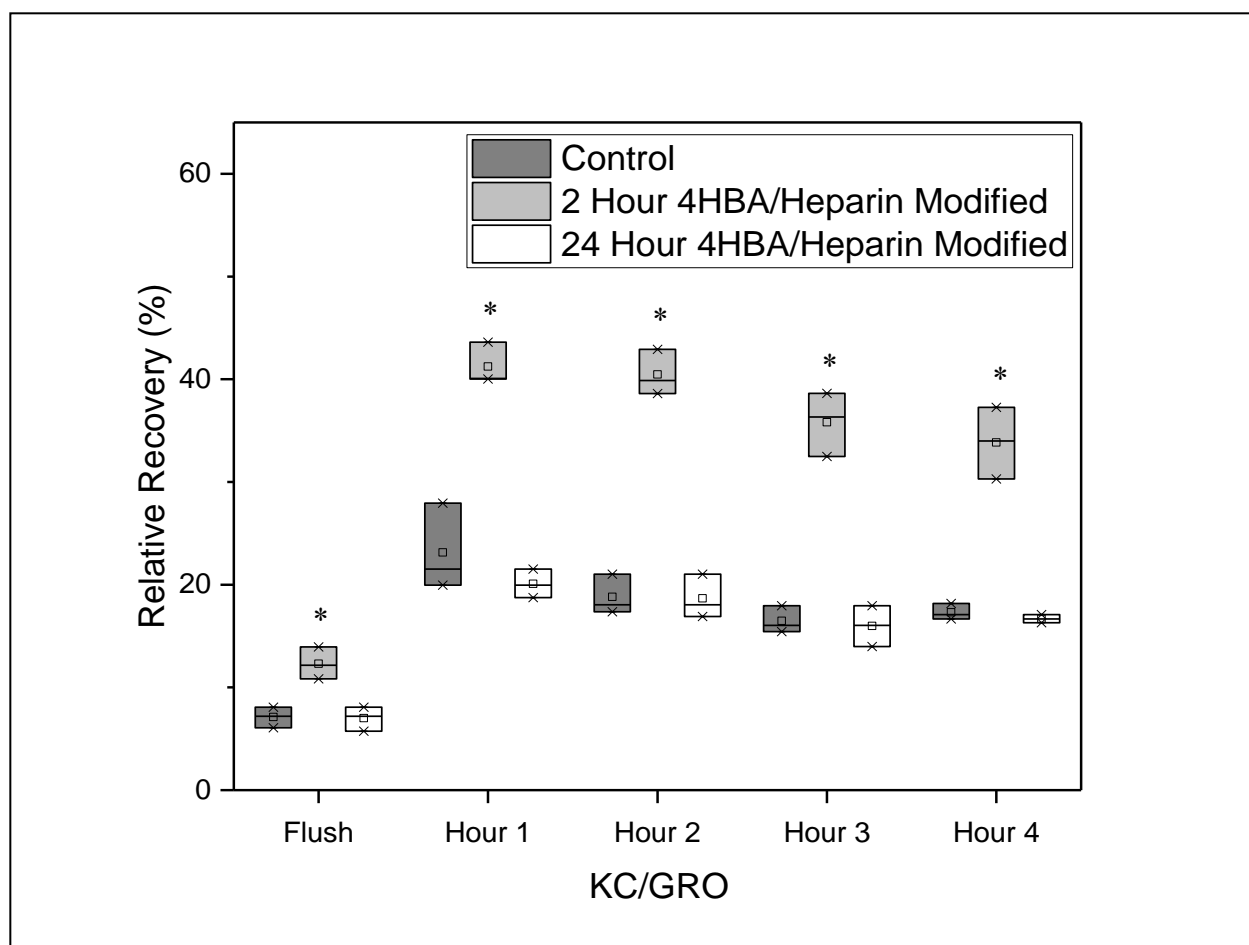
Figure 46. Box and whiskers plot of KC/GRO relative recovery of control 2 hour and 24 hour 4HBA-heparin modified microdialysis probes. N=3 * Indicates significantly different than the control at the 95% confidence level as determined by a 2 factor ANOVA with Bonferroni post hoc test.

Relative Recovery of CCL2, aFGF, and VEGF for Control, 2 Hour, and 24 Hour 4HBA-Heparin Modified Microdialysis Membranes

RR was calculated for CCL2, aFGF and VEGF. These three analytes are known heparin binding proteins and also have both fast (VEGF, aFGF) and slow off rates (CCL2). These are known heparin binding proteins, so RR was determined to test if by adding heparin as an affinity agent to the membrane surface would increase RR. From this information more insight will be given into the factors that affect the RR enhancement by affinity agents like heparin.

For the 24 hour 4HBA-heparin modified microdialysis probes, there is a significant increase in RR observed for hours 2 to 4 (Figure 47). The increase at hour 2 is approximately 20% and for hours 3-4 is close to 100%. For the 2 hour 4HBA-heparin modified microdialysis probes, there is no significant difference between the control and the 2 hour 4HBA-heparin modified microdialysis probes (Figure 48). For the 24 hour 4HBA-heparin modified membranes, the RR increase after hour 1 may be that the rate of binding of CCL2 to heparin is faster than the rate of release. After hour 1 an equilibrium phase where the rate of binding and releasing is equal; this allows for the increase in RR due to the blocking of irreversible binding sites by the addition of heparin onto the membrane surface. For the 2 hour 4HBA-heparin modified microdialysis membranes there may be insufficient heparin on the surface to observe a significant increase in RR.
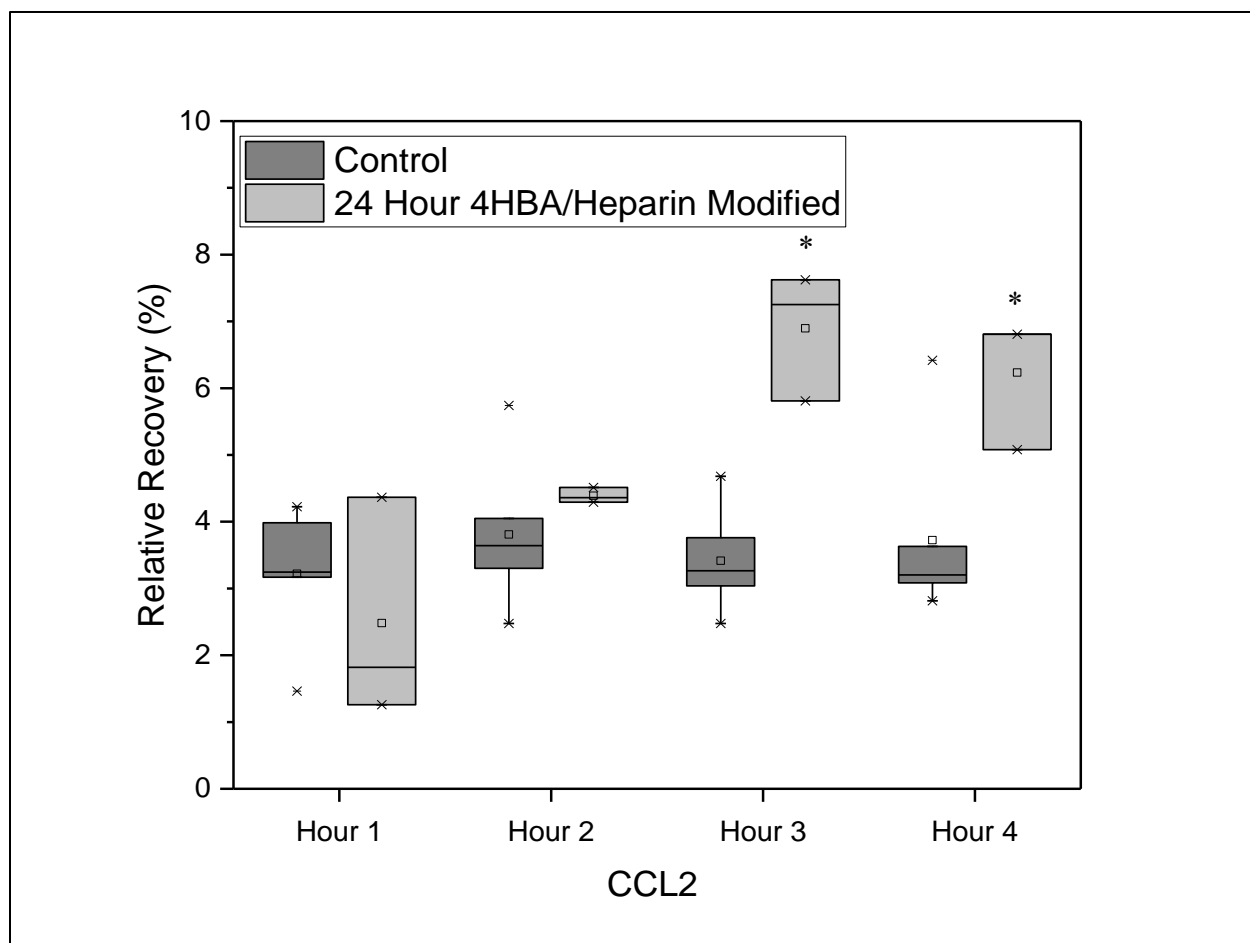
Figure 47. Box and whiskers plot of CCL2 RR of control and 24 hour 4HBA-heparin modified MD probes. N=6 for control, and N=3 for 24 hour 4HBA-heparin modified MD probes. * indicates significance at the 95% confidence level.
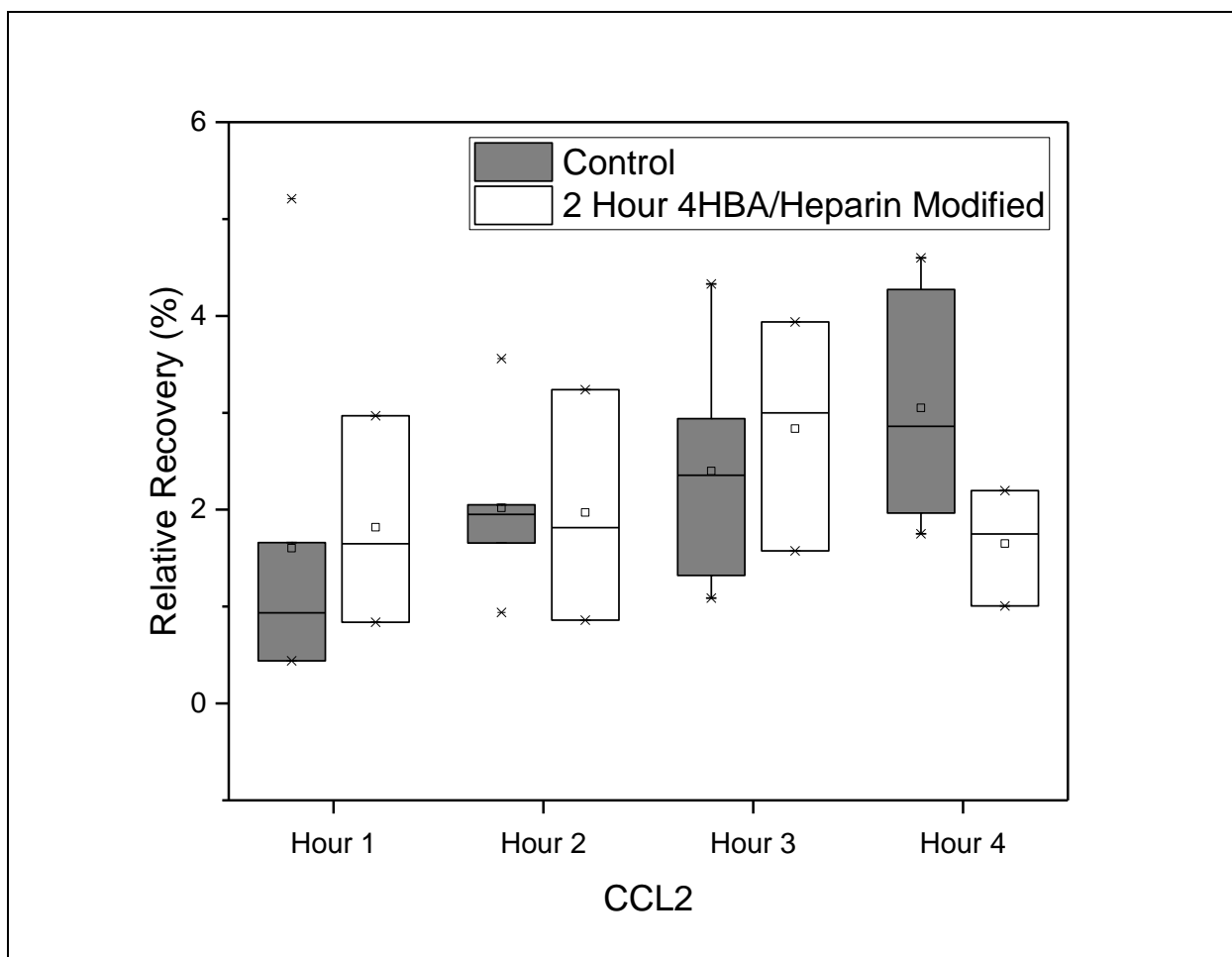
Figure 48. Box and whiskers plot of CCL2 RR of control and 2 hour 4HBA-heparin modified MD probes. N=6 for control MD probes and N=3 for 2 hour 4HBA-heparin modified microdialysis probes.
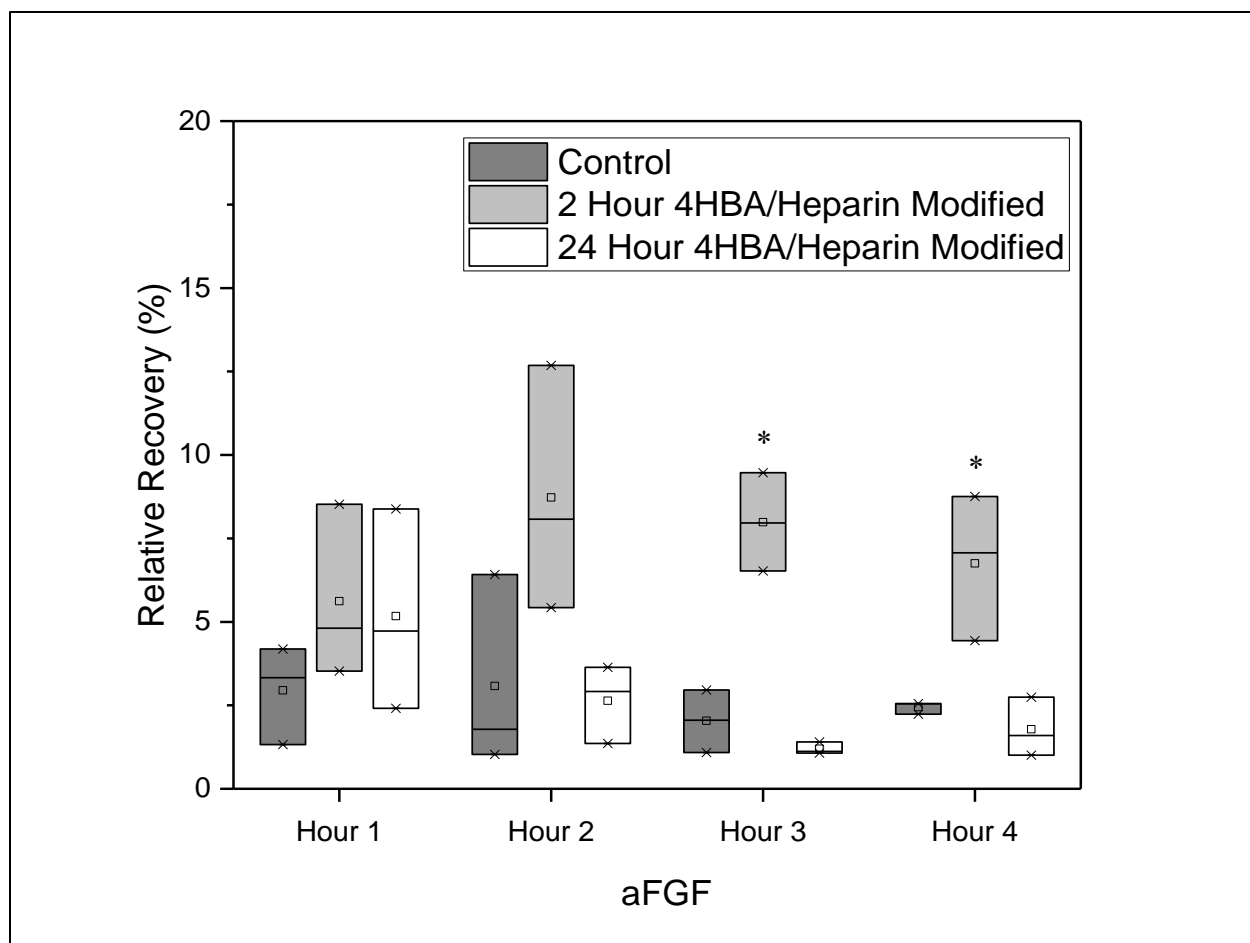
Figure 49. Box and whiskers plot of aFGF relative recovery of control, 2 hour and 24 hour 4HBA-heparin modified MD probes. N=3. * indicates significance at the 95% confidence level.

The next analyte that was tested was aFGF which has a fast off rate compared to CCL2. The results from the aFGF in vitro microdialysis experiment in Figure 49 show a significant increase in RR after hour 2 for the 2 hour 4HBA-heparin modified microdialysis probes. The RR for 24 hour 4HBA-heparin modified microdialysis probes did not change significantly. CCL2 is 13.1 kDa (pI 9.25) and is slightly smaller than aFGF at 15.5 kDa (pI 5.6). Since aFGF is approximately 2 kDa larger in mass compared to CCL2, the 24 hour 4HBA modification time may exclude more of the aFGF compared to the CCL2. This may be the reason the RR for aFGF did not increase for the 24 hour 4HBA-heparin modified microdialysis membranes. For the 2 hour 4HBA-heparin modifications since aFGF has a slightly higher on-rate and a faster off rate, more heparin may not need to be bound to the surface in order to see RR enhancement.

Next, VEGF relative recovery was determined for control, 2 hour and 24 hour 4HBA-heparin modified microdialysis membranes. VEGF RR results for 2 hour 4HBA-heparin modified and 24 hour 4HBA-heparin modified membranes are shown in Figure 50. For the 24 hour 4HBA-heparin modification there was a significant difference in RR for VEGF compared to the control. The increase in RR observed is slight compared to the control. VEGF is larger at 21 kDa than CCL2 and aFGF at 13.1 and 15.5 kDa. Since it is known that the modification with 4HBA can decrease the pore size, especially at the 24 hour reaction time, the transport of VEGF RR may decrease more due to the pore size decrease than can be compensated for by the affinity interaction on the membrane surface. This could also explain why there is no significant difference in the RR for the 2 hour 4HBA-heparin modification because there is possibly less heparin on the surface.
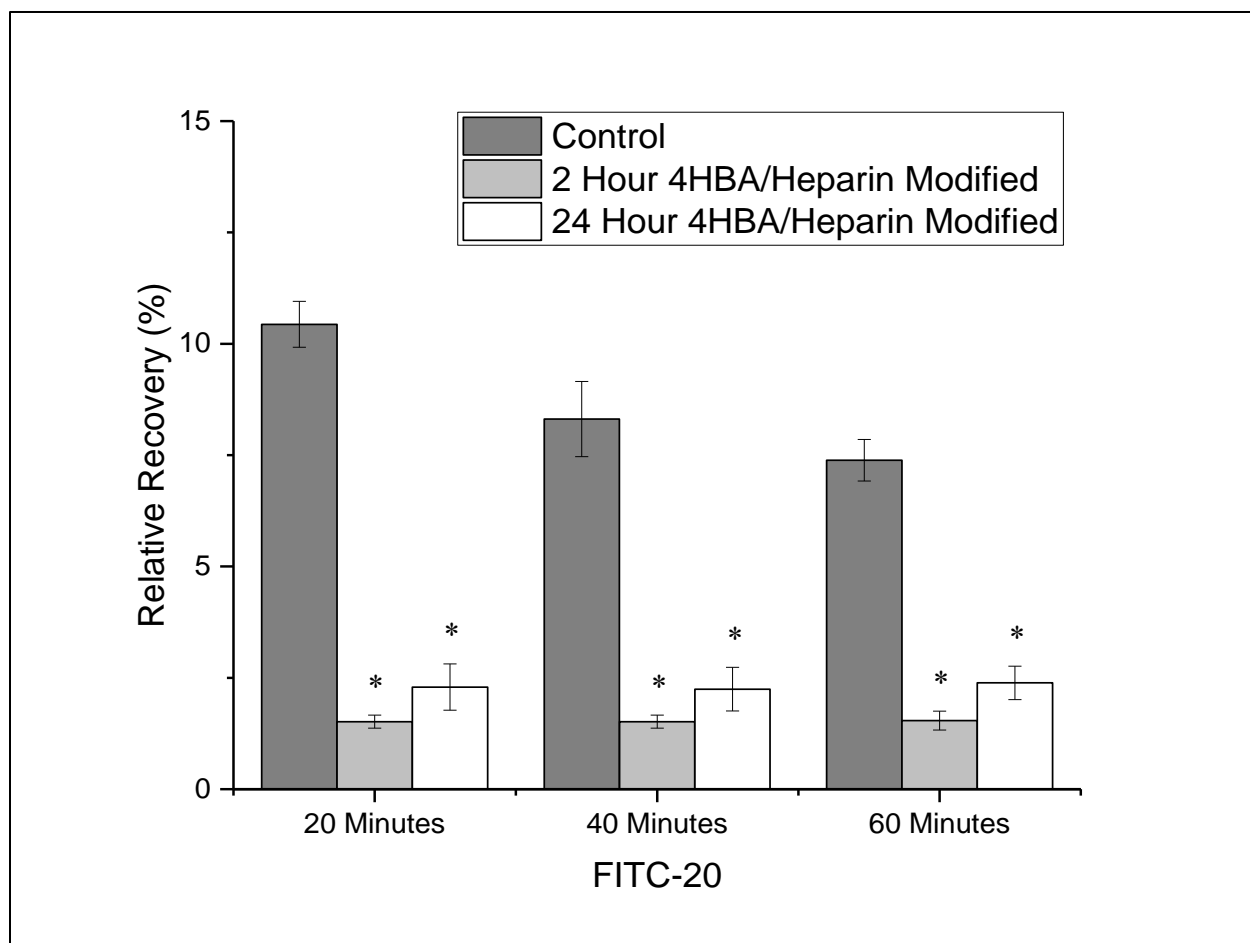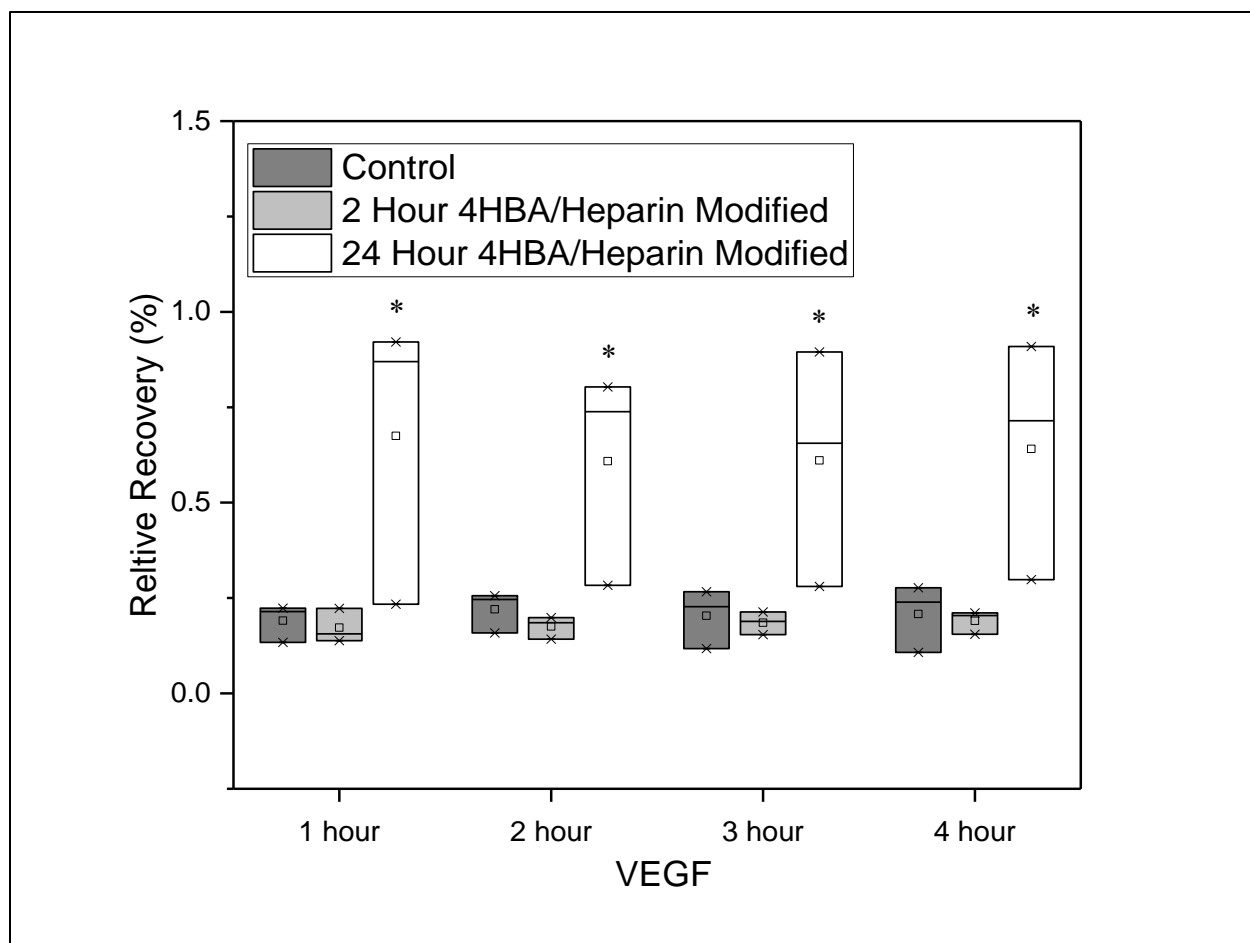
Figure 50. Box and whiskers plot of VEGF relative recovery of control, 2 and 24 hour 4HBA modified microdialysis probes. N=3 * Indicates significantly different than the control at the 95% confidence level as determined by a 2 factor ANOVA with Bonferroni post hoc test.

With the attachment of heparin onto the membrane surface, RR of CCL2, aFGF, and

VEGF were analyzed. CCL2 RR increased twofold at hours 3 and 4 for the 24 hour 4HBA-

heparin modification. For aFGF RR for the 2 hour 4HBA-heparin modified MD probes

increased twofold for hours 3 and 4. CCL2 is smaller at 13.1 kDa than aFGF at 15.5 kDa. Since

the 24 hour modification is shown to inhibit transport this could explain why the increase in RR

for aFGF is not observed for the 24 hour modification time. This may also explain why the

increase in RR for VEGF is also small for the 24 hour modification time because VEGF is 21

kDa.

Conclusions

This chapter shows successful attachment of heparin on to PES flat sheets and

microdialysis membranes shown by XPS and ATR-FTIR analysis. Protein adsorption

experiments show no significant change in adsorption for BSA and an increase in adsorption of

lysozyme for 12 and 24 hour modification times. Equilibrium dialysis experiments were

attempted with heparin modified flat sheets but there was a high amount of analyte binding to the

membrane surface and pores. FITC-4, FITC-10, and FITC-20, RR was calculated and showed

that upon addition of ED and heparin that the recovery did not decrease compared to the initial

decrease from addition of 4HBA. Relative recovery of CCL2 increased 2 fold at hours 3 and 4

and for VEGF at all collection times for the 24 hour 4HBA-heparin modified membranes. These

RR enhancements were less than what was observed with using heparin-immobilized

microspheres for CCL2 and VEGF of 4 fold and 2 fold increases, but this could be due to the

reduction in pore size due to the modification.[53] This could be improved upon by testing

different 4HBA, and heparin modification times. Also aFGF showed a 2 fold increase in RR for

hours 3 and 4 for 2 hour 4HBA-heparin modified membranes. This increase in RR was not

observed under the same flow rate conditions of 1 μL/min with heparin modified microspheres so by adding heparin to the membrane surface the RR was enhanced twofold which is an improvement on the previously used method.[53] By doubling the RR the concentration required to detect these analytes is reduced by half. For example for CCL2 the detection limit for the ELISA assay is 31 pg/mL so with a RR of 3.84% the minimum amount of CCL2 needed outside the probe to be detected by this assay would be 806 pg/mL. With the 24 hour 4HBA-heparin modification with an average RR of 6.56% at hours 3 and 4 the required amount of CCL2 needed outside the probe would be 472 pg/mL. By increasing the RR the analyte is able to be detected at a lower concentration. If the analyte is indicative of the onset of a specific condition or disease being able to detect this analyte at a lower concentration could ultimately lead to detecting the condition or disease marker sooner.

CHAPTER 6. CONCLUSIONS AND FUTURE PROSPECTS

Microdialysis is a technique which has the ability to sample the extracellular fluid space surrounding the membrane but one of the challenges to this technique is the ability to sample proteins which have low relative recovery and are at low concentrations (ng/mL-pg/mL range). This introduces a problem in detecting these proteins. An approach to solving this problem is to increase the relative recovery of these proteins across the microdialysis membrane. By increasing the relative recovery the amount of analyte external to the probe needed to detect this analyte is reduced. For example is the relative recovery is doubled then the external concentration needed for detection by the assay is reduced by half.

Introduction of perfusion fluid additives, such as BSA, antibodies, and heparin, have been previously shown to increase relative recovery.[7]   These perfusion fluid additives look at two different approaches to increasing relative recovery: reducing nonspecific adsorption (BSA), and introducing an affinity interaction (heparin, antibodies). In this dissertation the membrane surface was modified in order to study the enhancement of relative recovery using these two different methods. To study the enhancement of relative recovery by reducing nonspecific adsorption, 4-hydroxybenzoic acid polymers were covalently added to the membrane surface using a laccase catalyzed reaction. To study the effect of relative recovery by attaching an affinity agent, heparin was attached to the membrane surface.

Conclusions

To study how the addition of 4-hydroxybenzoic acid polymers altered relative recovery in microdialysis, a method was devised to modify the microdialysis membrane surface using the enzyme laccase. Laccase catalyzes the one-electron oxidation of four reducing-substrate

molecules followed by the four-electron reduction of molecular oxygen to water.[91] The overall outcome of the catalytic cycle is the reduction of one molecule of oxygen to two molecules of water and the concomitant oxidation of 4 substrate molecules to produce 4 radicals.[91] These 4HBA radicals can then react with the PES surface as well as with other 4HBA molecules. The reaction between 4-hydroxybenzoic acid and laccase was used to generate 4HBA polymers onto the microdialysis membrane surface.

Confirmation of attachment of 4-hydroxybenzoic acid polymers onto PES flat sheets was shown by the presence of hydroxyl peak from a conjugated carboxylic acid at approximately 3300 cm^{-1} on the IR spectrum, and the presence of carboxylic acid peak at 287.85 eV, a decrease in C-S at 288.81 eV, and a decrease in O-S at 533.35 eV from C1s and O1s high resolution XPS spectra. After confirming the attachment of 4-hydroxybenzoic acid polymers onto PES flat sheets, BSA and lysozyme adsorption was analyzed and showed an initial increase in BSA adsorption followed by a decrease in BSA adsorption with increasing modification time. This shows that in order to see reduction in nonspecific adsorption the amount of polymer on the surface in terms of both graft density and chain length must be reached in order to exclude BSA adsorption onto the surface. Lysozyme protein adsorption increased upon modification with 4-hydroxybenzoic acid possibly due to both charge-charge interactions with the carboxylic acid functional groups and insufficient graft density to exclude lysozyme from binding to the surface.

After confirming the attachment of 4-hydroxybenzoic acid polymers onto PES flat sheet membranes the reaction was performed on PES microdialysis probes and the attachment was confirmed using XPS by the introduction of a carboxylic acid peak at 387.90 eV and the reduction of the O-S peak at 532.99 eV to a non-detectable level. Two different modification times were chosen, 2 and 24 hours. FITC-4, FITC-10, and FITC-20 relative recovery was

initially tested to determine if the modification times selected inhibited transport across the membrane; it was confirmed that the 24 hour modification time reduced relative recovery by 60-70% and the 2 hour modification reduced relative recovery by 20-40%. To further confirm this reduction in relative recovery upon modification with 4-hydroxybenzoic acid, lysozyme relative recovery was not detected for the 24 hour modification, and the 2 hour modification was not significantly different than the control (no modification). Since the adsorption of BSA and lysozyme onto the PES flat sheets indicated that the adsorption was influenced by charge-charge interactions between the adsorbing molecule and the surface, relative recovery was analyzed for both proteins with pI greater and less than pH 7.4. These analytes were CCL2 (pI= 9.3), KC/GRO (pI= 9.1), and VEGF (pI= 8.5), which have isoelectric points greater than pH 7.4 and TNF-α (pI= 5.0), and aFGF (pI= 5.7), which have isoelectric points less than pH 7.4. The relative recovery results from these analytes showed a 2 to 3 fold increase in relative recovery for analytes that had an isoelectric point greater than pH 7.4 (CCL2, KC/GRO, VEGF) but no significant increase in relative recovery for analytes with isoelectric points less than pH 7.4 (TNF-α, aFGF) for the 2 hour 4-hydroxybenzoic acid modified microdialysis probes.

After analyzing the effect of the 4-hydroxybenzoic acid modification on relative recovery, this modification was used to further modify the membrane surface with heparin. This was performed by a two-step process, attaching ethylenediamine to the carboxylic acid modified membrane surface, and then attaching heparin to the amine modified membrane surface, both using EDC/NHS chemistry. Attachment of ethylenediamine and heparin was confirmed by the disappearance of the peak at 3300 cm^{-1}, indicating that the surface did not contain the carboxylic acid functional group at a significant quantity to be detected using ATR-FTIR; heparin modification was confirmed by the reappearance of the peak at 3300 cm^{-1}, indicating the

142

presence of the carboxylic acid functional group. XPS results for the heparin modified flat

sheets showed peaks at 287.85 eV indicative of the carboxylic acid functional group and 167.67

eV, and 168.87 eV for S2p. There was also a decrease in C-S at 288.82 eV. BSA and lysozyme

protein adsorption to the PES flat sheet membrane showed no change in BSA adsorption, but an

increase in protein adsorption for the 12 and 24 hour modification times for lysozyme. This

increase in protein adsorption could indicate a charge-charge interaction between the highly

negatively charged heparin and the overall positively charge lysozyme.

After confirming the attachment of heparin onto PES flat sheets the method was applied

to PES hollow fiber microdialysis probes. XPS results show the presence of a carboxylic acid

peak at 287.72 eV ± 0.35 at 3.23% ± 2.86 for the heparin modified microdialysis membranes,

which is not detected for the control membranes. Also the O-S peak at 533.54 eV ± 0.24 for the

heparin modified membranes was not detectable compared the control at 3.15% ± 0.64. The S2p

peak is also greater than the S2p peak in the 4HBA modified microdialysis membrane.

After confirming the attachment of heparin to PES microdialysis membranes FITC-4,

FITC-10, and FITC-20 relative recovery was determined and showed no further decrease in

relative recovery compared to the decrease in relative recovery after modification with 4HBA.

Relative recovery for heparin binding proteins, CCL2, aFGF, and VEGF, was determined.

CCL2 showed a twofold increase in relative recovery for hours 3 and 4 for the 24 hour 4HBA-

heparin modifications time. This RR enhancement was less than the observed fourfold RR

enhancement with heparin immobilized microspheres but by doubling the RR with the 24 hour

4HBA-heparin modified surface this is still considered to be an improvement compared to using

an unmodified microdialysis membrane.[53] The increase in RR CCL2 for the 24 hour 4HBA-

heparin modification could be due to the increase in heparin on the membrane surface with

increased 4HBA modification time but the size of CCL2 is not significantly blocked by the increase in modification. This may also explain why the RR enhancement was less than what was observed with the heparin-immobilized microspheres because the pore size of the membrane is, as was observed with the FITC-labeled dextrans, being reduced.

For aFGF the RR increased twofold for the 2 hour 4HBA-heparin modification. This was not observed under the flow rate conditions (1μL/min) with perfusing heparin immobilized microspheres so adding heparin to the membrane surface provided more significant enhancement to RR compared to using heparin immobilized microspheres under the same flow rate conditions.[53] For the aFGF molecular weight is greater than CCL2 so aFGF may be blocked by the 24 hour 4HBA-heparin modification which could explain why the RR did not increase with the 24 hour 4HBA-heparin modification.

VEGF relative recovery was significantly different than the control for the 24 hour 4HBA-heparin modification time. VEGF (21 kDa) relative recovery for 24 hour 4HBA-heparin modified membranes was significantly different than the control but the increase in relative recovery was slight this could be due to pore blockage caused by the 24 hour 4HBA-heparin modification leading reduced transport across the membrane. This could explain why with heparin-immobilized microsphere the RR enhancement was 3.5-fold but with a heparin modified surface the RR enhancement was approximately 25%.[53] This could also be the case for CCL2 but since CCL2 is smaller at 13.1 kDa, CCL2's diffusion through the modified membrane surface is not as hindered compared to VEGF.

KC/GRO was also analyzed since it is the rat analog of IL-8, a known heparin binding protein, and relative recovery increased with the 2 hour 4HBA-heparin modified microdialysis membranes. A similar increase in relative recovery was observed for KC/GRO with the 2 hour

144

4HBA modified microdialysis membranes.   This increase could be due to the electrostatic

interaction between a negatively charged surface and KC/GRO (pI=9.1) with an overall positive

charge. This portion of the dissertation showed successful attachment of heparin onto the

microdialysis membrane surface.

Future Prospects

In this dissertation the 4HBA modification showed a trend towards increasing RR of

proteins with a pI greater than the pH of the buffer (pH 7.4), but not for proteins with a pI less

than the pH of the buffer. This could indicate an electrostatic attraction between proteins and the

negatively charged surface. An interesting future project could be to test if the opposite trend

could occur with the ethylenediamine modification performed before attachment of heparin. The

pKa of the removal of a proton from the first amine is 7.564 and the second is 10.71, so at pH 7.4

the surface would have an overall positive charge. This could be tested with the set of analytes

used in this project to see if altering the charged nature of the PES membrane surface could

increase RR of analytes with a pI less than 7.4. This trend could also be further studied for both

the carboxylic acid and ethylenediamine functionalization using carboxylic acid functionalized

SPR sensors. This could be used to investigate the kinetic parameters (k_{on}, k_{off} and K_D) between

the protein and the surface.

A major area in membrane research is the modification of the membrane surface, and one

of the purposes of this project was to develop a method to attach molecules containing carboxyl

or amine functional groups onto the microdialysis membrane surface. With the attachment of

4HBA polymers onto the membrane surface, attachment of other amine or carboxyl containing

molecules can be attached to the membrane surface using EDC/NHS chemistry. This method

can be beneficial in a wide variety of ways. In this dissertation heparin was attached to the

surface as a proof of principle experiment to modify the surface as well as to test the effect this

modification could have on relative recovery of heparin binding proteins. Another one of the

future prospects of the project could be to attach different analytes to the membrane surface.

This could be tailored to a wide variety of applications that use functionalized membrane

surfaces, such as biomaterials, catalysts in fuel cell systems, and membrane separations.

REFERENCES

1.   Kjellstrom, S.; Appels, N.; Ohlrogge, M.; Laurell, T.; Marko-Varga, G., Microdialysis- a membrane based sampling technique for quantitative determination of proteins. *Chromatographia* **1999,** *50* (9-10), 539.

2.   Nady, N.; Schroen, K.; Franssen, M. C.; Lagen, B.; Murali, S.; Boom, R. M.; Mohyeldin, M. S.; Zuilhof, H., Mild and highly flexible enzyme-catalyzed modification of poly(ethersulfone) membranes. *ACS applied materials & interfaces* **2011,** *3* (3), 801-810.

3.   Duo, J.; Fletcher, H.; Stenken, J. A., Natural and synthetic affinity agents as microdialysis sampling mass transport enhancers: current progress and future perspectives. *Biosensors & bioelectronics* **2006,** *22* (3), 449-457.

4.   Cooper, G. M., Signaling molecules and their receptors. **2000**.

5.   Nirogi, R.; Kandikere, V.; Bhyrapuneni, G.; Benade, V.; Saralaya, R.; Irappanavar, S.; Muddana, N.; Ajjala, D. R., Approach to reduce the non-specific binding in microdialysis. *Journal of neuroscience methods* **2012,** *209* (2), 379-387.

6.   Schutte, R. J.; Oshodi, S. A.; Reichert, W. M., In vitro characterization of microdialysis sampling of macromolecules. *Anal Chem* **2004,** *76* (20), 6058-63.

7.   Ao, X.; Stenken, J. A., Microdialysis sampling of cytokines. *Methods (San Diego, Calif.)* **2006,** *38* (4), 331-341.

8.   Clough, G.; Noble, M., Microdialysis—A Model for Studying Chronic Wounds. *The International Journal of Lower Extremity Wounds* **2003,** *2* (4), 233-239.

9.   Anderson, C.; Svensson, C.; Sjogren, F.; Andersson, T.; Wardell, K., Human in vivo microdialysis technique can be used to measure cytokines in contact reactions. *Current problems in dermatology* **1995,** *23*, 121-130.

10.   Stenken, J. A.; Lunte, C. E.; Southard, M. Z.; Stahle, L., Factors that influence microdialysis recovery. Comparison of experimental and theoretical microdialysis recoveries in rat liver. *Journal of pharmaceutical sciences* **1997,** *86* (8), 958-966.

11.   Woodroofe, M. N.; Sarna, G. S.; Wadhwa, M.; Hayes, G. M.; Loughlin, A. J.; Tinker, A.; Cuzner, M. L., Detection of interleukin-1 and interleukin-6 in adult rat brain, following mechanical injury, by in vivo microdialysis: evidence of a role for microglia in cytokine production. *Journal of neuroimmunology* **1991,** *33* (3), 227-236.

12.   Tamime, A. Y., *Membrane Processing: Dairy and Beverage Applications*. John Wiley & Sons: 2012.

13.   Ståhle, L., On mathematical models of microdialysis: geometry, steady-state models, recovery and probe radius. *Use of Microdialysis in Drug Delivery* **2000,** *45* (2–3), 149-167.

14.   Wages, S. A.; Church, W. H.; Justice, J. B., Sampling considerations for on-line microbore liquid chromatography of brain dialysate. *Analytical Chemistry* **1986,** *58* (8), 1649-1656.

15.   Bungay, P. M.; Wang, T.; Yang, H.; Elmquist, W. F., Utilizing transmembrane convection to enhance solute sampling and delivery by microdialysis: Theory and in vitro validation. *Journal of membrane science* **2010,** *348* (1), 131-149.

16.   Müller, M., *Microdialysis in drug development*. Springer: 2013.

17.   Winter, C. D.; Iannotti, F.; Pringle, A. K.; Trikkas, C.; Clough, G. F.; Church, M. K., A microdialysis method for the recovery of IL-1β, IL-6 and nerve growth factor from human brain in vivo. *Journal of Neuroscience Methods* **2002,** *119* (1), 45-50.

18.   Klein, E., Affinity membranes: a 10-year review. *Journal of Membrane Science* **2000,** *179* (1), 1-27.

19.   Pendergast, M. M.; Hoek, E. M. V., A review of water treatment membrane nanotechnologies. *Energy & Environmental Science* **2011,** *4* (6), 1946-1971.

20.   Anuraj, N.; Bhattacharjee, S.; Geiger, J. H.; Baker, G. L.; Bruening, M. L., An all-aqueous route to polymer brush-modified membranes with remarkable permeabilites and protein capture rates. *J Memb Sci* **2012,** *389*, 117-125.

21.   Phillips, M.; Cormier, J.; Ferrence, J.; Dowd, C.; Kiss, R.; Lutz, H.; Carter, J., Performance of a membrane adsorber for trace impurity removal in biotechnology manufacturing. *Journal of Chromatography A* **2005,** *1078* (1–2), 74-82.

22.   Shiosaki, A.; Goto, M.; Hirose, T., Frontal analysis of protein adsorption on a membrane adsorber. *Journal of Chromatography A* **1994,** *679* (1), 1-9.

23.   Mohd Yusof, A. H.; Ulbricht, M., Polypropylene-based membrane adsorbers via photo-initiated graft copolymerization: Optimizing separation performance by preparation conditions. *Journal of Membrane Science* **2008,** *311* (1–2), 294-305.

24.   Ran, F.; Song, H.; Niu, X.; Yang, A.; Nie, S.; Wang, L.; Li, J.; Sun, S.; Zhao, C., Bionic design for surface optimization combining hydrophilic and negative charged biological macromolecules. *Int J Biol Macromol* **2014,** *67*, 260-9.

25.   Tang, M.; Xue J Fau - Yan, K.; Yan K Fau - Xiang, T.; Xiang T Fau - Sun, S.; Sun S Fau - Zhao, C.; Zhao, C., Heparin-like surface modification of polyethersulfone membrane and its biocompatibility. (1095-7103 (Electronic)).

26.   Wang, L.; Cai, Y.; Jing, Y.; Zhu, B.; Zhu, L.; Xu, Y., Route to hemocompatible polyethersulfone membranes via surface aminolysis and heparinization. *Journal of Colloid and Interface Science* **2014,** *422* (0), 38-44.

27.   Duo, J.; Stenken, J. A. In *Development of heparin-immobilized microspheres for enhanced microdialysis relative recovery of inflammatory cytokines*, American Chemical Society: 2006; p MRM.

28.   Herbaugh, A. W.; Stenken, J. A., Antibody-enhanced microdialysis collection of CCL2 from rat brain. *Journal of neuroscience methods* **2011,** *202* (2), 124-127.

29.   Khramov, A. N.; Stenken, J. A., Enhanced microdialysis recovery of some tricyclic antidepressants and structurally related drugs by cyclodextrin-mediated transport. *The Analyst* **1999,** *124* (7), 1027.

30.   Stenken, J. A.; Chen, R.; Yuan, X., Influence of geometry and equilibrium chemistry on relative recovery during enhanced microdialysis. *Analytica Chimica Acta* **2001,** *436* (1), 21.

31.   Green, R. J.; Frazier, R. A.; Shakesheff, K. M.; Davies, M. C.; Roberts, C. J.; Tendler, S. J. B., Surface plasmon resonance analysis of dynamic biological interactions with biomaterials. *Biomaterials* **2000,** *21* (18), 1823-1835.

32.   Cussler, E. L., *Diffusion : mass transfer in fluid systems*. 3rd ed.; Cambridge University Press: Cambridge ; New York, 2009; p xxii, 631 p.

33.   Khramov, A. N.; Stenken, J. A., Enhanced Microdialysis Extraction Efficiency of Ibuprofen in Vitro by Facilitated Transport with Î²-Cyclodextrin. *Analytical Chemistry* **1999,** *71* (7), 1257.

34.   Wang, Y. X.; Stenken, J. A., Affinity-based microdialysis sampling using heparin for in vitro collection of human cytokines. *Analytica Chimica Acta* **2009,** *651* (1), 105-111.

35.   Dagouassat, M.; Suffee N Fau - Hlawaty, H.; Hlawaty H Fau - Haddad, O.; Haddad O Fau - Charni, F.; Charni F Fau - Laguillier, C.; Laguillier C Fau - Vassy, R.; Vassy R Fau - Martin, L.; Martin L Fau - Schischmanoff, P.-O.; Schischmanoff Po Fau - Gattegno, L.; Gattegno L Fau - Oudar, O.; Oudar O Fau - Sutton, A.; Sutton A Fau - Charnaux, N.; Charnaux, N., Monocyte chemoattractant protein-1 (MCP-1)/CCL2 secreted by hepatic myofibroblasts promotes migration and invasion of human hepatoma cells. (1097-0215 (Electronic)).

36.   Zhang, F.; McLellan, J. S.; Ayala, A. M.; Leahy, D. J.; Linhardt, R. J., Kinetic and Structural Studies on Interactions between Heparin or Heparan Sulfate and Proteins of the Hedgehog Signaling Pathway. *Biochemistry* **2007,** *46* (13), 3933-3941.

37.   Hartmann, G.; Prospero, T.; Brinkmann, V.; Ozcelik, Ö.; Winter, G.; Hepple, J.; Batley, S.; Bladt, F.; Sachs, M.; Birchmeier, C.; Birchmeier, W.; Gherardi, E., Engineered mutants of HGF/SF with reduced binding to heparan sulphate proteoglycans, decreased clearance and enhanced activity in vivo. *Current Biology 8* (3), 125-135.

38.   Lin, Y.; Pixley, R. A.; Colman, R. W., Kinetic Analysis of the Role of Zinc in the Interaction of Domain 5 of High-Molecular Weight Kininogen (HK) with Heparin. *Biochemistry* **2000,** *39* (17), 5104-5110.

39.   Ibrahimi, O. A.; Zhang, F.; Lang Hrstka, S. C.; Mohammadi, M.; Linhardt, R. J., Kinetic Model for FGF, FGFR, and Proteoglycan Signal Transduction Complex Assembly. *Biochemistry* **2004,** *43* (16), 4724-4730.

40.   Amara, A.; Lorthioir, O.; Valenzuela, A.; Magerus, A.; Thelen, M.; Montes, M.; Virelizier, J.-L.; Delepierre, M.; Baleux, F.; Lortat-Jacob, H.; Arenzana-Seisdedos, F., Stromal Cell-derived Factor-1α Associates with Heparan Sulfates through the First β-Strand of the Chemokine. *Journal of Biological Chemistry* **1999,** *274* (34), 23916-23925.

41.   Guo, N. H.; Krutzsch, H. C.; Negre, E.; Zabrenetzky, V. S.; Roberts, D. D., Heparin-Binding Peptides from the Type-I Repeats of Thrombospondin - Structural Requirements for Heparin Binding and Promotion of Melanoma Cell-Adhesion and Chemotaxis. *Journal of Biological Chemistry* **1992,** *267* (27), 19349-19355.

42.   Rabenstein, D. L., Heparin and heparan sulfate: structure and function. *Natural Product Reports* **2002,** *19* (3), 312-331.

43.   Li, G.; Steppich, J.; Wang, Z.; Sun, Y.; Xue, C.; Linhardt, R. J.; Li, L., Bottom-up low molecular weight heparin analysis using liquid chromatography-Fourier transform mass spectrometry for extensive characterization. *Anal Chem* **2014,** *86* (13), 6626-32.

44.   Chung, H.; Kim, H.; Yoon, J.; Park, T., Heparin Immobilized Porous PLGA Microspheres for Angiogenic Growth Factor Delivery. *Pharmaceutical research* **2006,** *23* (8), 1835.

45.   Lau, E. K.; Paavola, C. D.; Johnson, Z.; Gaudry, J. P.; Geretti, E.; Borlat, F.; Kungl, A. J.; Proudfoot, A. E.; Handel, T. M., Identification of the glycosaminoglycan binding site of the CC chemokine, MCP-1: implications for structure and function in vivo. *The Journal of biological chemistry* **2004,** *279* (21), 22294-22305.

46.   Gibbs, R. V., Cytokines and glycosaminoglycans (GAGs). *Advances in Experimental Medicine and Biology* **2003,** *535*, 125-143.

47.   Powell, A. K.; Yates, E. A.; Fernig, D. G.; Turnbull, J. E., Interactions of heparin/heparan sulfate with proteins: appraisal of structural factors and experimental approaches. *Glycobiology* **2004,** *14* (4), 17R-30R.

48.   Capila, I.; Linhardt, R. J., Heparin-protein interactions. *Angewandte Chemie (International ed.in English)* **2002,** *41* (3), 391-412.

49.   Li, J.; Huang, X. J.; Ji, J.; Lan, P.; Vienken, J.; Groth, T.; Xu, Z. K., Covalent Heparin Modification of a Polysulfone Flat Sheet Membrane for Selective Removal of Low-Density Lipoproteins: A Simple and Versatile Method. *Macromolecular Bioscience* **2011,** *11* (9), 1218-1226.

50.   Lin, W. C.; Tseng, C. H.; Yang, M. C., In-vitro hemocompatibility evaluation of a thermoplastic polyurethane membrane with surface-immobilized water-soluble chitosan and heparin. *Macromolecular Bioscience* **2005,** *5* (10), 1013-1021.

51.   Wang, L. R.; Su, B. H.; Cheng, C.; Ma, L.; Li, S. S.; Nie, S. Q.; Zhao, C. S., Layer by layer assembly of sulfonic poly(ether sulfone) as heparin-mimicking coatings: scalable fabrication of super-hemocompatible and antibacterial membranes. *Journal of Materials Chemistry B* **2015,** *3* (7), 1391-1404.

52.   Lang, M.; Baihai, S.; Chong, C.; Zehua, Y.; Hui, Q.; Jiaming, Z.; Shudong, S.; Changsheng, Z., Toward highly blood compatible hemodialysis membranes via blending with heparin-mimicking polyurethane: Study in vitro and in vivo. *Journal of Membrane Science* **2014,** *470*, 90-101.

53.   Duo, J.; Stenken, J. A., In vitro and in vivo affinity microdialysis sampling of cytokines using heparin-immobilized microspheres. *Analytical and bioanalytical chemistry* **2011,** *399* (2), 783-793.

54.   Nady, N.; El-Shazly, H. A.; Soliman, M. H.; Kandil, H. S., Protein-Repellence PES Membranes Using Bio-grafting of Ortho-aminophenol. *Polymers* **2016,** *8* (8).

55.   Mansourpanah, Y.; Madaeni, S. S.; Rahimpour, A.; Farhadian, A.; Taheri, A. H., Formation of appropriate sites on nanofiltration membrane surface for binding TiO2 photo-catalyst: Performance, characterization and fouling-resistant capability. *Journal of Membrane Science* **2009,** *330* (1–2), 297-306.

56.   Pieracci, J.; Crivello, J. V.; Belfort, G., Photochemical modification of 10 kDa polyethersulfone ultrafiltration membranes for reduction of biofouling. *Journal of Membrane Science* **1999,** *156* (2), 223-240.

57.   Fan, L.; Nguyen, T.; Roddick, F. A.; Harris, J. L., Low-pressure membrane filtration of secondary effluent in water reuse: Pre-treatment for fouling reduction. *Journal of Membrane Science* **2008,** *320* (1–2), 135-142.

58.   Boi, C., Membrane adsorbers as purification tools for monoclonal antibody purification. *Journal of Chromatography B* **2007,** *848* (1), 19-27.

59.   Helmerhorst, E.; Chandler, D. J.; Nussio, M.; Mamotte, C. D., Real-time and Label-free Bio-sensing of Molecular Interactions by Surface Plasmon Resonance: A Laboratory Medicine Perspective. *Clin Biochem Rev* **2012,** *33* (4), 161-73.

60.   Rich, R. L.; Myszka, D. G., Advances in surface plasmon resonance biosensor analysis. *Current Opinion in Biotechnology* **2000,** *11* (1), 54-61.

61.   Liu, S. X.; Kim, J.-T., Characterization of Surface Modification of Polyethersulfone Membrane. *Journal of Adhesion Science and Technology* **2011,** *25* (1-3), 193-212.

62.   Singh, A. K.; Prakash, S.; Kulshrestha, V.; Shahi, V. K., Crosslinked hybrid nanofiltration membrane with antibiofouling properties and self-assembled layered morphology. *ACS Appl. Mater. Interfaces* **2012,** *4* (3), 1683-1692.

63.   Stenken, J. A., Methods and issues in microdialysis calibration. *Analytica Chimica Acta* **1999,** *379* (3), 337-358.

64.   Duo, J.; Stenken, J. A. In *Affinity-Based Microdialysis Sampling of Cytokines Using Heparin-Immobilized Microspheres*, American Chemical Society: 2008; p SWRM.

65.   Kochkodan, V.; Johnson, D. J.; Hilal, N., Polymeric membranes: Surface modification for minimizing (bio)colloidal fouling. *Advances in Colloid and Interface Science* **2014,** *206*, 116-140.

66.   Field, R. In *Fundamentals of fouling*, Wiley-VCH Verlag GmbH & Co. KGaA: 2010; p 1.

67.   Nady, N.; Franssen, M. C. R.; Zuilhof, H.; Boom, R. M.; Schroën, K., Enzymatic Modification of Polyethersulfone Membranes. *Water* **2012,** *4* (4), 932-943.

68.   Irfan, M.; Idris, A., Overview of PES biocompatible/hemodialysis membranes: PES–blood interactions and modification techniques. *Materials Science and Engineering: C* **2015,** *56*, 574-592.

69.   Snyder, K. L.; Nathan, C. E.; Yee, A.; Stenken, J. A., Diffusion and calibration properties of microdialysis sampling membranes in biological media. *Analyst* **2001,** *126* (8), 1261-8.

70.   Shenfu, C.; Lingyan, L.; Chao, Z.; Jie, Z., Surface hydration: Principles and applications toward low-fouling/nonfouling biomaterials. *Polymer* **2010,** *51* (23), 5283-5293.

71.   Frederix, F.; Bonroy, K.; Reekmans, G.; Laureyn, W.; Campitelli, A.; Abramov, M. A.; Dehaen, W.; Maes, G., Reduced nonspecific adsorption on covalently immobilized protein surfaces using poly(ethylene oxide) containing blocking agents. *J Biochem Biophys Methods* **2004,** *58* (1), 67-74.

72.   Zhou, Y.; Wang, Z.; Zhang, Q.; Xi, X.; Zhang, J.; Yang, W., Equilibrium and thermodynamic studies on adsorption of BSA using PVDF microfiltration membrane. *Desalination* **2012,** *307* (0), 61-67.

73.   Hirt, D. E.; Ning, L.; Chun, Z.; Husson, S. M., Adsorption of fluorescently labeled protein residues on poly(ethylene- co-acrylic acid) films modified with affinity functionalities. *Colloids and Surfaces B (Biointerfaces)* **2006,** *50* (2), 89-96.

74.   Nady, N.; Schroen, K.; Franssen, M. C.; Fokkink, R.; Mohy Eldin, M. S.; Zuilhof, H.; Boom, R. M., Enzyme-catalyzed modification of PES surfaces: reduction in adsorption of BSA, dextrin and tannin. *Journal of colloid and interface science* **2012,** *378* (1), 191-200.

75.   Chen, S.; Cao, Z.; Jiang, S., Ultra-low fouling peptide surfaces derived from natural amino acids. *Biomaterials* **2009,** *30* (29), 5892-5896.

76.   Dahlin, A. P.; Hjort, K.; Hillered, L.; Sjodin, M. O.; Bergquist, J.; Wetterhall, M., Multiplexed quantification of proteins adsorbed to surface-modified and non-modified microdialysis membranes. *Anal Bioanal Chem* **2012,** *402* (6), 2057-67.

77.   Loos, W. J.; Zamboni, W. C.; Engels, F. K.; de Bruijn, P.; Lam, M. H.; de Wit, R.; Verweij, J.; Wiemer, E. A. C., Pitfalls of the application of microdialysis in clinical oncology: Controversial findings with docetaxel. *Journal of pharmaceutical and biomedical analysis* **2007,** *45* (2), 288.

78.   Nirogi, R.; Kandikere, V.; Bhyrapuneni, G.; Benade, V.; Saralaya, R.; Irappanavar, S.; Muddana, N.; Ajjala, D. R., Approach to reduce the non-specific binding in microdialysis. *Journal of neuroscience methods* **2012,** *209* (2), 379.

79.   Ratner, B. D., *Biomaterials science : an introduction to materials in medicine*. 3rd ed.; Elsevier Academic Press: Amsterdam ; Boston, 2013; p 57, 241 p.

80.   Kull, K. R.; Steen, M. L.; Fisher, E. R., Surface modification with nitrogen-containing plasmas to produce hydrophilic, low-fouling membranes. *Journal of Membrane Science* **2005,** *246* (2), 203-215.

81.   Cao, L.; Chang, M.; Lee, C.-Y.; Castner, D. G.; Sukavaneshvar, S.; Ratner, B. D.; Horbett, T. A., Plasma-deposited tetraglyme surfaces greatly reduce total blood protein adsorption, contact activation, platelet adhesion, platelet procoagulant activity, and in vitro thrombus deposition. *Journal of Biomedical Materials Research, Part A* **2007,** *81A* (4), 827-837.

82.   McArthur, S. L.; McLean, K. M.; Kingshott, P.; St, J. H. A. W.; Chatelier, R. C.; Griesser, H. J., Effect of polysaccharide structure on protein adsorption. *Colloids and Surfaces, B: Biointerfaces* **2000,** *17* (1), 37-48.

83.   Luk, Y.-Y.; Kato, M.; Mrksich, M., Self-Assembled Monolayers of Alkanethiolates Presenting Mannitol Groups Are Inert to Protein Adsorption and Cell Attachment. *Langmuir* **2000,** *16* (24), 9604-9608.

84.   Chapman, R. G.; Ostuni, E.; Liang, M. N.; Meluleni, G.; Kim, E.; Yan, L.; Pier, G.; Warren, H. S.; Whitesides, G. M., Polymeric Thin Films That Resist the Adsorption of Proteins and the Adhesion of Bacteria. *Langmuir* **2001,** *17*, 1225.

85.   Statz, A. R.; Meagher, R. J.; Barron, A. E.; Messersmith, P. B., New peptidomimetic polymers for antifouling surfaces. *Journal of the American Chemical Society* **2005,** *127* (22), 7972-7973.

86.   Chelmowski, R.; Koester, S. D.; Kerstan, A.; Prekelt, A.; Grunwald, C.; Winkler, T.; Metzler-Nolte, N.; Terfort, A.; Woell, C., Peptide-Based SAMs that Resist the Adsorption of Proteins. *Journal of the American Chemical Society* **2008,** *130* (45), 14952-14953.

87.   Ali, N. a.; Tari, S. S. M., Surface modification of polyethersulfone ultrafiltration (PES-UF) membrane using myoglobin as modifying agent. *Desalination and Water Treatment* **2012,** *47* (1-3), 171-181.

88.   Kouwonou, Y.; Malaisamy, R.; Jones, K. L., Modification of PES Membrane: Reduction of Biofouling and Improved Flux Recovery. *Separation Science and Technology* **2008,** *43* (16), 4099-4112.

89.   Kurniawati, S.; Nicell, J. A., Characterization of Trametes versicolor laccase for the transformation of aqueous phenol. *Bioresource Technology* **2008,** *99* (16), 7825-7834.

90.   Schroeder, M.; Fatarella, E.; Kovač, J.; Guebitz, G. M.; Kokol, V., Laccase-Induced Grafting on Plasma-Pretreated Polypropylene. *Biomacromolecules* **2008,** *9* (10), 2735-2741.

91.   Piontek, K.; Antorini, M.; Choinowski, T., Crystal structure of a laccase from the fungus Trametes versicolor at 1.90-A resolution containing a full complement of coppers. *J Biol Chem* **2002,** *277*, 37663-37669.

92.   Nady, N.; Schroen, K.; Franssen, M. C. R.; Eldin, M. S. M.; Zuilhof, H.; Boom, R. M., Laccase-catalyzed modification of PES membranes with 4-hydroxybenzoic acid and gallic acid. *Journal of Membrane Science* **2012,** *394*, 69-79.

93.   Chandra, R. P.; Felby, C.; Ragauskas, A. J., Improving Laccase-Facilitated Grafting of 4-Hydroxybenzoic Acid to High-Kappa Kraft Pulps. *Journal of wood chemistry and technology* **2005,** *24* (1), 69-81.

94.   Nady, N.; Schroen, K.; Franssen, M. C. R.; Lagen, B. v.; Murali, S.; Boom, R. M.; Mohyeldin, M. S.; Zuilhof, H., Mild and Highly Flexible Enzyme-Catalyzed Modification of Poly(ethersulfone) Membranes. *ACS Applied Materials & Interfaces* **2011,** *3* (3), 801.

95.   Ikeda, R.; Sugihara, J.; Uyama, H.; Kobayashi, S., Enzymatic oxidative polymerization of 4-hydroxybenzoic acid derivatives to poly(phenylene oxide)s[J]. *Polym Int* **1998,** *47*, 295-301.

96.   Aktas, N.; Cicek, H.; Unal, A. T.; Kibarer, G.; Kolankaya, N.; Tanyolac, A., Reaction kinetics for laccase-catalyzed polymerization of 1-napthol. *Bioresour Technol* **2001,** *80*, 29-36.

97.   Hind, A. R.; Bhargava, S. K.; McKinnon, A., At the solid/liquid interface: FTIR/ATR — the tool of choice. *Advances in Colloid and Interface Science* **2001,** *93* (1–3), 91-114.

98.   Sun, C.; Ji, H.; Qin, H.; Nie, S.; Zhao, W.; Zhao, C., A facile approach toward multifunctional polyethersulfone membranes via in situ cross-linked copolymerization. *Journal of biomaterials science. Polymer edition* **2015,** *26* (15), 1013-34.

99.   Ma, J.; Luan, S. F.; Song, L. J.; Jin, J.; Yuan, S. S.; Yan, S. J.; Yang, H. W.; Shi, H. C.; Yin, J. H., Fabricating a Cycloolefin Polymer Immunoassay Platform with a Dual-Function Polymer Brush via a Surface-Initiated Photoiniferter-Mediated Polymerization Strategy. *Acs Applied Materials & Interfaces* **2014,** *6* (3), 1971-1978.

100.	Xiang, T.; Zhang, L. S.; Wang, R.; Xia, Y.; Su, B. H.; Zhao, C. S., Blood compatibility comparison for polysulfone membranes modified by grafting block and random zwitterionic copolymers via surface-initiated ATRP. *Journal of Colloid and Interface Science* **2014,** *432*, 47-56.

101.	Zhu, J.; Sun, G., Facile Fabrication of Hydrophilic Nanofibrous Membranes with an Immobilized Metal-Chelate Affinity Complex for Selective Protein Separation. *Acs Applied Materials & Interfaces* **2014,** *6* (2), 925-932.

102.	Xu, G. C.; Hibino, Y.; Suzuki, Y.; Tanihara, M.; Imanishi, Y.; Awazu, K., Free electron laser induces specific immobilization of heparin on polysulfone films. *Journal of Biomaterials Science-Polymer Edition* **2001,** *12* (5), 503-514.

103.	Tripathi, B. P.; Dubey, N. C.; Stamm, M., Polyethylene glycol cross-linked sulfonated polyethersulfone based filtration membranes with improved antifouling tendency. *Journal of Membrane Science* **2014,** *453*, 263-274.

104.	Belfer, S.; Fainchtain, R.; Purinson, Y.; Kedem, O., Surface characterization by FTIR-ATR spectroscopy of polyethersulfone membranes-unmodified, modified and protein fouled. *Journal of Membrane Science* **2000,** *172* (1–2), 113-124.

105.	Liu, S. X.; Kim, J. T.; Kim, S., Effect of polymer surface modification on polymer-protein interaction via hydrophilic polymer grafting. *Journal of Food Science* **2008,** *73* (3), E143-E150.

106.	Watts, J. F.; Wolstenholme, J., An Introduction to Surface Analysis by XPS and AES. Wiley Online Library: 2004; p 166.

107.	Chen, Y.-Y.; Yu, B.-Y.; Wang, W.-B.; Hsu, M.-F.; Lin, W.-C.; Lin, Y.-C.; Jou, J.-H.; Shyue, J.-J., X-ray Photoelectron Spectrometry Depth Profiling of Organic Thin Films Using C60 Sputtering. *Analytical Chemistry* **2008,** *80* (2), 501-505.

108.	Li, Q.; Matuana, L. M., Surface of cellulosic materials modified with functionalized polyethylene coupling agents. *Journal of Applied Polymer Science* **2003,** *88* (2), 278-286.

109.	Himstedt, H. H.; Qian, X.; Weaver, J. R.; Wickramasinghe, S. R., Responsive membranes for hydrophobic interaction chromatography. *Journal of Membrane Science* **2013,** *447* (0), 335-344.

110.	Chen, X.; Zhao, Y.; Moutinho, J.; Shao, J.; Zydney, A. L.; He, Y., Recovery of small dye molecules from aqueous solutions using charged ultrafiltration membranes. *J Hazard Mater* **2015,** *284*, 58-64.

111.	Murgasova, R.; Hercules, D. M., Polymer characterization by combining liquid chromatography with MALDI and ESI mass spectrometry. *Analytical and Bioanalytical Chemistry* **2002,** *373* (6), 481-489.

112. Su, W.-F., Polymer Size and Polymer Solutions. In *Principles of Polymer Design and Synthesis*, Springer: 2013; pp 9-26.

113. Mojsiewicz-Pienkowska, K., Size exclusion chromatography with evaporative light scattering detection as a method for speciation analysis of polydimethylsiloxanes. III. Identification and determination of dimeticone and simeticone in pharmaceutical formulations. *Journal of Pharmaceutical and Biomedical Analysis* **2012,** *58*, 200-207.

114. Podzimek, S.; Vlcek, T.; Johann, C., Characterization of branched polymers by size exclusion chromatography coupled with multiangle light scattering detector. I. Size exclusion chromatography elution behavior of branched polymers. *Journal of Applied Polymer Science* **2001,** *81* (7), 1588-1594.

115. Nielen, M. W. F.; Malucha, S., Characterization of polydisperse synthetic polymers by size-exclusion chromatography matrix-assisted laser desorption/ionization time-of-flight mass spectrometry. *Rapid Communications in Mass Spectrometry* **1997,** *11* (11), 1194-1204.

116. Zhou, Y. N.; Wang, Z.; Zhang, Q.; Xi, X. J.; Zhang, J.; Yang, W. T., Equilibrium and thermodynamic studies on adsorption of BSA using PVDF microfiltration membrane. *Desalination* **2012,** *307*, 61-67.

117. Liu, S. X.; Kim, J. T.; Kim, S.; Singh, M., The Effect of Polymer Surface Modification Via Interfacial Polymerization on Polymer-Protein Interaction. *Journal of Applied Polymer Science* **2009,** *112* (3), 1704-1715.

118. Cowan, S.; Ritchie, S., Modified polyethersulfone (PES) ultrafiltration membranes for enhanced filtration of whey proteins. *Separation Science and Technology* **2007,** *42* (11), 2405-2418.

119. Demneh, S. M. G.; Nasernejad, B.; Modarres, H., Modeling investigation of membrane biofouling phenomena by considering the adsorption of protein, polysaccharide and humic acid. *Colloids and Surfaces B-Biointerfaces* **2011,** *88* (1), 108-114.

120. Ma, Z. W.; Lan, Z. W.; Matsuura, T.; Ramakrishna, S., Electrospun polyethersulfone affinity membrane: Membrane preparation and performance evaluation. *Journal of Chromatography B-Analytical Technologies in the Biomedical and Life Sciences* **2009,** *877* (29), 3686-3694.

121. Lin, W. C.; Liu, T. Y.; Yang, M. C., Hemocompatibility of polyacrylonitrile dialysis membrane immobilized with chitosan and heparin conjugate. *Biomaterials* **2004,** *25* (10), 1947-1957.

122. Ma, Z. W.; Kotaki, M.; Ramakrishna, S., Electrospun cellulose nanofiber as affinity membrane. *Journal of Membrane Science* **2005,** *265* (1-2), 115-123.

123.	Zhang, N.; Weir, M. D.; Romberg, E.; Bai, Y. X.; Xu, H. H. K., Development of novel dental adhesive with double benefits of protein-repellent and antibacterial capabilities. *Dental Materials* **2015,** *31* (7), 845-854.

124.	Kratz, F.; Grass, S.; Umanskaya, N.; Scheibe, C.; Muller-Renno, C.; Davoudi, N.; Hannig, M.; Ziegler, C., Cleaning of biomaterial surfaces: Protein removal by different solvents. *Colloids and Surfaces B-Biointerfaces* **2015,** *128*, 28-35.

125.	Wu, H. X.; Tan, L.; Yang, M. Y.; Liu, C. J.; Zhuo, R. X., Protein-resistance performance of amphiphilic copolymer brushes consisting of fluorinated polymers and polyacrylamide grafted from silicon surfaces. *Rsc Advances* **2015,** *5* (16), 12329-12337.

126.	Lin, P.; Ding, L.; Lin, C. W.; Gu, F., Nonfouling Property of Zwitterionic Cysteine Surface. *Langmuir* **2014,** *30* (22), 6497-6507.

127.	Kirdeciler, S. K.; Ozen, C.; Akata, B., Fabrication of nano- to micron-sized patterns using zeolites: Its application in BSA adsorption. *Microporous and Mesoporous Materials* **2014,** *191*, 59-66.

128.	Mohan, T.; Ristic, T.; Kargl, R.; Doliska, A.; Kostler, S.; Ribitsch, V.; Marn, J.; Spirk, S.; Stana-Kleinschek, K., Cationically rendered biopolymer surfaces for high protein affinity support matrices. *Chemical Communications* **2013,** *49* (98), 11530-11532.

129.	Aitken, A.; Learmonth, M. P., Protein Determination by UV Absorption. In *The Protein Protocols Handbook*, Walker, J. M., Ed. Humana Press: Totowa, NJ, 2002; pp 3-6.

130.	Walker, J. M., The Bicinchoninic Acid (BCA) Assay for Protein Quantitation. In *The Protein Protocols Handbook*, Walker, J. M., Ed. Humana Press: Totowa, NJ, 2009; pp 11-15.

131.	McKinney, R. M.; Spillane, J. T.; Pearce, G. W., A simple method for determining the labeling efficiency of fluorescein isothiocyanate products. *Analytical Biochemistry* **1966,** *14* (3), 421-428.

132.	Zou, W.; Qin, H.; Shi, W. B.; Sun, S. D.; Zhao, C. S., Surface Modification of Poly(ether sulfone) Membrane with a Synthesized Negatively Charged Copolymer. *Langmuir* **2014,** *30* (45), 13622-13630.

133.	Shao, L.; Kumar, G.; Lenhart, J. L.; Smith, P. J.; Payne, G. F., Enzymatic modification of the synthetic polymer polyhydroxystyrene. *Enzyme Microb. Technol.* **1999,** *25* (8-9), 660-668.

134.	Duo, J., Affinity microdialysis sampling of cytokines. **2009**.

135.	Diamond, R., Real-space refinement of the structure of hen egg-white lysozyme. *Journal of Molecular Biology* **1974,** *82* (3), 371-391.

136.	Maina, N. H.; Tenkanen, M.; Maaheimo, H.; Juvonen, R.; Virkki, L., NMR spectroscopic analysis of exopolysaccharides produced by Leuconostoc citreum and Weissella confusa. *Carbohydr Res* **2008,** *343* (9), 1446-55.

137.	Hlady, V.; Buijs, J.; Jennissen, H. P., Methods for Studying Protein Adsorption. *Methods in enzymology* **1999,** *309*, 402-429.

138.	Ferreira, L. F.; Souza, L. M.; Franco, D. L.; Castro, A. C. H.; Oliveira, A. A.; Boodts, J. F. C.; Brito-Madurro, A. G.; Madurro, J. M., Formation of novel polymeric films derived from 4-hydroxybenzoic acid. *Materials Chemistry and Physics* **2011,** *129* (1-2), 46-52.

139.	Goger, B.; Halden, Y.; Rek, A.; Mosl, R.; Pye, D.; Gallagher, J.; Kungl, A. J., Different affinities of glycosaminoglycan oligosaccharides for monomeric and dimeric interleukin-8: A model for chemokine regulation at inflammatory sites. *Biochemistry* **2002,** *41* (5), 1640-1646.